NASA-CR-194229

7N-24-CR
183167
p- 105

MCI 85-0458

FINAL REPORT

MAGNESIUM COMPOSITE MATERIAL FOR ADVANCED ROTARY AIRCRAFT ENGINES

SBIR 1983 Phase II

Contract Number NAS3-24546
SBIR - 02.07-5785
Release Date: 9-1-87
May 29, 1987

N94-70558

Unclas

Z9/24 0183167

(NASA-CR-194229) MAGNESIUM COMPOSITE MATERIAL FOR ADVANCED ROTARY AIRCRAFT ENGINES Final Report (Material Concepts) 105 p

Prepared for:

NASA-LEWIS RESEARCH CENTER
Aeronautics Section
21000 Brookpark Rd., M.S. 500-305
Cleveland, OH 44135

By:

WALTER R. WHITMAN
DR. DAVID M. GODDARD

MATERIAL CONCEPTS, INC.
666 North Hague Avenue
Columbus, Ohio 43204

PROJECT SUMMARY

Inasmuch as some of the data and experimental results are currently incomplete, a comprehensive project summary cannot be written at present. It will be provided as part of the final version of this report.

NOTICE - SBIR DATA - PHASE II

This SBIR data is furnished under NASA Contract No. NAS3-24546. It is furnished in confidence with the understanding that it will not, without permission of the contractor, be used for other than Governmental purposes nor disclosed outside the Government. This notice shall be affixed to any reproduction of this data, in whole or in part.

This report/paper contains information which falls under the purview of the U.S. Munitions List, Section 121.01, International Traffic in Arms Regulations. It shall not be transferred to foreign nationals in the U.S., or abroad, without a validated export license. Penalty for violation is described in ITAR, Section 127.

PREFACE

This program was performed by Material Concepts, Inc. for NASA Lewis Research Center under Contract No. NAS3-24546. NASA Project Manager was Mr. Chi-Ming Lee. Dr. David M. Goddard was the MCI Principal Investigator for the program, with Mr. Walter R. Whitman serving as Project Engineer.

1.0 INTRODUCTION

Rotary engines are attractive power sources for general aviation aircraft because of their potential for high efficiency and durability, which are a result of the low number of movable parts, compactness, and extremely high horsepower-to-weight ratio of these engines. In order to adapt the rotary engine to aircraft use, it is essential to reduce the weight of such components as the engine housings, rotors, and crankshaft. One method of reducing weight is to employ high performance, lightweight materials. Graphite/magnesium (Gr/Mg) composites, consisting of continuous graphite fibers in a magnesium alloy matrix, possess excellent mechanical properties combined with a very low density. In addition, these materials maintain both their integrity and their properties at the operating temperatures encountered in a rotary engine, plus they offer essentially metallic thermal conductivity.

This Final Report summarizes the results of a Phase II SBIR program, sponsored by NASA Lewis Reseach Center, on the development of cast Gr/Mg rotary engine components. In Phase I, an intermediate housing was successfully cast; this component had been selected because it represented a major, but not impossible, casting challenge. For Phase II, the target component was changed to a rotor housing, because it was determined that the performance requirements of this housing would better demonstrate the advantageous properties of Gr/Mg castings. The ultimate goal of this program was the fabrication of a cast Gr/Mg rotor housing which would perform under the service conditions of an operating rotary engine.

2.0 TECHNICAL OBJECTIVES

The technical objectives of this Phase II effort were as follows:

1. Fully characterize cast Gr/Mg composite materials with respect to those physical and mechanical properties which are pertinent to the performance of a rotary engine housing.

2. Use the material properties to determine optimum fiber contents and orientations for a cast Gr/Mg rotor housing.

3. Develop the optimum techniques for producing wear-resistant and chemical-resistant surfaces on cast Gr/Mg.

4. Develop the technology to produce commercial quality complex Gr/Mg castings.

5. Demonstrate the fabrication of a commercial quality cast Gr/Mg rotor housing, consisting of material which has been optimized for performance requirements.

3.0 TECHNICAL APPROACH

The technical approach in this research program was designed to achieve each of the individual technical objectives as separate and well-defined Tasks.

3.1 TASK 1: CHARACTERIZATION OF CAST Gr/Mg

Three fiber orientations were studied: 0^{o} (unidirectional), $0^{o}/90^{o}$, and $+45^{o}/-45^{o}$. For the two orientations that involve cross-plying, both equal fiber amounts--20 volume percent (vol %)--in the two directions and a 30%/10% ratio were studied. All tests were conducted in both the 0^{o} and the 90^{o} directions except in cases where the material is equivalent in these two directions. A total of seven directional material properties were thus determined for each type of test described below.

Tests were conducted on cast Gr/Mg to determine the following properties: tensile strength and modulus, compressive strength and modulus, flexural strength, fatigue, thermal expansion, and thermal conductivity. Room temperature tensile, compressive, and flexure (4-point bending) tests were conducted at MCI. Elevated temperature (300^{o}C) mechanical tests were performed at the Energy Materials Testing Laboratory (EMTL), Biddeford, ME. EMTL also performed the thermal expansion and thermal conductivity tests, in the range of room temperature to 400^{o}C (750^{o}F). The fatigue tests were conducted at Battelle Memorial Institute's Columbus Laboratories (BCL), Columbus, OH; these tests studied the zero-tension-zero behavior of the material and were used to determine the stress level for infinite (10^{7} cycles) life. All data was analyzed at MCI to determine reproducibility and predictability of properties. Where encessary, additional verification tests were performed.

3.2 TASK 2: MATERIAL DESIGN FOR CAST Gr/Mg ROTOR HOUSING

MCI interfaced with manufacturers and research organizations knowledegable in rotary engine design and performance requirements. The purpose of this interfacing was to establish the appropriate considerations for optimum material performance in a rotary engine rotor housing. The mechanical properties of interest had been determined under Task 1.

What was obtained from the rotary engine experts was a "wish list" of material properties that would be optimum for service performance of the housing. This information, together with the material property data generated under Task 1, was supplied to a composite materials analysis and design organization. MCI utilized the services of Material Science Corporation (MSC), Spring House, PA, for this purpose.

The thrust of the MSC effort was to combine the performance requirements of the rotary engine rotor housing, the physical and mechanical properties of cast Gr/Mg, and composites reinforcement theory to design a material with optimum performance for the application.

3.3 TASK 3: DEVELOPMENT OF COMPATIBILITY COATINGS FOR Gr/Mg

This task involved two areas of conern: one was the wear resistance of the housing surface in contact with the rotor, and the other was the chemical compatibility of the material with the coolants and lubricants used in the rotary engine.

The first area involved the review of a wear resistant coating on the trochoid surface of the rotor housing. The review was limited in scope, but was directed toward establishing a trochoid wear surface capable of withstanding the operational parameters of the rotary engine.

Chemical compatibility of Gr/Mg with coolants and lubricants was another area of concern. The engine coolant used is ethylene glycol, while the lubricants are paraffin-base and synthetic oils. Tests performed in this portion of the task involved submerging cast Gr/Mg, uncoated or coated with various protective materials, in these liquids and ascertaining if any attack took place.

3.4 TASK 4: DEVELOPMENT OF COMMMERCIAL QUALITY Gr/Mg CASTINGS

The Phase I effort in this program was very successful. However, from a commercial standpoint, much remained to be accomplished in demonstrating that Gr/Mg castings can be produced which exhibit the same level of soundness and surface finish as standard magnesium alloy castings.

The specific activities under this task consisted of utilizing foundry techniques to produce castings which demonstrated good surface finish and soundness. These castings were subsize, to facilitate greater experimentation within the time and financial constraints of this task. However, the castings were designed to accurately represent portions, or smaller versions, of the rotor housing; specifically, achieving full soundness in thick sections was addressed. Exterior surface finish was assessed by visual observation, while soundness was evaluated by metallographic methods. The goal of the task was to establish the technology for producing generic fiber reinforced castings whose overall quality is equal to that of commercially cast non-reinforced products.

3.5 TASK 5: FABRICATION OF ROTARY ENGINE ROTOR HOUSING

In this task, the design results of Task 2, the surface compatibility approach defined by Task 3, and the optimized casting techniques developed under Task 4 were combined to produce a representative commercial-quality cast Gr/Mg rotary engine rotor housing. This housing was not optimized, as the physical configuration was a retrofit for a conventional alloy housing rather than a design specifically modified for composite materials. However, within this constraint, the Gr/Mg material itself was optimized for the physical and mechanical performance requirements of the rotary engine application. The casting was designed to have optimized surface finish and soundness, with the soundness being verified by NDE techniques. The appropriate chemically compatible surfaces were applied to the casting, based on the Task 3 technology. The wear resistant surface was tested and specified. In summary, this part was essentially ready for testing under service conditions.

4.0 RESULTS AND DISCUSSION

For clarity, the results of this program will be discussed by Task.

4.1 TASK 1: CHARACTERIZATION OF CAST Gr/Mg

4.1.1 Tensile, Compressive, and Flexural Properties

The results of the tensile, compressive, and flexural tests conducted on samples of cast Gr/Mg flat plates are given in Table 1. A few tests were deleted from the original plan; the deleted tests, and the reasons for the deletion, are shown in Table 2.

An analysis of the Table 1 results reveals no major or inexplicable deviations from anticipated behavior. The tensile strength of the unidirectional (40% in the 0^{o} direction) fiber orientation material is lower than that predicted from rule-of-mixtures theory. However, it is believed that this discrepancy can be explained by fiber misalignment which occurs during the procedure involving fiber layup, prepregging with a fugitive binder, and flattening of the prepreg. Furthermore, it is not unusual for composite materials to fail to exhibit full theoretical properties when tested in bulk form. What is significant about the Table 1 data is that it represents by far the most complete compilation of mechanical property data on cast Gr/Mg. And, while there are deviations from straight-line behavior as the fiber content in the test direction increases from 0% to 40%, the general trend of each property is decidedly upward, as would be expected (Figures 1 through 5). The fact many of the data points for the 30% fiber samples fall below the average line is undoubtedly related to the casting quality of the plates from which these samples were cut, and is probably irrelevant to the general property trend. Note that the relationship between fiber content and tensile modulus is generally good (Figure 3), with the only significant deviation occurring at the 10% value.

In general, it is believed that, with more experience in casting test plates, all strength values will tend to improve; also, a linear relationship between properties and fiber content will be shown to exist throughout the available range of reinforcement. For the present program, Table 1 data is adequate as a baseline for the Task 2 design study, since it provides at least approximate (and probably conservative) values for the properties required.

Not surprisingly, Gr/Mg castings maintain their mechanical properties quite well at elevated temperatures, except in cases such as the $\pm 45^{\circ}$ fiber orientations, where there are no fibers parallel to the test direction. In these materials, transfer of the load to the fibers is by shear stresses in the matrix, and the matrix shear strength is significantly reduced as the test temperature is increased. It is also apparent, however, that even the room temperature properties of the $\pm 45^{\circ}$ fiber samples are not especially attractive, again, because of the necessity of shear stress transfer through the matrix and the relatively weak fiber/matrix interfaces. This fact was given strong consideration in the Task 2 design study, as will be dis- cussed later. On the positive side, the compressive strength of Gr/Mg is quite good, even at elevated temperatures, and even perpendicular to the primary fiber direction. (Compressive modulus at elevated temperatures could not be measured using the equipment employed by EMTL). The only exception to this rule is the $\pm 45^{\circ}$ fiber samples, because compressive stresses cause shear failure at the fiber/matrix interfaces.

It is interesting to note that, in a few cases, the strength of the material appears to be higher at elevated temperatures than at room temperature. This could have been the result of higher quality material being tested at elevated temperatures. On the other hand, misaligned fibers are especially detrimental to composite strength if they are contained by a high modulus matrix. Since the effective modulus of the matrix decreases at elevated temperatures, the apparent increase in strength could be real. Of course, this will not happen when the misalignment problems are solved.

4.1.2 Thermal Properties

The thermal diffusivity/thermal conductivity, specific heat, and thermal expansion of a variety of cast Gr/Mg materials were measured at EMTL.

4.1.2.1 Thermal Conductivity

The thermal conductivities were calculated from the measured thermal diffusivities and the specific heat, the latter being a material property independent of fiber orientation. In the procedure employed, thermal diffusivity is measured by a flash method. A short-duration pulse of thermal energy is absorbed on one face of a slab specimen and allowed to propagate through the thickness of the specimen. The thermal response of the opposite face is monitored as a function of time, and recorded with an oscilloscope. Thermal diffusivity is then calculated as a relation of this time function and the specimen thickness. This measurement method conforms generally to Specification ASTM-C-714-72, with modifications to permit accurate measurements to elevated temperatures.

The simplified relationship which has been derived to relate diffusivity with specimen thickness and heat pulse traverse time is basically:

$$\alpha = \frac{\omega L^2}{t_{1/2}}$$

where:

α = thermal diffusivity
L = specimen thickness
$t_{1/2}$ = time for back-face temperature to reach one-half its maximum
ω = parameter which is a function of heat loss from the specimen. For the ideal case of zero heat loss, the value of this parameter is 0.139.

More specific to this discussion, the relationship of thermal conductivity and thermal diffusivity is expressed as:

$$\gamma = \alpha \, \rho \, C_p$$

where:

γ = thermal conductivity
α = thermal diffusivity
ρ = material density
C_p = specific heat

Specific heat is derived as the slope of the curve describing the enthalpy-temperature relationship. Enthalpy is measured with a Bunsen-type ice calorimeter; sufficient data are recorded so that the relationship can be well defined. Specific heat is then derived graphically from the smoothed enthalpy data.

In the Bunsen ice calorimeter, heat given up from a preheated specimen to the well is measured in terms of a volume change in a closed water-ice chamber in equilibrium at $0^{o}C$. The heat melts some of the ice in the chamber, causing a net change in the water-ice volume. To measure this change, mercury is used as the volume transfer agent; a reservoir of mercury in the bottom of the well is connected to an external accounting system such that small volume changes can be related to weight changes in the mercury volume. The heat equivalent for mercury in this system has been determined by the National Bureau of Standards and other laboratories to be 270.48 joules per gram. This is the constant of the measuring method, and should not vary among Bunsen ice calorimeters. It is a function of the volume change of ice melting to water and the heat of fusion involved in the change of state. All heat transfer is measured at the ice point; there is no need to measure temperatures in the calorimeter.

The specific heat of cast Gr/Mg containing 40 volume % fiber, as a function of temperature, is shown in Figure 6. The thermal conductivities of a variety of Gr/Mg materials (different combinations of various fiber orientations, tested in various directions) are shown in Figures 7 through 10. Several important facts are apparent from these figures. First, the increasing thermal conductivity with increasing temperatures is evidently a matrix phenomenon, since the alloy (AZ91) exhibits similar behavior. Second, the thermal conductivities of composites are generally lower than that of the matrix, which ranges from approximately 0.6 to 1 watts $cm^{-1}C^{-1}$, depending on temperature. The reason for this can be deduced from Figures 7 and 10. Although these curves are not identical, in theory they should be: in both cases, all fibers are oriented perpendicular to the direction of measured conductivity. From a material fabrication standpoint, the material in Figure 7 contains successive planes of fibers oriented in two orthogonal directions, but the planes of both the 0^{o} and the 90^{o} fibers are perpendicular to the heat pulse direction of travel. In Figure 10, the heat pulse traveled parallel to the planes of fibers, but the fibers in all planes were oriented perpendicular to the travel direction. It seems probable that something in the processing sequence created enough difference between these two situations to account for the difference between Figures 7 and 10. Regardless of this discrepancy, it is clear that the thermal conductivity of Gr/Mg, perpendicular to the fibers, is in the approximate range of 0.1 to 0.2 watts cm^{-1} C^{-1}.

This fact has some important implications for designing Gr/Mg materials for circumstances under which thermal conductivity is a primary concern. Although the transverse thermal conductivity of the fibers is not known, simplistic reasoning would suggest that the conductivity of a Gr/Mg material containing 40 volume % fiber, in a direction perpendicular to the fibers, would be 60 percent of the matrix conductivity plus 40 percent of the transverse fiber conductivity. This is clearly not the case. In fact, to a first approximation, it appears that the thermal conductivity of any portion of the composite which does not contain fibers parallel to the measurement direction, but which does contain any significant amount of perpendicular fibers, falls in the 0.1 to 0.2 watts cm^{-1} C^{-1} range. In other words,

$$C_c = C_f V_f + C_t(1-V_f)$$

where C_c = directional conductivity of the composite

C_f = longitudinal conductivity of the fibers

V_f = volume fraction of fibers oriented in conductivity direction

C_t = conductivity of bulk material containing transverse fibers

= 0.1 to 0.2 watts cm_{-1} C_{-1} (approximately)

Thus, even though $C_f = 1$ for P55 fibers and the matrix thermal conductivity is approximately 0.8, Figure 9 shows that, for a $0^o/90^o$ valanced cross-ply, the 0^o direction conductivity is

$$C_c = (1)(.2) + (0.15)(.8) = 0.32$$

which is the approximate value shown in the Figure. The thermal conductivity would undoubtedly be higher if a higher modulus fiber were used. For example, the same configuration using P100 fiber (C_f = 5.2 watts cm^{-1} C^{-1}) would yield:

$$C_c = (5.2)(.2) + (.15)(.8) = 1.16 \text{ watts } cm^{-1}\ C^{-1}$$

or a higher thermal conductivity than the matrix alone. Unfortunately, the 0^o fiber orientaion sample, tested in the 0^o direction, was cracked, and the results were therefore invalid; experimental difficulties in preparing samples for this test precluded fabricating a replacement. However, it seems reasonable to assume that if there are no fibers oriented perpendicular to the direction of heat travel, the matrix conductivity will become fully effective, and therefore:

$$C_c = C_f V_f + C_m(1-V_f)$$

where C_m is the matrix conductivity (approximately 0.7 watts cm^{-1} C^{-1}). Unfortunately, the Table 1 data shows that the transverse strength of a unidirectionally reinforced Gr/Mg composite is not sufficient for most structural applications. Therefore, for portions of a structure where thermal conductivity in one particular direction is especially important, the best compromise might be to use the minimum transverse fiber content neccesary to maintain structural integrity, together with the maximum content of high conductivity (high modulus) fibers in the critical direction. This approach is certainly feasible for rotary engine housings. It was not attempted on this program, partly because the confirming property data was not available, and partly because the incorporation of the high modulus fibers into an already complex fiber layup was felt to be beyond the scope of what could be reasonably accomplished.

4.1.2.2 Thermal Expansion

The method employed to measure thermal expansion is frequently identified as the quartz (fused silica) recording dilatometer. In this procedure, illustrated schematically in Figure B-1, the specimen is supported between members of a quartz frame and push-rod assembly. The assembly is inserted into a furnace capable of uniformly heating the specimen zone. As the specimen temperature is changed, changes in its length dimension result in relative displacement of the quartz push-rod and frame assembly. The amount of displacement is sensed by a linear variable differential transformer and recorded on one scale of an X-Y plotter. Specimen temperature, sensed by a thermocouple, is recorded on the other scale. Thus, a continuous record of dilation versus temperature is produced.

The thermal expansion behavior of the various Gr/Mg materials studied is shown in Figures 11 through 15. Table 3 lists the coefficient of thermal expansion (CTE) over various temperature ranges. Three facts are obvious from this data. First, the thermal expansion of Gr/Mg is much lower than that of conventional alloys. Second, the CTE becomes lower (and often even negative) as the temperature increases. Third, there is a hysteresis loop between the heating and cooling portions of the expansion curve.

When a composite material containing unidirectionaly aligned fibers is heated, the theoretical CTE is defined by the equation:

$$CTE_c = \frac{(CTE_f)(E_f)(V_f) + (CTE_m)(E_m)(1-V_f)}{E_f V_f + E_m(1-V_f)}$$

where CTE_c = CTE of composite
CTE_f = CTE of fiber
CTE_m = CTE of matrix

E_f, E_m = Elastic moduli of fiber and matrix
V_f = Volume fraction fiber

For P55 fibers in an AZ91 matrix,

CTE_f = -0.5 PPM/^{o}F
CTE_m = 14 PPM/^{o}F
E_f = 55 msi
E_m = 6.5 msi

It seems reasonable to assume that, for a material containing $0^{o}/90^{o}$ cross-plied fibers, the effective matrix modulus is the modulus of the material containing transverse fibers; from Table 1, this value is 3.4 msi at room temperature. The CTE of this matrix should be close to 14 PPM/^{o}F, as seen in Figures 12 and 13 and Table 3. Using these numbers, the CTE values for Gr/Mg composites containing 10, 20, 30, and 40 volume percent fibers in the test direction (40 volume percent fibers total, the balance being in the transverse direction) are calculated to be, respectively, 4.7, 2.4, 1.3, and 1.7 PPM/^{o}F. The fact that the calculated CTE for 30% fibers is lower than that for 40% fibers is related to the assumption used for matrix modulus; it is, undoubtedly, not correct to assume this modulus drop from 6.5 to 3.4 msi with the addition of only a few transverse fibers. In spite of this simplification, it can be seen that the agreement with experimental results is reasonably good up to 400^{o}F. Above this temperature, other factors become dominant.

The reason for the low CTE in Gr/Mg is, of course, the negative CTE and relatively high modulus of the fibers. As the material is heated, the fibers attempt to contract in length, while the matrix attempts to expand. The two components therefore exert stresses on each other (tensile stress on the fibers and compressive stresses on the matrix during heating). The balance of these stresses determines the CTE, as shown in the equation. However, the use of the matrix modulus is valid only until the yield strength of the matrix (compressive, on heating) is reached. Further heating not only increases the contraction stress exerted by the fiber, but the matrix, having yielded, is less able to resist this stress, so the CTE becomes lower. Note in Figure 11 that the CTE of all materials appears to become negative above approximately 300°C (575°F). This is an interesting result which, to the author's knowledge, has not previously been documented. Gr/Mg composites have been designed to achieve a zero CTE under certain conditions, primarily in a space environment. However, these materials generally contain much higher modulus fibers, and the temperature range over which the CTE has been measured has been typically -250 to +250°F. Quite probably, the CTE of these materials would become very negative at the temperatures encountered in a rotary engine housing.

Returning to the CTE studies in this program: after the maximum test temperature has been reached and the specimen begins to cool, the fibers now exert a tensile stress on the matrix. Until the matrix tensile yield stress is reached, the matrix modulus again becomes effective in resisting the fiber induced stresses. Therefore, initial contraction is greater than the final expansion on heating, resulting in hysteresis. Note that all composite cooling curves exhibit a lower expansion, at a given temperature, than the corresponding heating curves. Final cooling to room temperature is an asymptotic process, and therefore impractical under the experimental conditions.

However, all cooling curves appear to be heading towards approximately zero net expansion at room temperature. One sample was indeed re-heated, and the expansion curve that was generated closely followed the original heating curve; therefore, any concerns about "ratcheting" (cumulative permanent changes in length after several thermal cycles) appear to be unwarranted. Furthermore, these CTE tests were conducted under unrestrained conditions. In a rotary engine, a Gr/Mg housing would be restrained by, and exert restraint upon, surrounding housings. Since the rotor housing is the hot housing, a low CTE Gr/Mg rotor housing would exert less stress (than would a conventional rotor housing) on the adjoining cooler housings during operation, and also have a lower stress exerted on it because its expansion tendency is less. After shut-down, the dimensional constraints imposed by the adjoining housings would ensure that the rotor housing maintain its original dimensions.

4.1.3 Fatigue Properties

Ambient and elevated temperature fatigue testing was conducted at Battelle. Initially, the cast Gr/Mg fatigue samples were of the configuration shown in Figure 16. This sample design had reportely been used successfully for various types of mechanical tests on other composite materials. In the first few tests at Battelle, however, the Gr/Mg samples failed at unexpectedly low combinations of stress and fatigue cycles. Samples of this configuration were therefore tensile tested at MCI, and these results, too, were poor, with ultimate strengths much lower than had been measured using straight sided test samples. In view of this result, the fatigue samples were remachined into a straight sided configuration, 0.5 in. wide x 6 in. long; adhesively bonded tabs were attached at the grip ends. The first fatigue tests using this new sample design duplicated the conditions of the earlier tests, and it was found that the indicated fatigue behavior was indeed much improved.

The fatigue tests are currently in progress. Full results will be documented in the final version of this report.

4.2 Task 2: Material Design for Cast Gr/Mg Rotor Housing

The material design studies were performed at Materials Sciences Corporation. The complete MSC report, in viewgraph format, is included in the Appendix. In summary, MSC statistically analyzed the mechanical and thermal property data for the Gr/Mg castings and deduced typical properties as a function of fiber orientation. Simplified one dimensional heat transfer analyses were performed at various crank angles in the rotor housing, in order to obtain estimates of wall temperatures. Two dimensional finite element analyses of the rotor housing were performed for internal pressure and temperature loads. Two different Gr/Mg fiber configurations were analyzed and compared to the baseline aluminum design, and the maximum allowable stresses determined from the Task 1 test program were used to assess housing structural integrity.

MSC found generally good correlation between the material test data and predicted properties, although considerable scatter existed primarily in the compression data. Thermal analysis indicated that the temperature which the material must withstand during rotor housing operation will be in the 400^{o}F range. Under these conditions, MSC determined that a simple $0^{o}/90^{o}$ cross-ply fiber layup would not withstand the shear stresses encountered in the housing. However, a $0^{o}/ 45^{o}/90^{o}$ fiber layup, while sacrificing some bi-directional tensile and compressive strength and modulus, has a better balance of properties and is much better suited for the design loads. MSC concluded that the $0^{o}/\pm 45^{o}/90^{o}$ P55/Mg material constitutes a viable fiber configuration under rotor housing operating conditions, although post processing heat treatment to reduce residual stresses was recommended.

It should be noted that MSC's analysis was performed under the constraint that three-dimensional fiber orientations (X-Y plane plus Z axis) are not currently feasible in Gr/Mg composites. Thus, the originally proposed fiber orientation (Figure 17) was not selected. In this figure, let us refer to the plane of the sketch as the X-Y plane, with the Y direction vertical. If the indicated "circumferential" fibers had been used, any "cross-ply" fibers would have had an orientation component in the Z direction (normal to the plane of the sketch). Therefore, because of the three-dimensional restriction, additional fibers oriented in various directions in the X-Y plane would not have been possible. Only the "circumferential" fibers shown would be in the X-Y plane; "radial" fibers (normal at all points to the "circumferential" fibers and lying in the X-Y plane) would be geometrically disadvantageous, because the area being reinforced increases with increasing distance from the housing centerline and would be extremely difficult from a fiber layup standpoint.

MSC's analysis revealed that the reinforcement of a variety of directions in the X-Y plane was much more important than reinforcement in the Z direction. This seems logical, since the Z direction stresses appear to be primarily compressive; and the Table 1 data indicates that the compressive strength of cast Gr/Mg perpendicular to all fibers is nearly 20 ksi at 575^{o}F, which should be adequate for the housing. In fact, although MCI had openly speculated that the Figure 17 fiber orientation would be selected as optimum, we had an unvoiced concern that an "onion skin" effect could be created during thermal cycling, with layers of circumferentially reinforced material delaminating from one another because of the poor tensile properties normal to the fibers. The X-Y plane $0^{o}/\pm45^{o}/90^{o}$ orientation selected by MSC alleviates this problem. It might also be noted that the selected configuration is probably much easier to achieve in fabrication than the circumferential orientation would have been.

4.3 TASK 3: DEVELOPMENT OF COMPATIBILITY CASTINGS FOR Gr/Mg

4.3.1 Wear Resistant Coatings

After considerable discussion with cognizant personnel at both NASA Lewis Research Center and the John Deere Rotary Engine group, two wear resistant coatings were selected for study in this program to determine their suitability for the trochoid surface of the rotor housing. A number of spray-coating processes have been used to apply wear-resistant coatings to the trochoid surfaces of conventional rotor housings. The most effective process has been the Union Carbide Detonation-Gun (D-Gun) process using tungsten carbide in a cobalt matrix (87%/13%). Therefore, this coating was selected as the "standard" coating for this program; specifically, the coating was defined as UCAR LW-In30, 2 to 4 mils thick. Two Gr/Mg samples were coated in this manner. The coating on the first sample did not appear to be smooth or well bonded, but the second sample was satisfactory. This sample was therefore machined into three properly configured specimens for wear testing; the preparation included polishing of the coated surface to a 2-5 RMS finish.

Based on discussions with NASA, it was decided to include a wear resistant coating in this program which might also serve as a thermal barrier during engine operation. The coating selected was a two-layer coating consisting of 4-6 mils of UCAR LCO-35 (CoNiCrAlY) and 20-25 mils of UCAR LZ-8 ($ZrO_2Y_2O_3$), applied by Union Carbide using a plasma spraying process. Two samples of Gr/Mg were coated in this fashion, and both appeared to exhibit excellent adhesion between the coating and the substrate. From one of these samples, three wear test specimens were prepared as previously described. Not surprisingly, polishing of these samples to the proper surface finish was easier because of the extra coating thickness. With the D-Gun applied material, breaking through the coating and exposing the substrate occurred in several places, although the wear test specimens appeared to be free of such defects.

Other approaches studied in this task included the incorporation of discontinuous glass or ceramic (oxide) fibers within the Gr/Mg casting and the imbedding of ceramic tiles in the composite as part of the coating process. It was found that the fibers, as well as a silicon carbide tile, could be successfully incorporated in, and thereby bonded to, the Gr/Mg casting, which indicates that the materials were wetted by the molten magnesium alloy. An attempt to incorporate silicon nitride tiles was unsuccessful, however, because wetting did not occur. None of these approaches was pursued to the wear testing stage, because the more fully developed coating processes appeared to be satisfactory.

The wear test specimens were supplied to the John Deere Rotary Engine group for testing. The results of these tests are not yet available; they will be included in the final version of this report.

4.3.2 Chemical Compatibility

Samples of cast Gr/Mg composite were submerged in baths of deionized water, 50%/50% by volume ethylene glycol and deionized water, and 100% 2 cycle AMS/oil; tests were conducted at both ambient temperature and 200°F and in both static and agitated baths, in an attempt to simulate the environment in various portions of an operating rotor housing. The composite matrix alloy used in most of the samples for this study, and in all later portions of this program, was the newly developed and more corrosion resistant AZ91D. This is basically the same alloy as the previously employed AZ91C, except with closer controls over impurity content. Initially, all composite corrosion samples were uncoated, in order to determine the behavior of the basic material. The samples were examined after every 24 hours of bath exposure to determine the extent of degradation.

It was found that the agitated solutions provided the best evidence of corrosive attack on the samples. In a room temperature/agitated bath of 100% deionized water, the specimen had undergone a significant amount of attack after 10 days of exposure. The specimen immersed in the 50%/50% by volume test of ethylene glycol and deionized water showed limited degradation after 10 days in solution. In the samples, the areas where a lack of fiber infiltration was present were those that showed some degradation. The 100% 2 cycle AMS/oil solution test showed no degradation after 10 days. An interesting fact was noted with this specimen: after the test was completed, it retained a surface film of oil even after three alcohol washes and 180^{o}C thermal cycles. The same specimen was then placed in the 100% deionized water bath for 10 days and showed limited degradation. This result raises the possibility of oil impregnation of the material as a possible means of corrosion protection. It also supports the previous evidence that uninfiltrated fiber areas are sites of increased corrosion attack. Oil would tend to fill these void areas and prevent the corroding medium from reaching the material surface. Of course, the best solution to the problem would be to eliminate the uninfiltrated areas. While this effort received major attention under Task 4, it is doubtful if any composite material can be produced which is initially 100% void-free. Possibly, hot isostatic pressing would eliminate most of the voids, but even this approach might not be entirely satisfactory with continuous fiber reinforcement, because of the difficulty of causing fiber movement.

Because of the poor performance of the material in the room temperature deionized water tests, elevated temperature ($200^{o}F$)/agitated solution tests were conducted on coated samples. Initially, two coatings were studied. One coating consisted of arc sprayed magnesium alloy; this approach was intended to cover any exposed fibers, so the composite would behave as a standard unreinforced alloy. The second coating was "Clevcoat", a material developed and provided by Imperial Clevite of Cleveland, Ohio. The high temperature tests resulted in severe degradation of the samples for both coatings studied. The least attack occurred in the oil immersion tests and the most severe occurred during the water immersion tests.

One final coating, polymethyl methacrylate, was studied for the high temperature/agitated 100% deionized water test only, since this had proven to be the most severely corrosive environment of those investigated. A Gr/Mg sample coated with this material showed limited degradation after 10 days' exposure under these conditions. It is believed that polymethyl methacrylate, which is applied as a solution in an organic solvent and dries to a semi-viscous solid, acts much like the oil in that it penetrates and coats all void areas, and does not become brittle or flakey after drying. Thus, while superior coating materials might exist, polymethyl methacrylate was selected as the most promising coating material identified in this program.

4.4 TASK 4: DEVELOPMENT OF COMMERCIAL QUALITY CASTINGS

Although this effort was identified as a separate task, in actual fact it supported the work in Tasks 1 and 3 as well. Specifically, in order for the mechanical and thermal property tests to be valid, they had to be conducted on material of a quality which was representative of that to be found in the ultimate rotor housing. The need for minimization of voids, especially surface voids, in the corrosion tests has already been mentioned. Perhaps the greatest challenge of this task was the satisfactory and repeatable casting of the flat plates from which all test samples were cut. This turned out to be much more difficult than had been anticipated, for numerous reasons. First, it was decided that a fiber content of 40 volume percent would be achieved in all material, in order to optimize properties. This is significantly higher than the 30 volume percent fiber present in the Phase I intermediate housing casting, and the tighter fiber packing makes metal infiltration more difficult. In order to improve infiltration, it is desirable to retard metal solidification, thereby allowing more time for penetration of the fiber groups. Solidification can usually be retarded by increasing the mold preheat temperature, the melt pouring temperature, or both. Unfortunately, when investment casting is used (as it was exclusively in this program) with magnesium, great caution must be exercised, because magnesium can react violently with the plaster of the investment mold; and higher temperatures promote this reaction. If one is fortunate, the reaction will only produce a roughened surface on the casting. Increasing degrees of reaction, however, can cause burning molten magnesium to be rejected upward from the mold sprue, volcano-like, while additional superheated magnesium breaches the mold walls, literally melts the supporting steel can, and pours uncontrolled onto the floor where it can be conclusively proven to have a corrosive effect on concrete!

The solution to this problem lies in carefully controlling the maximum mold and melt temperatures. Improved metal feeding through the fibers is then achieved only by decreasing the spacing of the ingates, which connect the various metal feeding runners to the casting cavity. Increasing the size of runners is also helpful. However, more ingates means more required machining of the casting, and more chances for fiber misalignment at these points because of the lack of restraint. Larger runners mean more metal must be poured for the same size casting, and more scrap generally results. It was found that the most difficult casting to produce was a long, thin plate, such as the

12 in. long x 0.080 in. thick plates cast for the fatigue samples. It is indeed ironic that, after all the effort expended on making and remaking these plates, the fatigue samples were changed to a 6-inch length, as previously described. Thicker castings were actually easier to make, for a given length and width, than thinner ones, probably because the incoming molten metal did not have to undergo such an abrupt directional change to fill the distances between the ingates.

In spite of the difficulties, the casting problems were eventually solved. Not only did violent reactions become rare, but the casting surfaces exhibited a reproducible and commendable 125 rms as cast finish. After all the required 0.080 in. thick test plates were produced, effort was directed at increasing the casting thickness. The goal was to cast a plate 1.28 in. thick, since this would exceed the maximum feeding thickness required in the rotor housing. This goal was successfully achieved; although the attempted casting thickness was increased in increments (0.240, 0.640, 0.960, and finally 1.28 in.), no problems were encountered. It must be emphasized, however, that this success was achieved only after the effects of the various casting parameters had been fully researched and understood during the lengthy production of the plates for the Task 1 test samples.

One of the original Task 4 objectives had been the development of suitable nondestructive evaluation (NDE) techniques for Gr/Mg castings. Indeed, appreciable effort was spent identifying and considering suitable methods, which included conventional radiography, ultrasonic scan, ultrasonic modulus, real-time microfocus radiography, and computerized tomography. Unfortunately, most of these methods rely on a comparison of the results with the results on a "standard" sample of the material. As discussed above, it required a great deal of development time, and many destructive tests performed under Task 1, before it was possible to define a standard for Gr/Mg castings. Even then, the problems of inspecting thicker sections or complex shapes had to await the successful casting of these variations before they could be addressed. By this time in the program, the more important objective was determined to be the casting of the rotor housing. It is still planned to evaluate this housing nondestructively by some basic techniques such as ultrasonic modulus determination and radiography. However, a more complete NDE technique development will have to be conducted in a future program, when the material development challenges are not as great. A description of any NDE tests employed on the rotor housing will be included in the final version of this report.

4.5 TASK 5: FABRICATION OF THE ROTARY ENGINE ROTOR HOUSING

The optimum fiber configuration for the rotor housing, as defined by the Task 2 results, was a balanced $0^{o}/\pm45^{o}/90^{o}$ layup. The fabrication approach employed started with isolating the various structural components of the housing (Figure 18) into regions with similar cross-sectional areas. The graphite fibers were coated with MCI's proprietary wettable coating, drum wound to the required width, treated with a fugitive binder, cut into appropriate lengths, flattened, and stacked in the proper orientation for each structural component. These components were then pressed and assembled, and the entire fiber group was given a final pressing to achieve the 40 volume percent packing density. Next, because the binder rigidized the fibers, this assembly was machined into the final rotor housing configuration. In effect, a graphite/organic composite rotor housing was produced (Figure 19).

The details of the metal feeding system for casting were designed, based on technology developed under Task 4. These details were added to the fiber preform in the form of wax strips, which is standard investment casting practice. The resulting waxed preform was invested (covered with plaster), and the wax and fugitive binder were removed as part of the mold baking process.

Two rotor housings were cast. The only structural difference between the two was that the first contained only $0^o/90^o$ orientation fibers, while the second contained the $\pm 45^o$ fibers as well. The results of these castings will be discussed in the final version of this report.

ILLUSTRATIONS

FIGURE 1

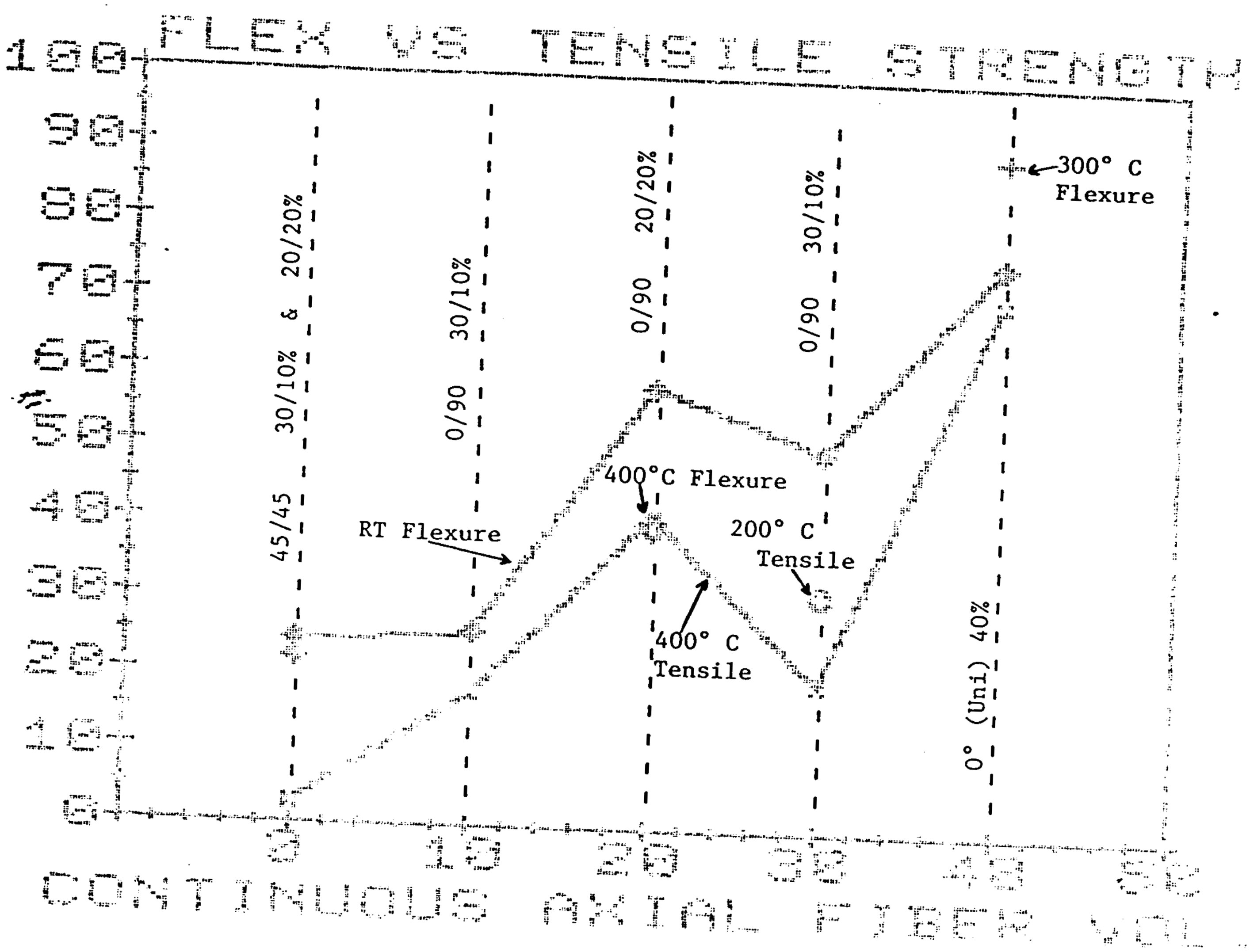

ORIGINAL PAGE IS
OF POOR QUALITY

FIGURE 2

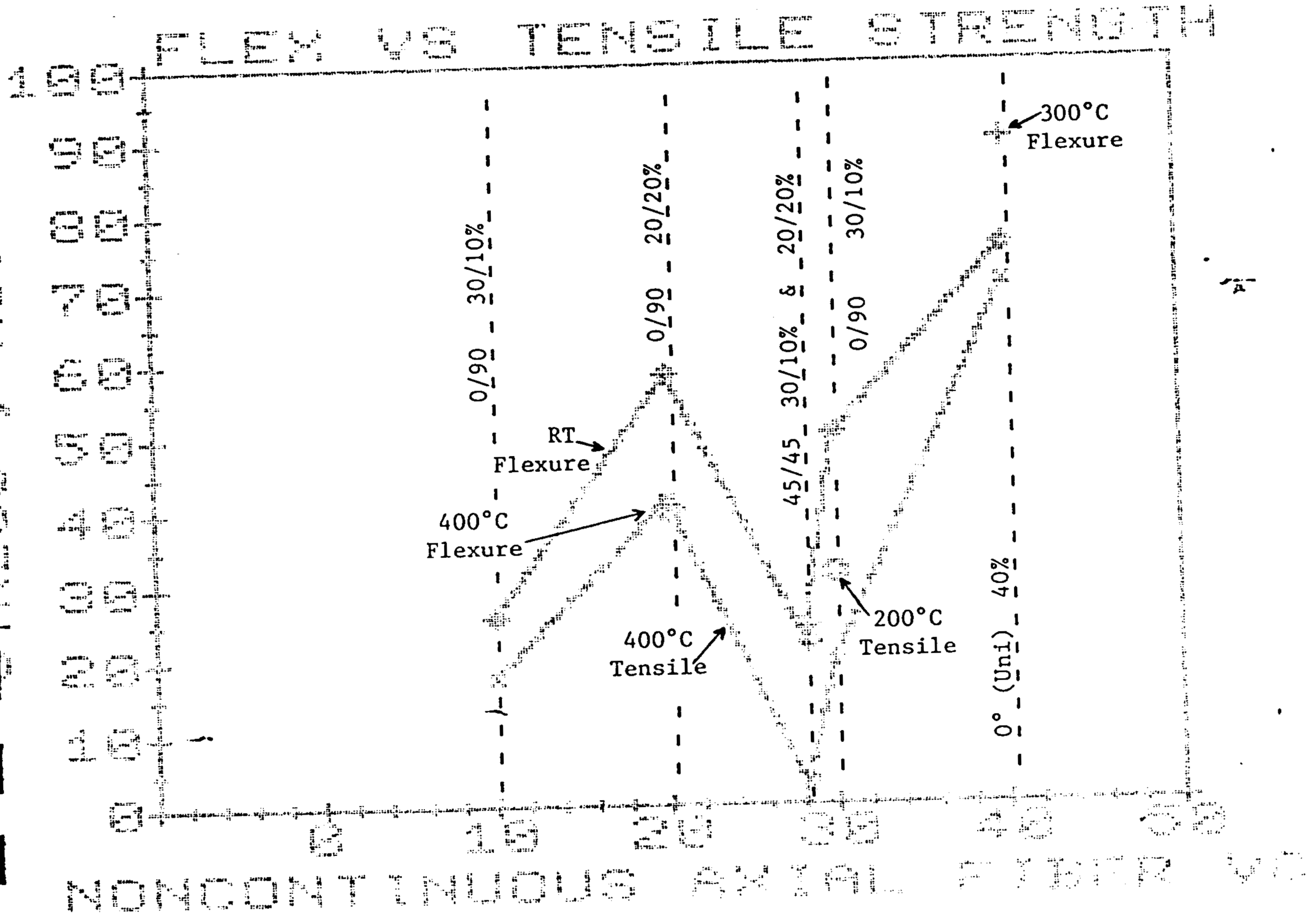

ORIGINAL PAGE IS
OF POOR QUALITY

FIGURE 3

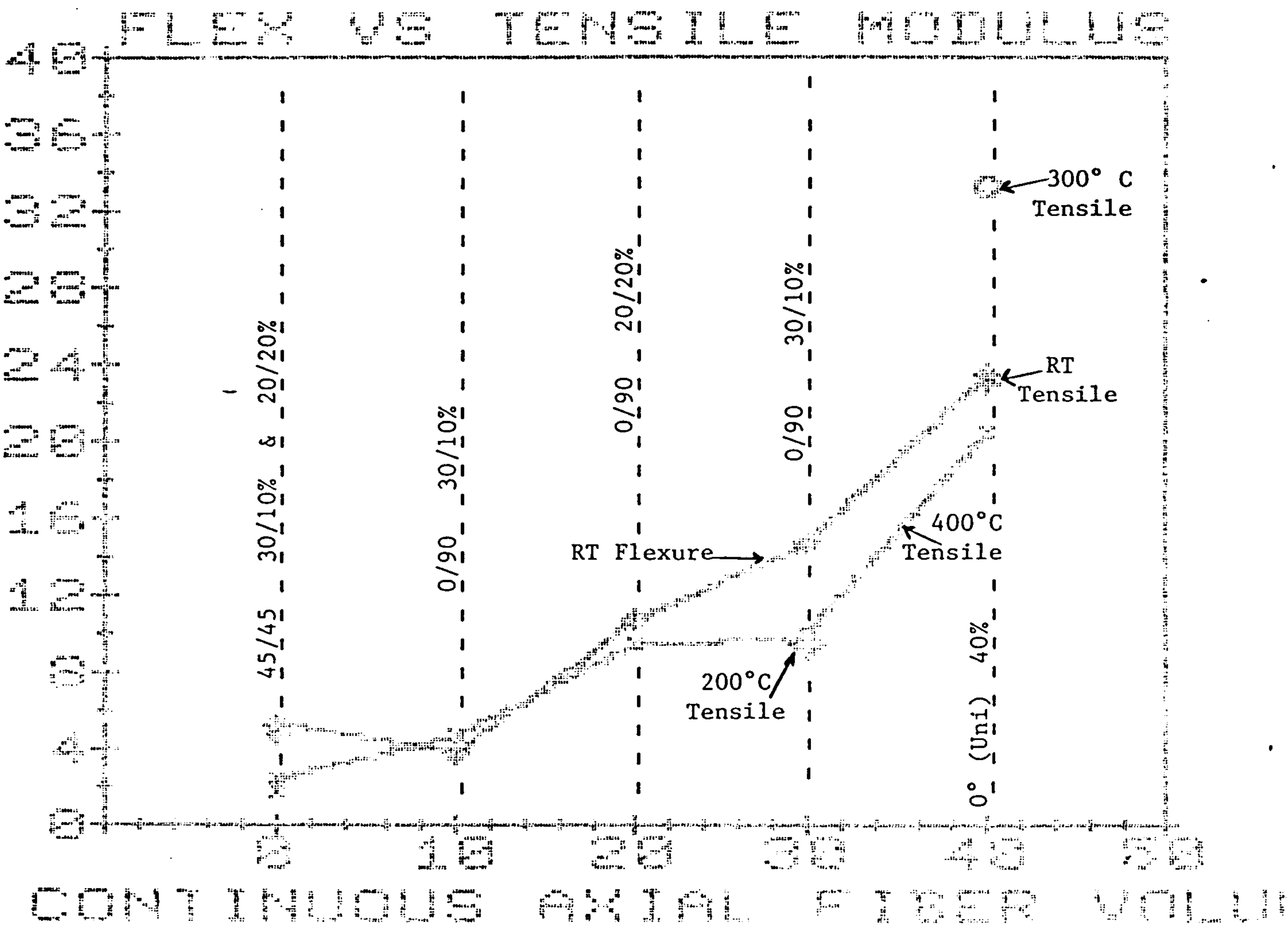

FLEX VS TENSILE MODULUS
45/45
30/10% & 20/20%
0/90 30/10%
0/90 20/20%
0/90 30/10%
0° (Uni) 40%
300° C Tensile
RT Tensile
400°C Tensile
RT Flexure
200°C Tensile
0
10
20
30
40
50
CONTINUOUS AXIAL FIBER VOLU

FIGURE 4

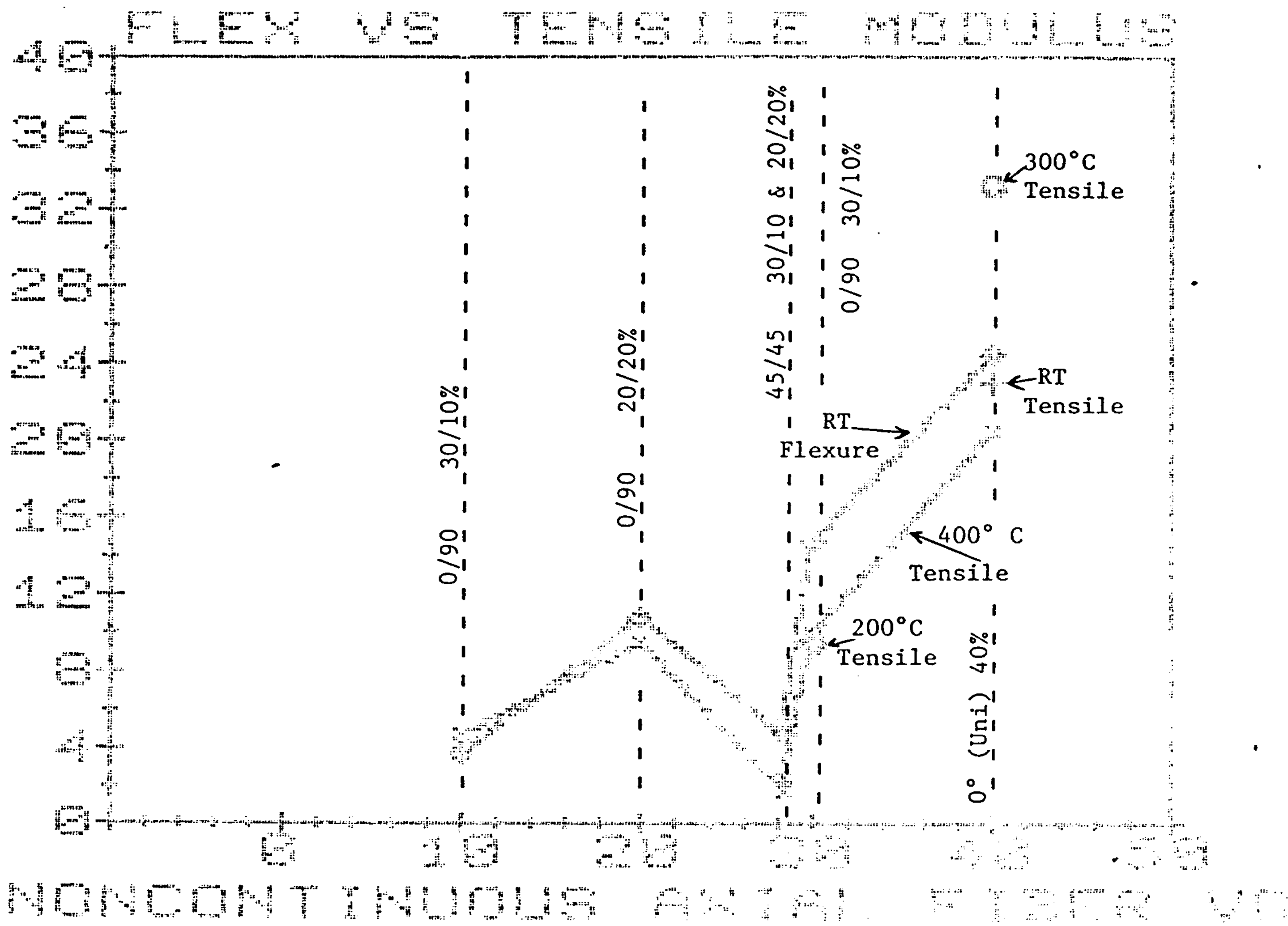

FLEX VS TENSILE MODULUS
NONCONTINUOUS
0/90 30/10%
0/90 20/20%
45/45 30/10 & 20/20%
0/90 30/10%
0° (Uni) 40%
300°C Tensile
RT Tensile
RT Flexure
400° C Tensile
200°C Tensile

FIGURE 5

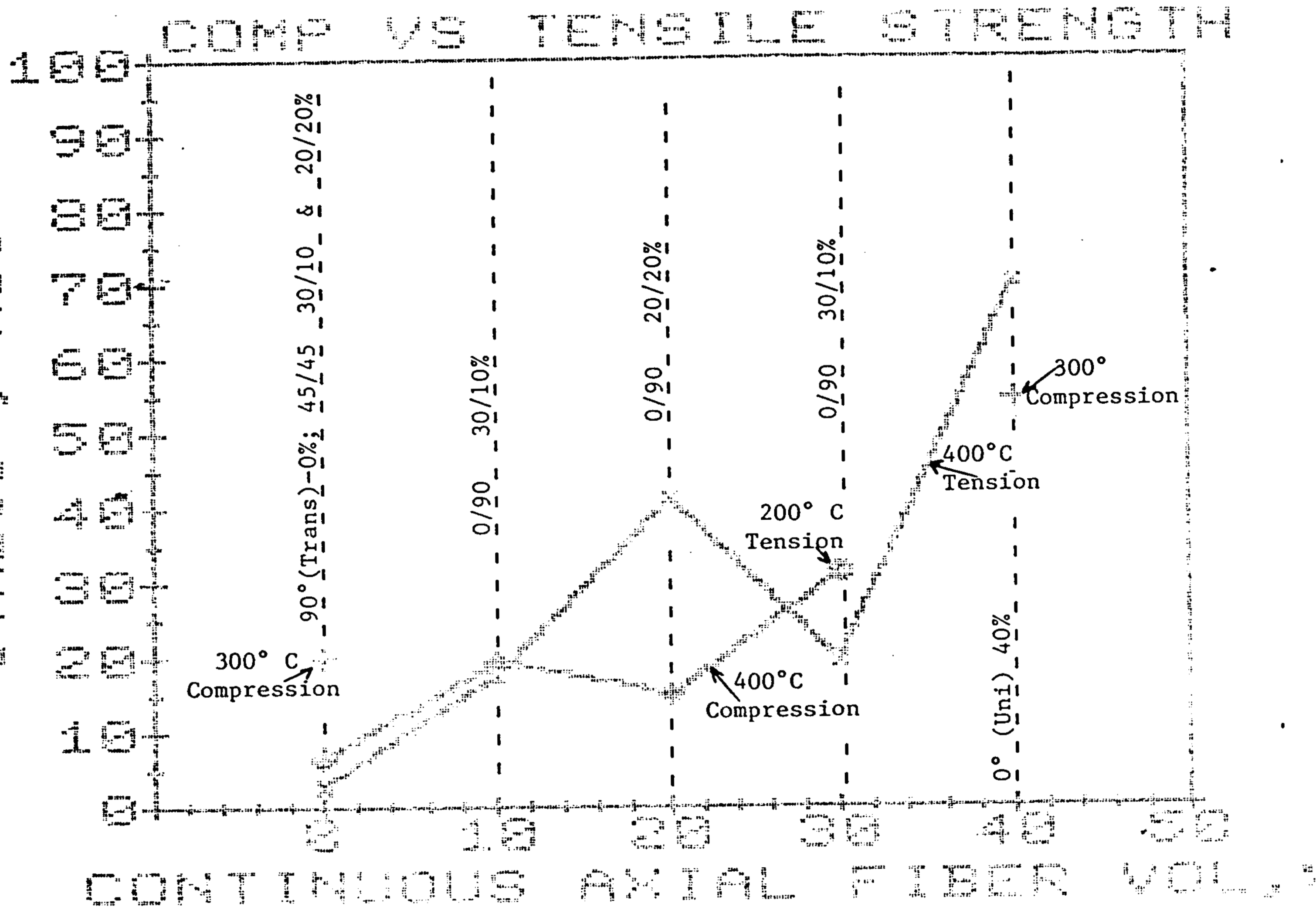

ORIGINAL PAGE IS OF POOR QUALITY

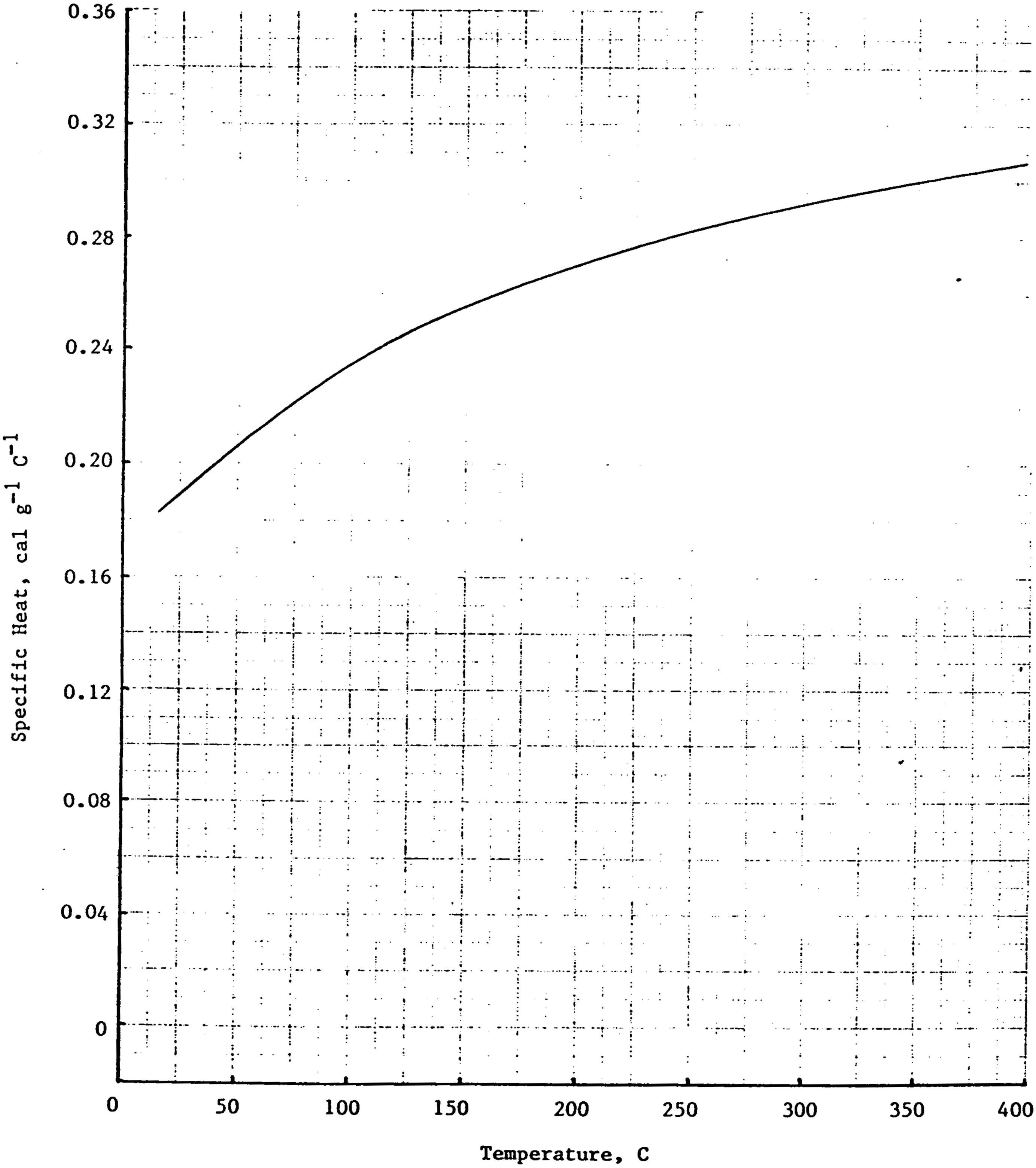

FIGURE 6. Specific Heat of P55/AZ 91C

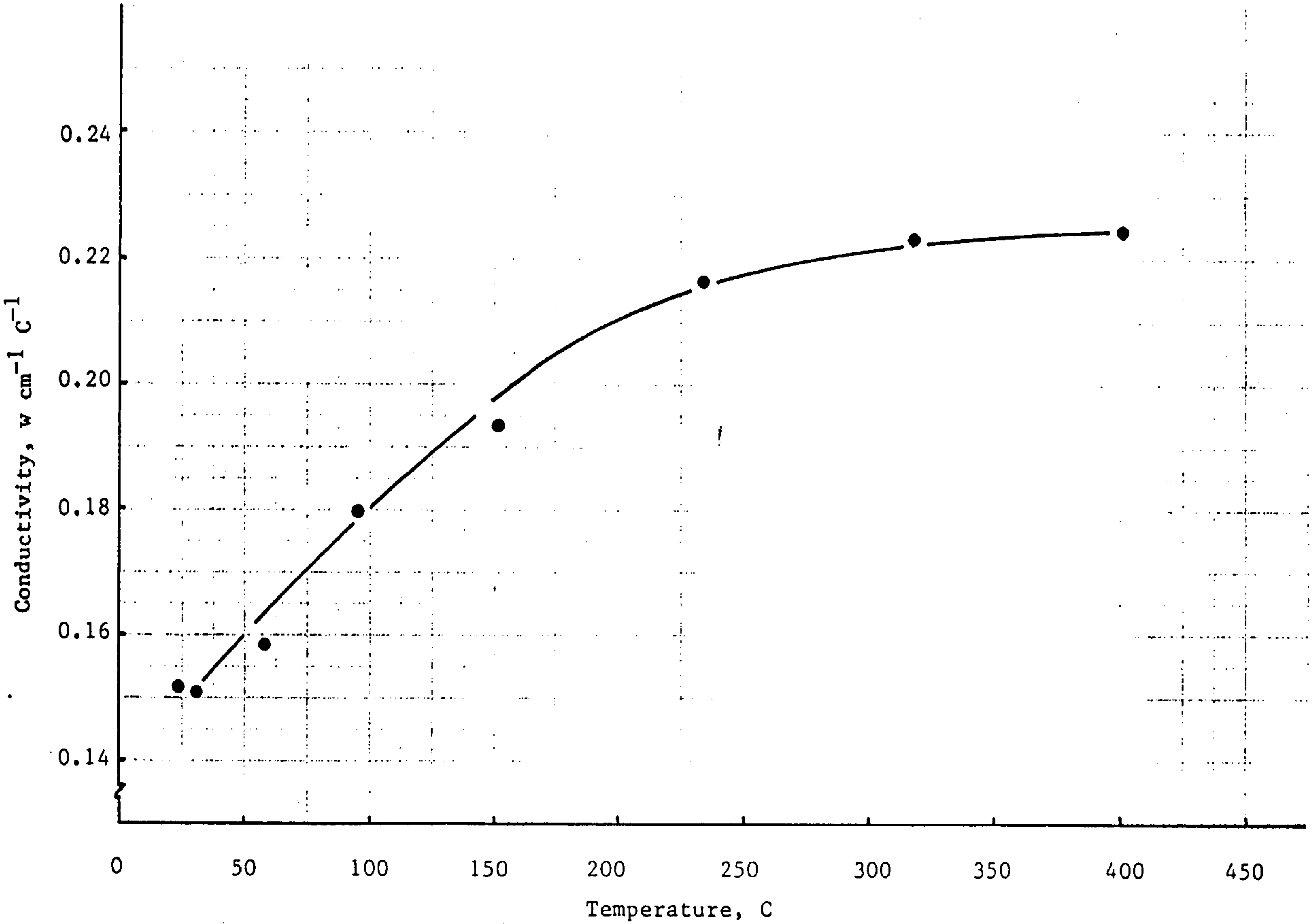

FIGURE 7. THERMAL CONDUCTIVITY OF P55/AZ91C, $0^{o}/90^{o}$, 20%/20%, TESTED IN Z DIRECTION

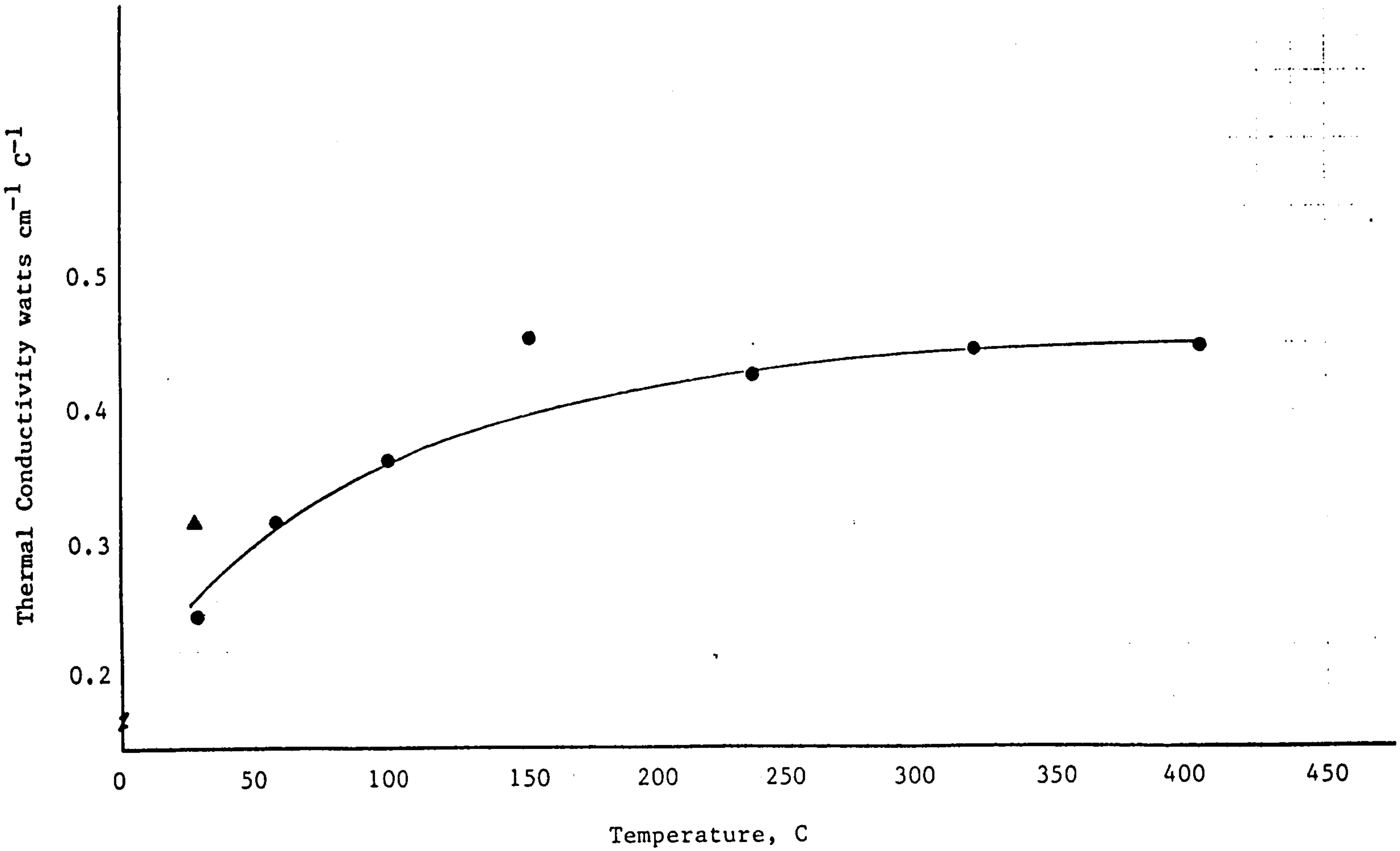

FIGURE 8: Thermal Conductivity of P55/A291 30/10 Vol % +45°/-45°

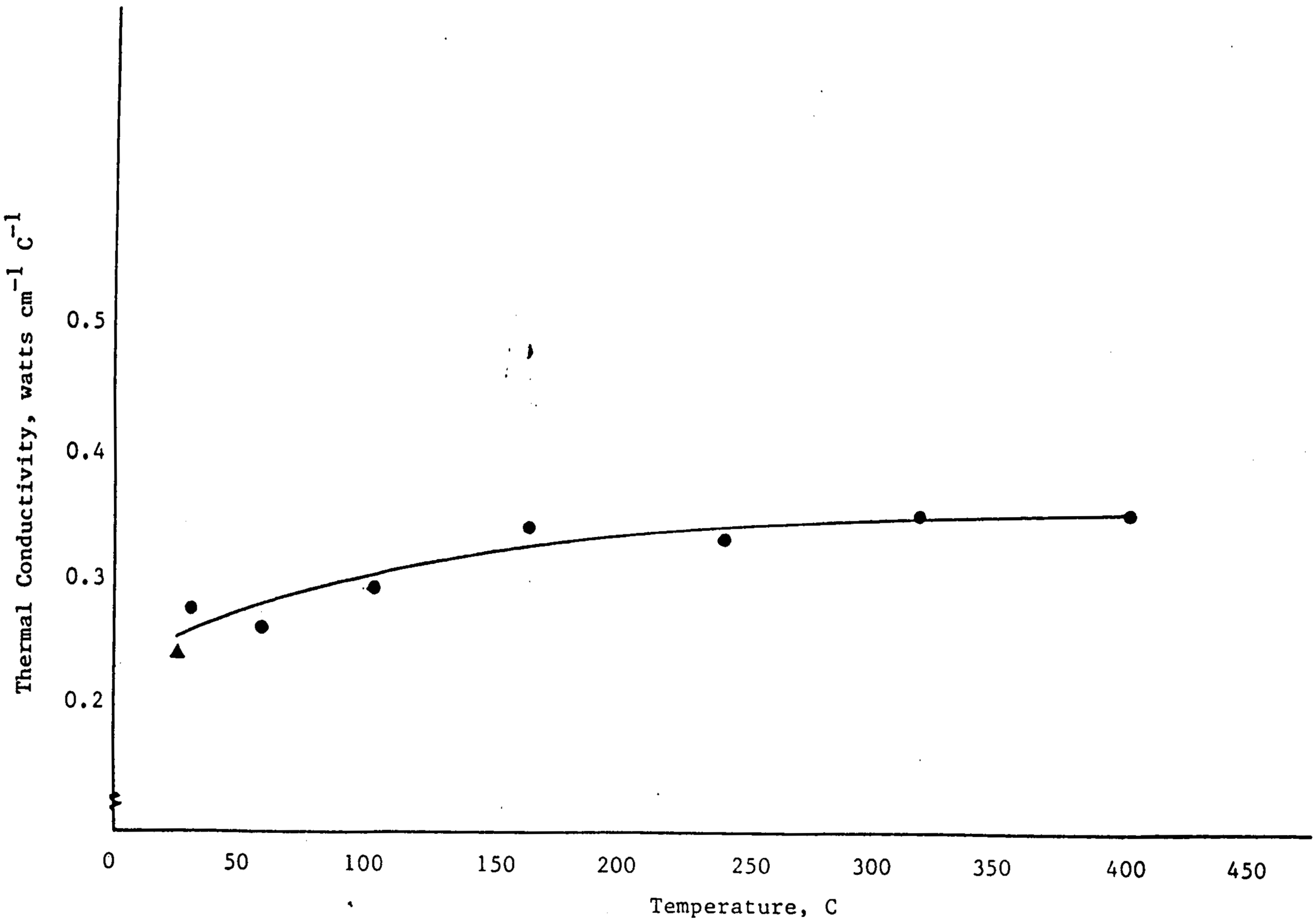

FIGURE 9. Thermal Conductivity of P55/A291 20/20 Vol % 0/90, 0° Test Direction

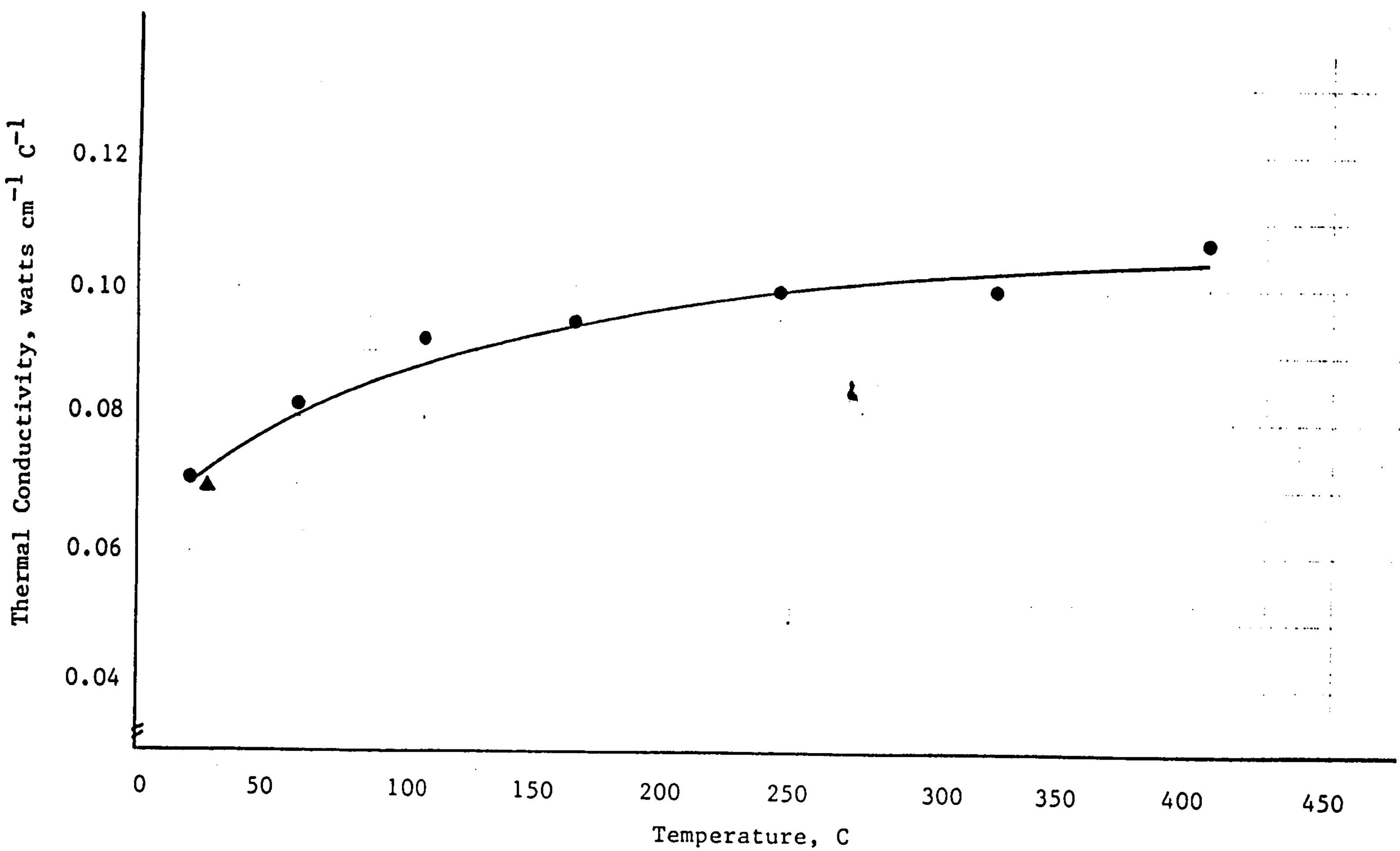

FIGURE 10. Thermal Conductivity of P55/A291, Unidirectional 40 v/o 90° Test Direction

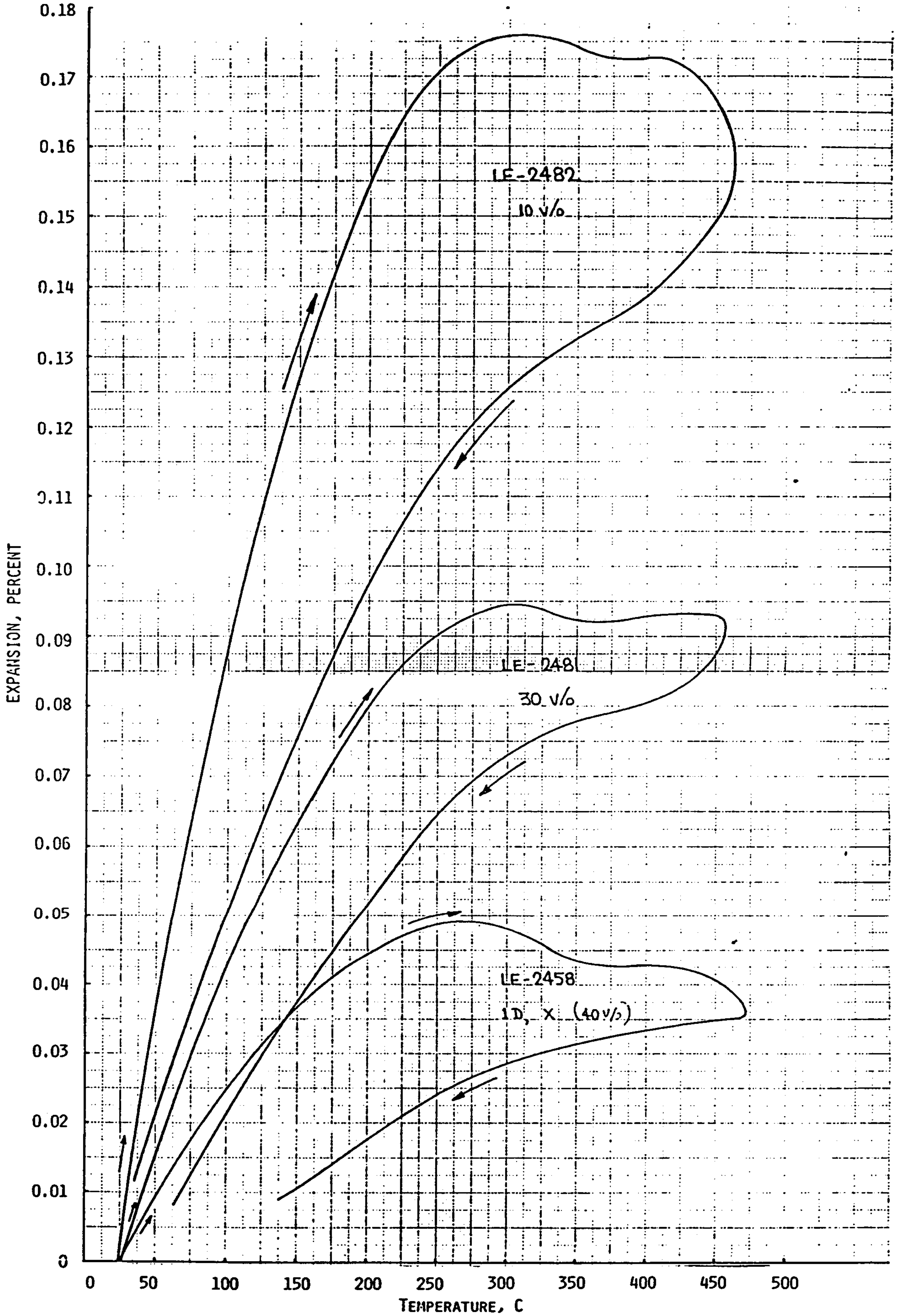

FIGURE 11. THERMAL EXPANSION OF P55/AZ 91 C

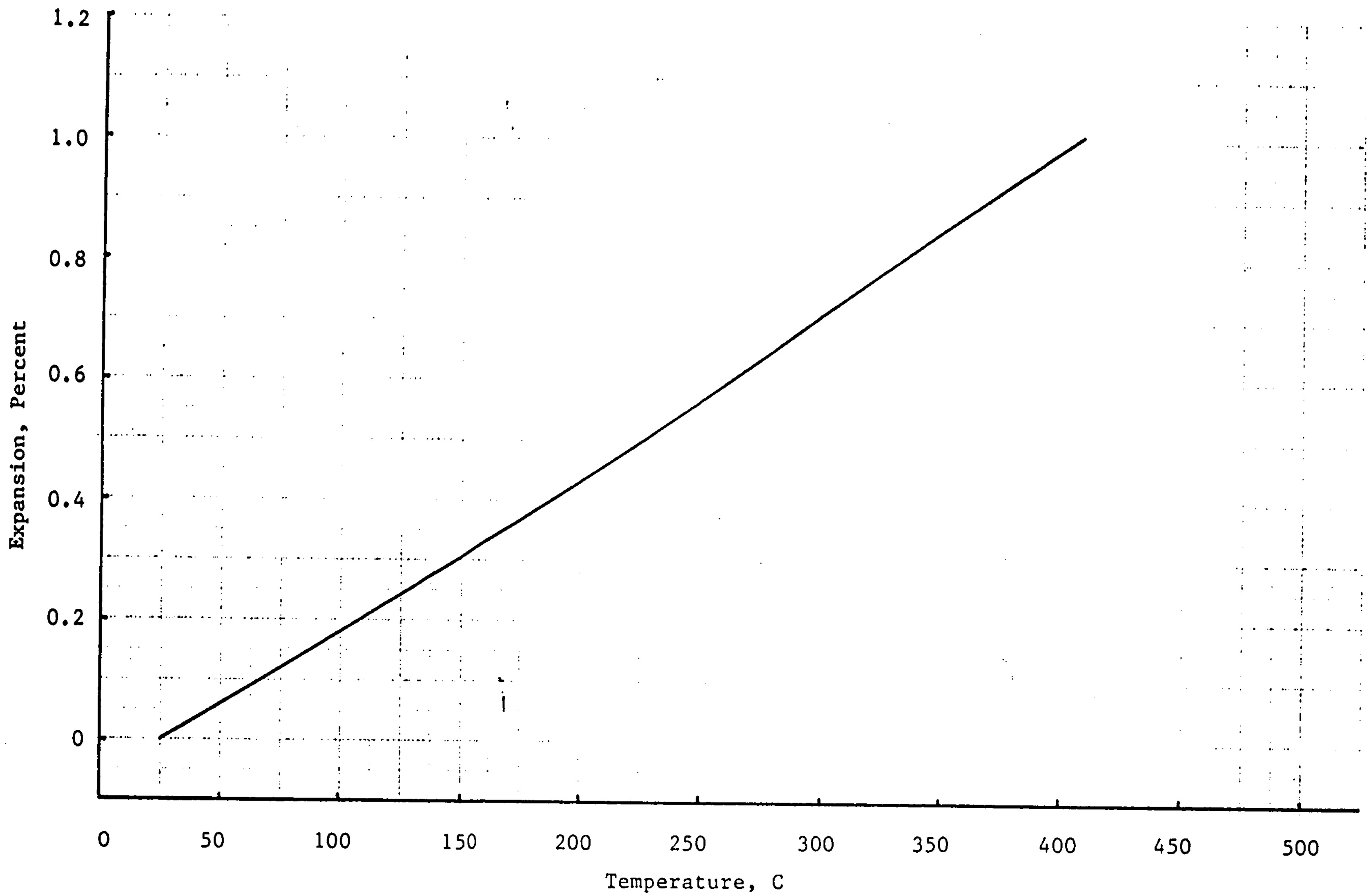

FIGURE 12. Thermal Expansion of P55/AZ 91C Y (90°)

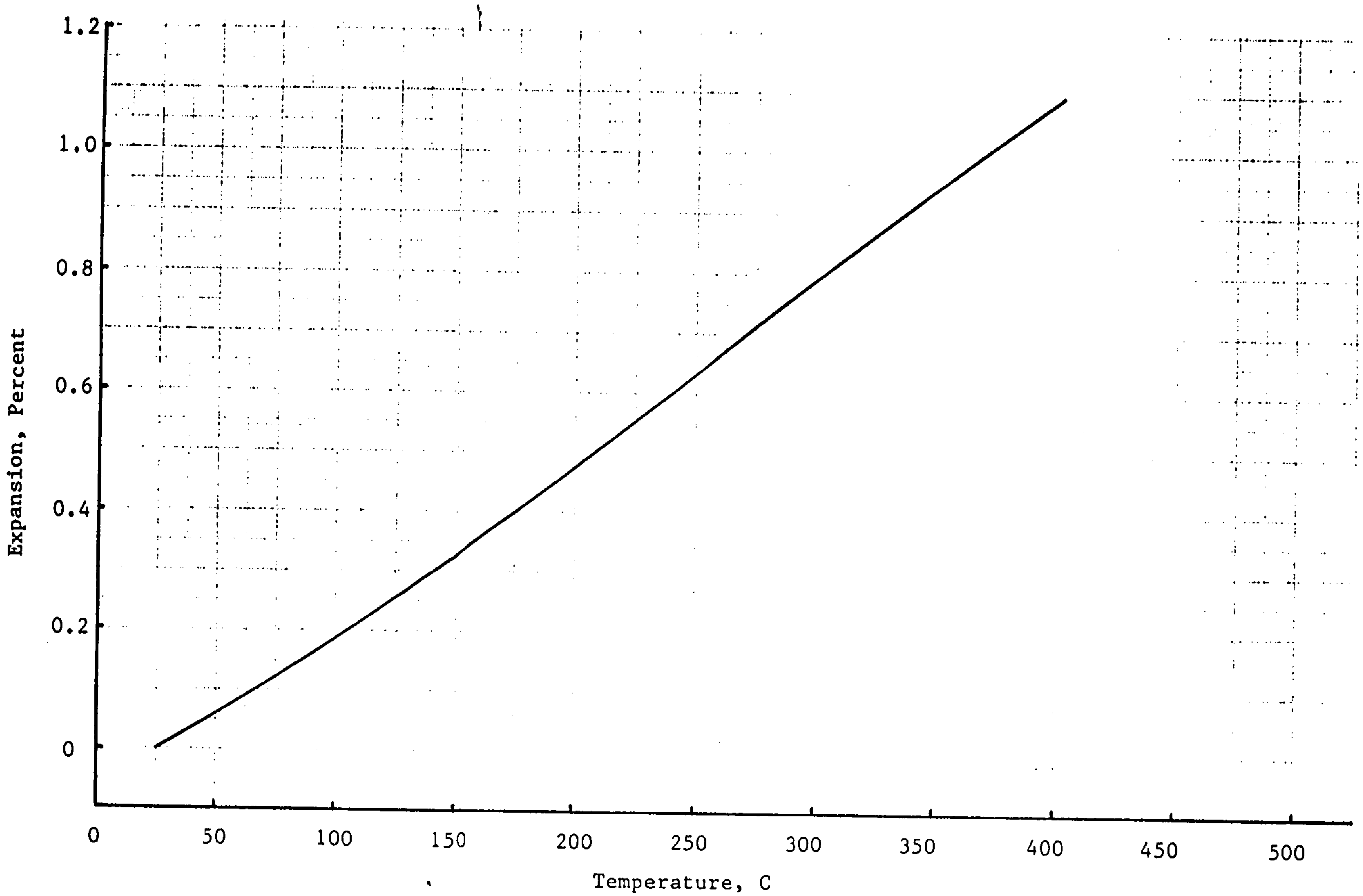

FIGURE 13. Thermal Expansion of P55/AZ 91 C Z (Thickness)

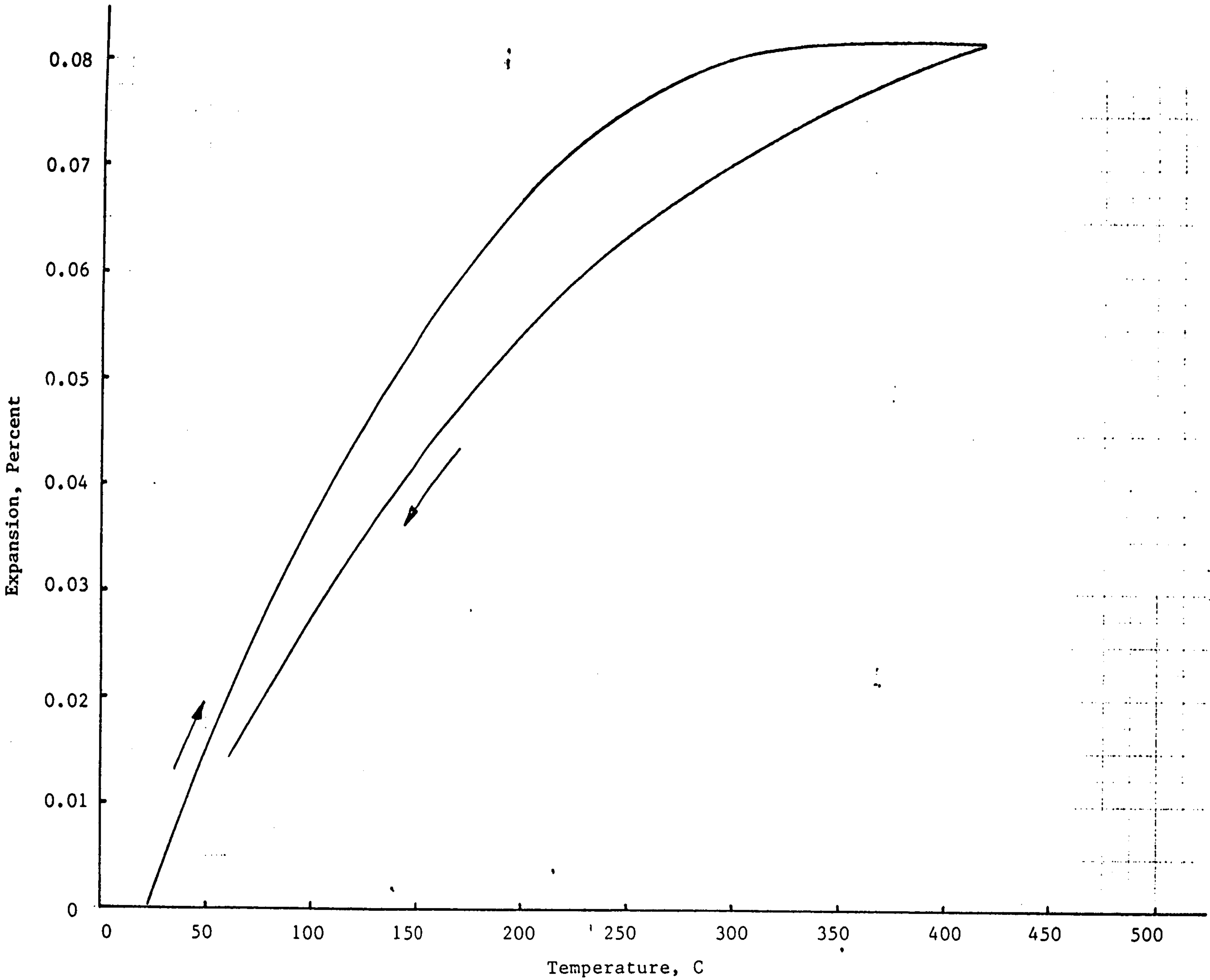

FIGURE 14. Thermal Expansion of P55/AZ 291 C 0°/90°

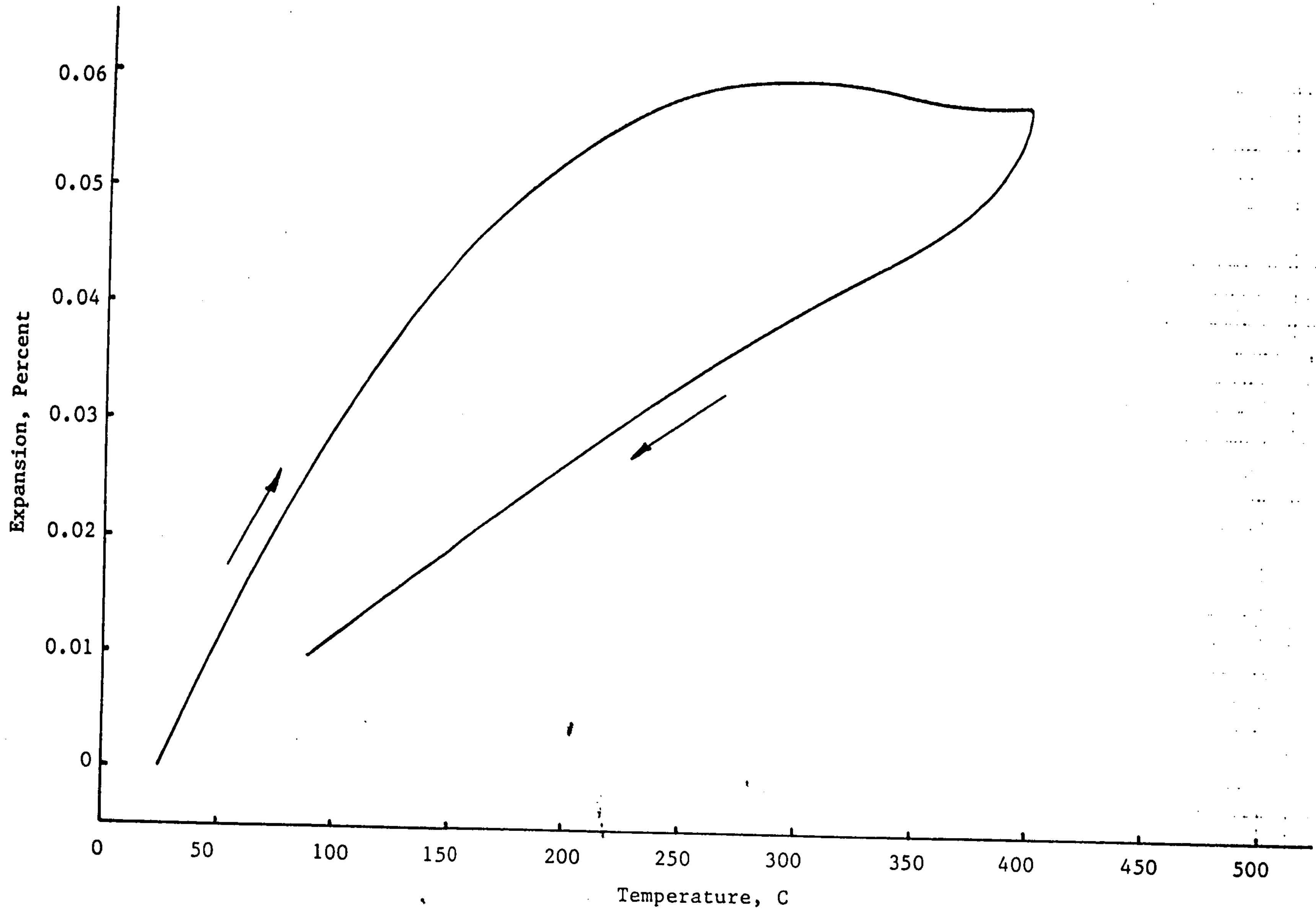

FIGURE 15. Thermal Expansion of P55/AZ 291 C +45°/-45°

CENTER COORDINATES FOR 0.500" TOOL
(ONE QUARTER SEGMENT)

± X, in.	Y, in.
0.000	0.266
0.250	0.266
0.375	0.266
0.500	0.267
0.750	0.270
1.000	0.274
1.250	0.281
1.500	0.293
1.704	0.305
1.895	0.320
2.097	0.337
2.313	0.357
2.545	0.378
2.796	0.400
3.065	0.423
3.350	0.442
3.648	0.459
3.956	0.472
4.272	0.483
4.500	0.488
4.750	0.494
5.000	0.497
5.250	0.499
5.500	0.500
5.750	0.500
6.000	0.500

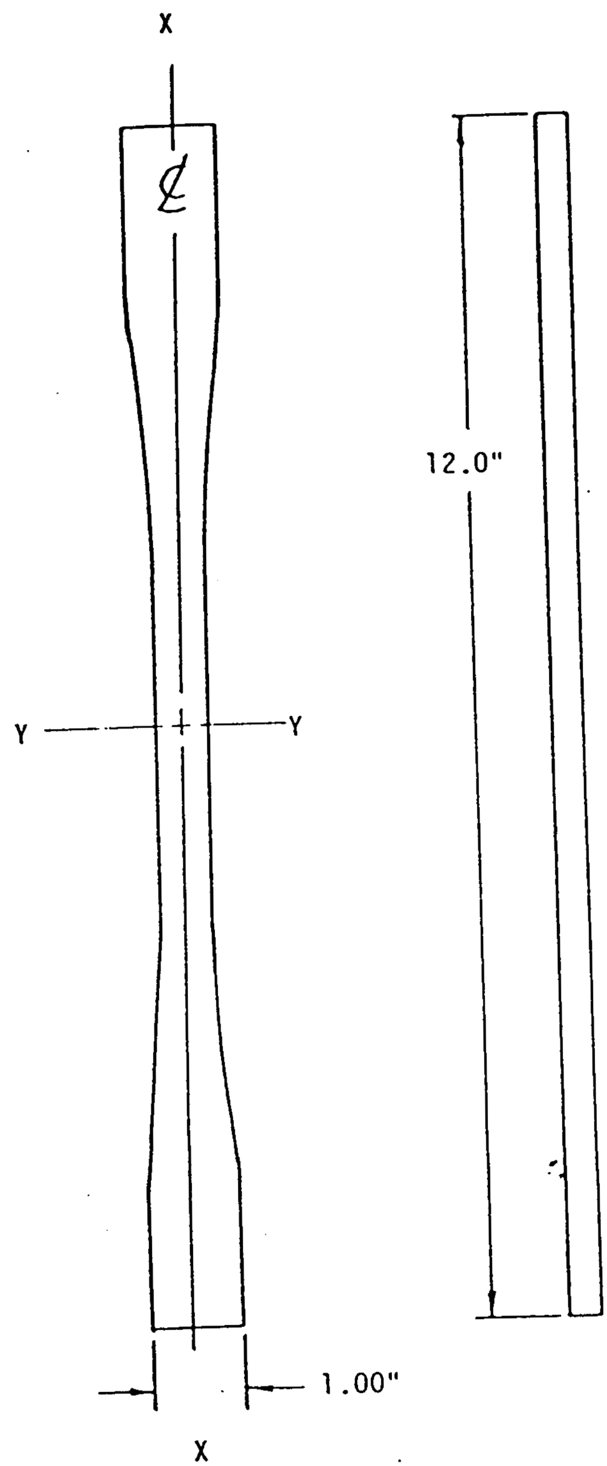

FIGURE 16. ORIGINAL FATIGUE SPECIMEN CONFIGURATION
("AMMRC Streamline Specimen")

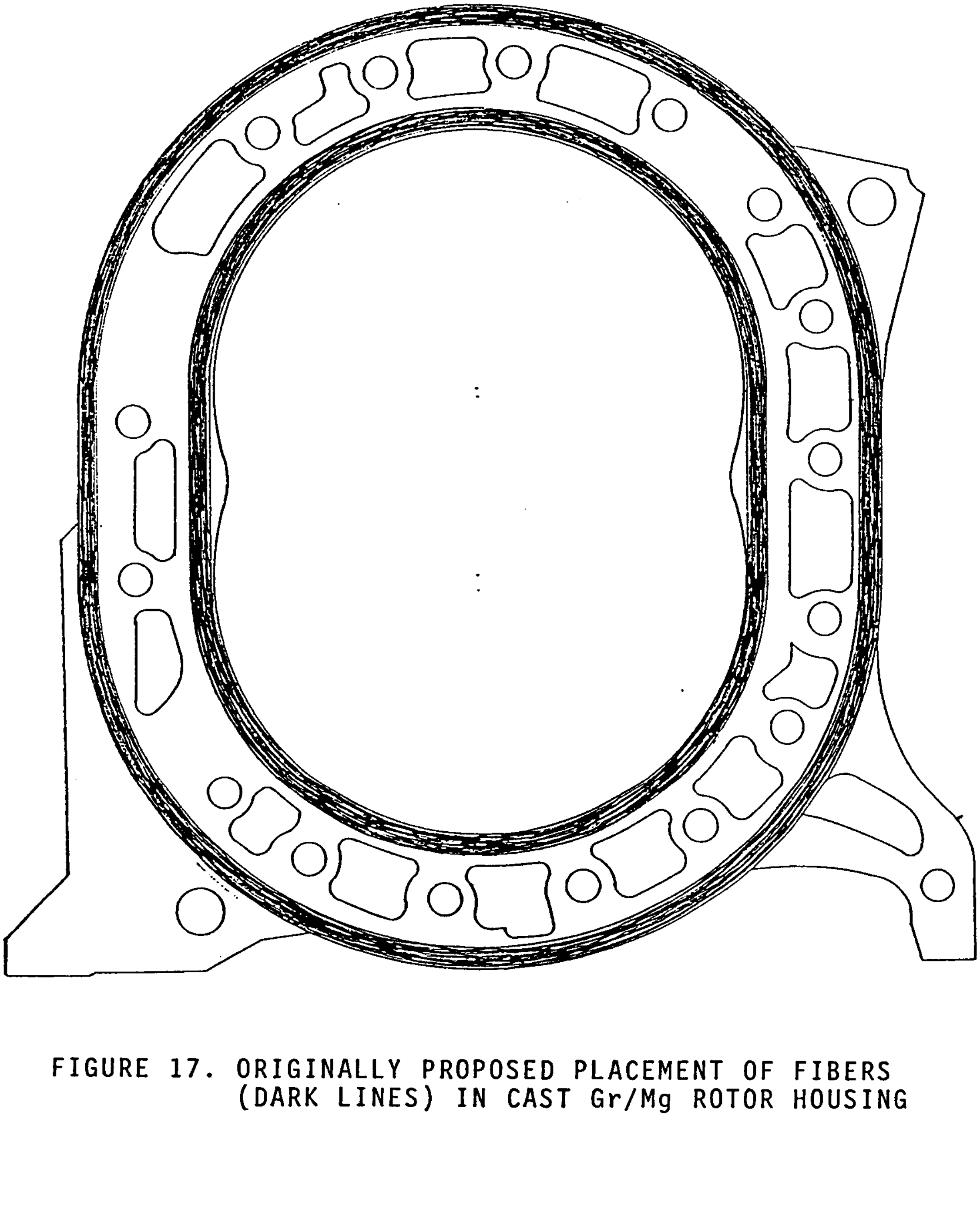

FIGURE 17. ORIGINALLY PROPOSED PLACEMENT OF FIBERS (DARK LINES) IN CAST Gr/Mg ROTOR HOUSING

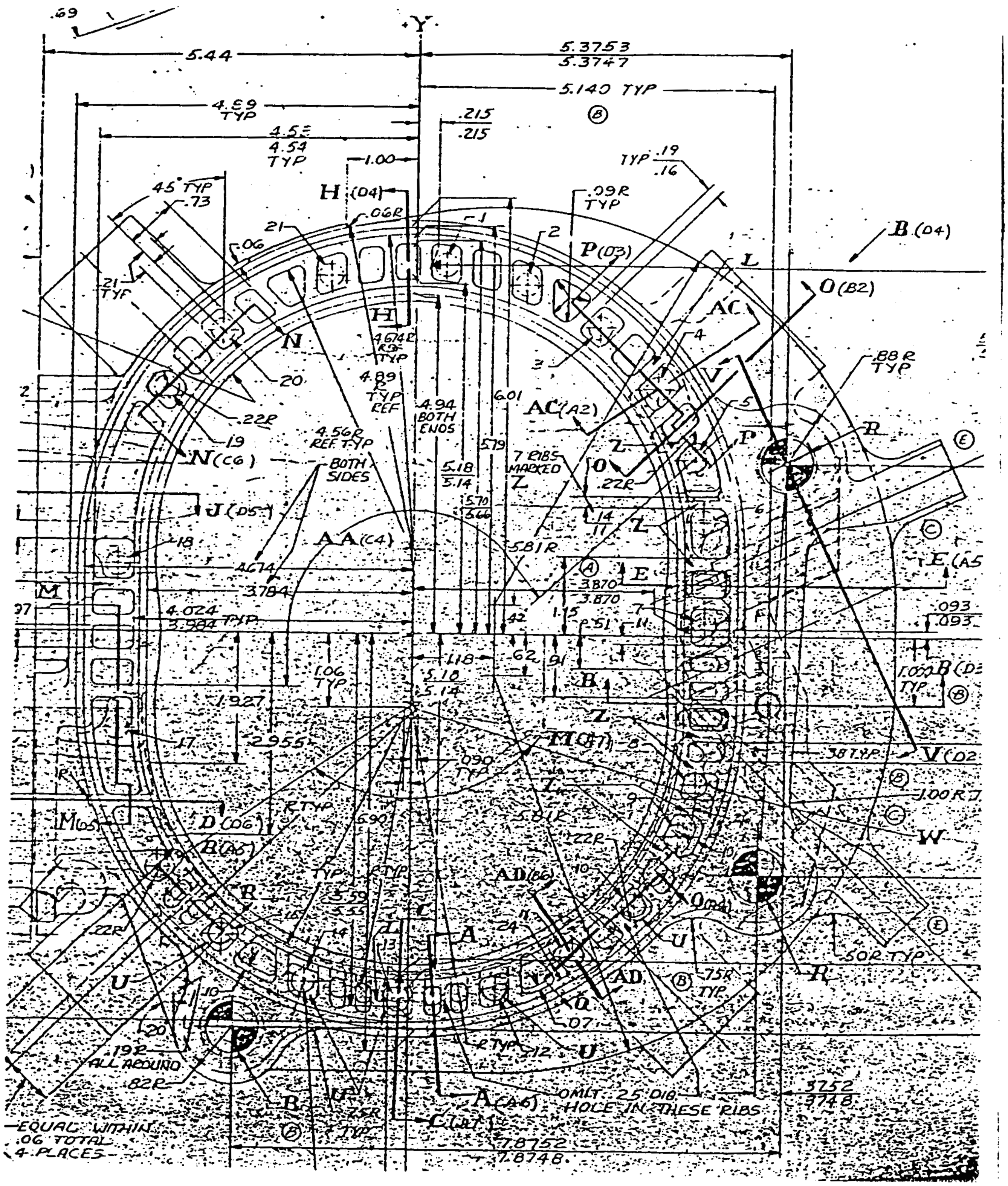

FIGURE 18. ENGINEERING DRAWING OF ROTOR HOUSING

FIGURE 19. ROTOR HOUSING FIBER PREFORM

TABLES

TABLE 1

MEASURED AVERAGE MECHANICAL PROPERTIES OF P55/AZ91 Gr/Mg CASTINGS

Fiber Content (Vol %)				Test			Ultimate Strength (KSI)	Modulus (MSI)
0°	$+45^\circ$	-45°	90°	Type	Direction	Temp ($^\circ$F)		
40	--	--	--	Tension	0°	RT	68.3	21.8
					90°	RT	3.9	3.4
					0°	750	69.4	20.3
				Compression	0°	RT	69.7	17.0
					90°	RT	36.7	2.5
					0°	575	53.8	*
					90°	575	19.5	*
				Flexure	0°	RT	75.0	24.3
					0°	575	89.1	*
30	--	--	10	Tension	0°	RT	35.7	16.8
					90°	RT	15.0	5.6
					0°	750	21.8	10.0
					90°	750	17.0	4.7
				Compression	0°	RT	47.3	15.7
					90°	RT	33.4	4.8
					0°	750	30.9	*
					90°	750	19.0	*
				Flexure	0°	RT	49.8	14.6
					90°	RT	25.1	3.7
20	--	--	20	Tension	0°	RT	34.9	12.8
					0°	750	40.8	9.3
				Compression	0°	RT	43.1	9.4
					0°	750	14.6	*
				Flexure	0°	RT	58.1	10.6
					0°	750	39.6	*
--	30	10	--	Tension	0°	RT	9.2	4.6
					0°	750	2.3	1.7
				Compression	0°	RT	15.4	3.9
					0°	750	6.7	*
				Flexure	0°	RT	21.4	4.5
--	20	20	--	Tension	0°	RT	11.4	4.3
					0°	750	2.6	2.4
				Compression	0°	RT	16.7	5.0
					0°	750	6.0	*
				Flexure	0°	RT	24.3	5.2

NOTES: 1. Tensile Specification — ASTM D 3552-77(A82)
2. Compressive Specification — ASTM D 3410-75
3. Flexure Specification — ASTM D 790-82

* Elevated Temperature Properties Unavailable

TABLE 2. DELETED MECHANICAL TESTS AND THEIR JUSTIFICATIONS

Deleted Tests	Justification
1. 40% in 0^{o} direction, 90^{o} test, 750^{o}F tensile	1. Property too poor to measure
2. 40% in 0^{o} direction, 90^{o} test, RT & 750^{o}F flexure	2. See Justification #1
3. 0/90, 30%/10%, 0 and 90^{o} 750^{o}F flexure	3. MSC indicated high temp. flexure data not needed for design
4. 0/90, 20%/20%, all 90^{o} tests	4. Should be equivalent to 0^{o} properties (confirmed by a few tests)
5. $\pm 45^{o}$, 30%/10% and 20%/20%, all 90^{o} tests	5. See Justification #4
6. $\pm 45^{o}$, 30%/10% and 20%/20%, 750^{o}F flexure	6. See Justification #3

TABLE 3

THERMAL EXPANSION DATA
FOR Gr/Mg CASTINGS
(P55/AZ91C)

% Fiber in Test Direction	Temp. Range, °F	CTE, PPM/°F	Thermal Expansion, %
40	RT to 400	1.3	0.04
	400 to 750	0.0	0.00
	RT to 750 (av.)	0.6	0.04
30	RT to 400	2.5	0.08
	400 to 750	0.4	0.01
	RT to 750 (av.)	1.4	0.09
10	RT to 400	4.9	0.15
	400 to 750	0.5	0.02
	RT to 750 (av.)	2.6	0.17
0	RT to 750 (av.)	14.4	0.97
Aluminum (Calculated)	RT to 400	13	0.41
	RT to 750		0.88
Steel (Calculated)	RT to 400	7	0.22
	RT to 750		0.47

APPENDIX

MSC®

ANALYTICAL SUPPORT FOR THE FABRICATION OF GRAPHITE/MAGNESIUM ROTOR HOUSING

PREPARED FOR:

MATERIALS CONCEPTS, INC.

UNDER PURCHASE ORDER NO. C12142

MARCH, 1987

Materials' Sciences Corporation

OBJECTIVES

- MATERIAL DATA CORRELATIONS FOR P55/MG COMPOSITES
- SIMPLIFIED THERMAL ANALYSES TO OBTAIN ESTIMATES OF ROTOR HOUSING TEMPERATURES
- TWO-DIMENSIONAL STRESS ANALYSES UNDER TEMPERTURE AND PRESSURE LOADS TO ASSESS HOUSING STRUCTURAL INTEGRITY

APPROACH

- DATA CORRELATION STUDIES WERE CARRIED OUT IN ORDER TO ESTABLISH CONSISTENT SET OF PROPERTIES FOR STRESS ANALYSES
  - TEST PROGRAM WAS CONDUCTED BY MCI ON VARIOUS P55/MG COMPOSITES AT RT AND ELEVATED TEMPERATURES

- SIMPLIFIED ONE DIMENSIONAL HEAT TRANSFER ANALYSES WERE DONE FOR VARIOUS CRANK ANGLES IN ORDER TO OBTAIN ESTIMATES OF HOUSING WALL TEMPERATURES
  - AVAILABLE INFORMATION ON BASELINE ALUMINUM DESIGN WAS USED AS A GUIDELINE

- TWO DIMENSIONAL FINITE ELEMENT ANALYSES OF THE ROTOR HOUSING WERE DONE FOR INTERNAL PRESURE AND TEMPERATURE LOADS
  - TWO DIFFERENT P55/MG CONFIGURATIONS WERE ANALYZED AND COMPARED TO THE BASELINE ALUMINUM DESIGN
  - MATERIAL ALLOWABLE STRENGTHS DETERMINED FROM TEST PROGRAM WERE USED TO ASSESS HOUSING STRUCTURAL INTEGRITY

MATERIAL DATA CORRELATIONS

- FOR IMPROVED UNDERSTANDING OF MATERIAL BEHAVIOR AT ROOM TEMPERATURE AND ELEVATED TEMPERATURES

- TO PROVIDE CONSISTENT SET OF INPUT PROPERTIES FOR FINITE ELEMENT AND THERMAL ANALYSES

DETAILS OF STATIC TEST PROGRAM

- ROOM TEMPERATURE AND ELEVATED TEMPERATURE TESTS (575°F OR 750°F)
- MATERIAL ORIENTATIONS
  - 0°
  - $0^\circ/90^\circ$
  - $0^\circ_3/90^\circ$
  - $\pm 45^\circ$
  - $\pm 45^\circ_3/-45^\circ$
- IN-PLANE TENSILE AND COMPRESSIVE MODULI AND STRENGTHS
- LIMITED THERMAL EXPANSION AND THERMAL CONDUCTIVITY TESTS

RESULTS OF RT DATA CORRELATIONS

- CORRELATION STUDIES INDICATED MATRIX IS IN YIELDED CONDITION AND EXHIBITS REDUCED MODULUS DUE TO PROCESSING STRESSES
  - RESIDUAL STRESSES ALSO AFFECT EFFECTIVE MATRIX TENSILE AND COMPRESSIVE STRENGTHS
- IN GENERAL, THE RESULTS ARE IN GOOD AGREEMENT
  - FAIRLY LARGE DATA SCATTER EXISTS FOR COMPRESSION SAMPLES
  - PREDICTED AND MEASURED VALUES DIFFER QUITE SIGNIFICANTLY FOR SOME COMPRESSION TESTS
- THERMAL EXPANSION TEST DATA WERE AVAILABLE ONLY FOR UNIDIRECTIONAL COMPOSITES AND HENCE WERE USED AS THE BASIS FOR COMPUTING THERMAL EXPANSION COEFFICIENTS FOR OTHER LAMINATES

ALUMINUM HOUSING UNDER TEMPERATURE AND PRESSURE LOADS

SIGY

MAX: 29.8
MIN: -24.8

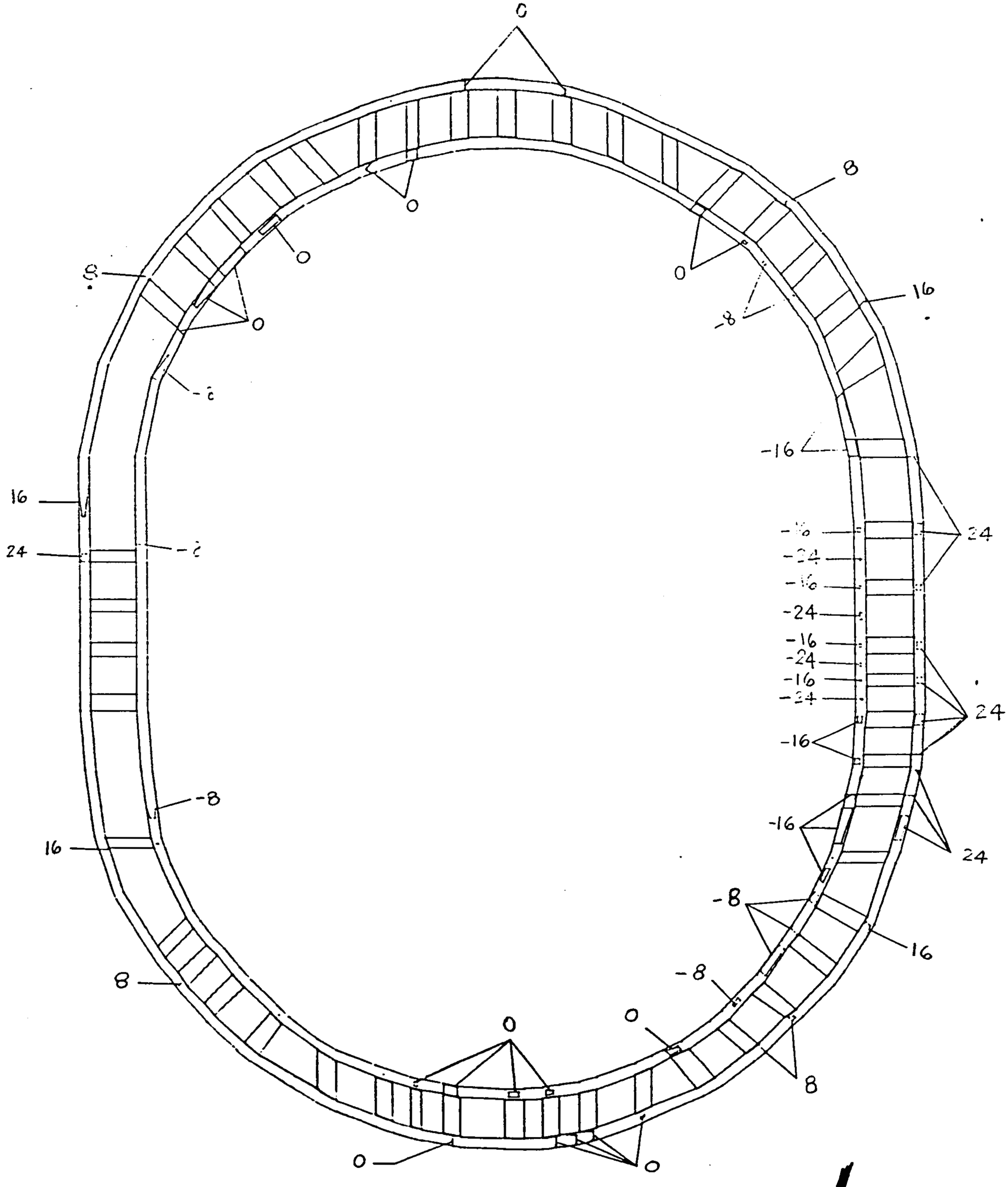

Note: Stresses are in ksi

ALUMINUM HOUSING UNDER TEMPERATURE AND PRESSURE LOADS

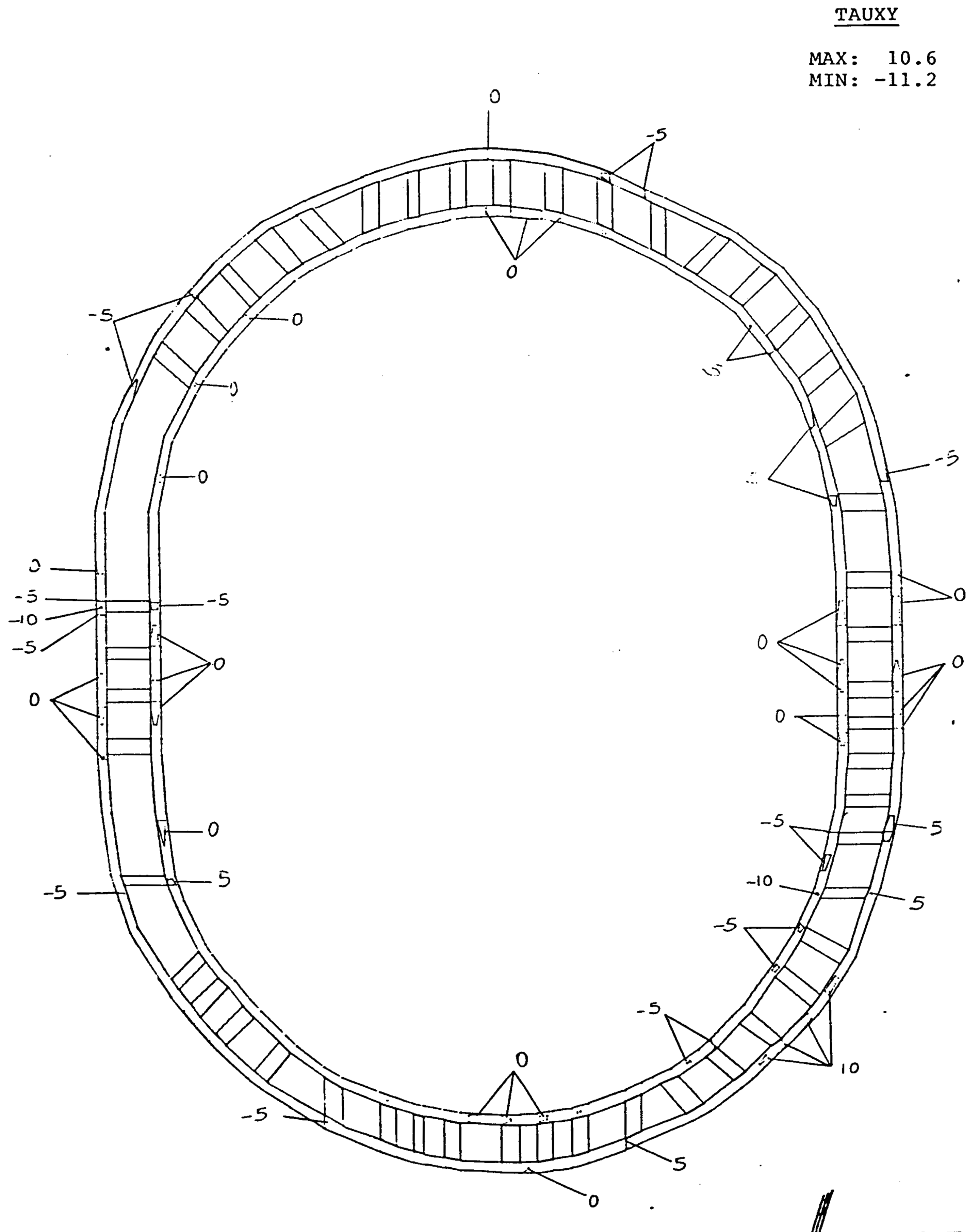

Note: Stresses are in ksi

0/90 P55/MG HOUSING UNDER PRESSURE LOADS ONLY

SIGX

MAX: 6.2
MIN: -9.3

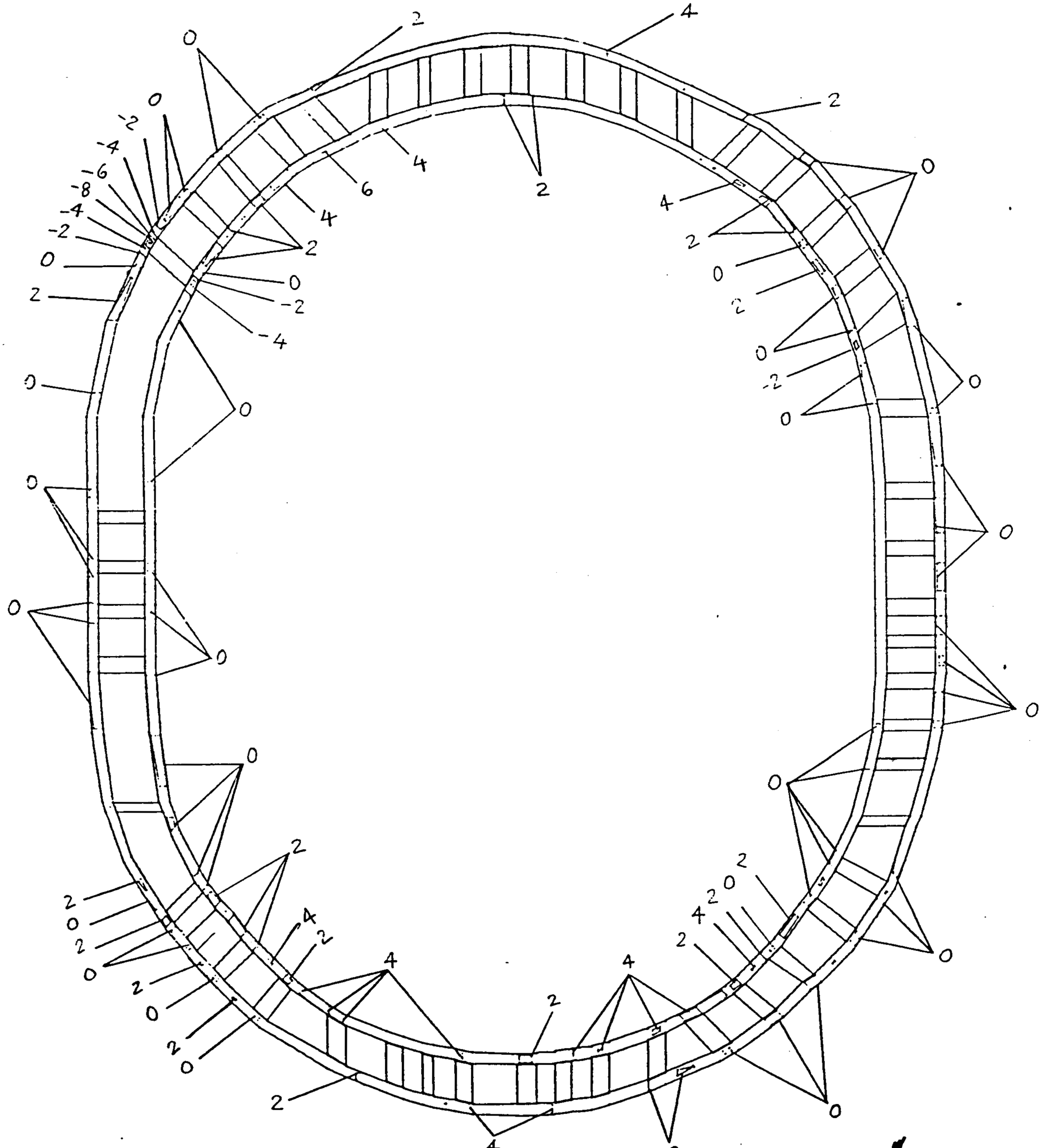

5

Note: Stresses are in ksi

0/90 P55/MG HOUSING UNDER PRESSURE LOADS ONLY

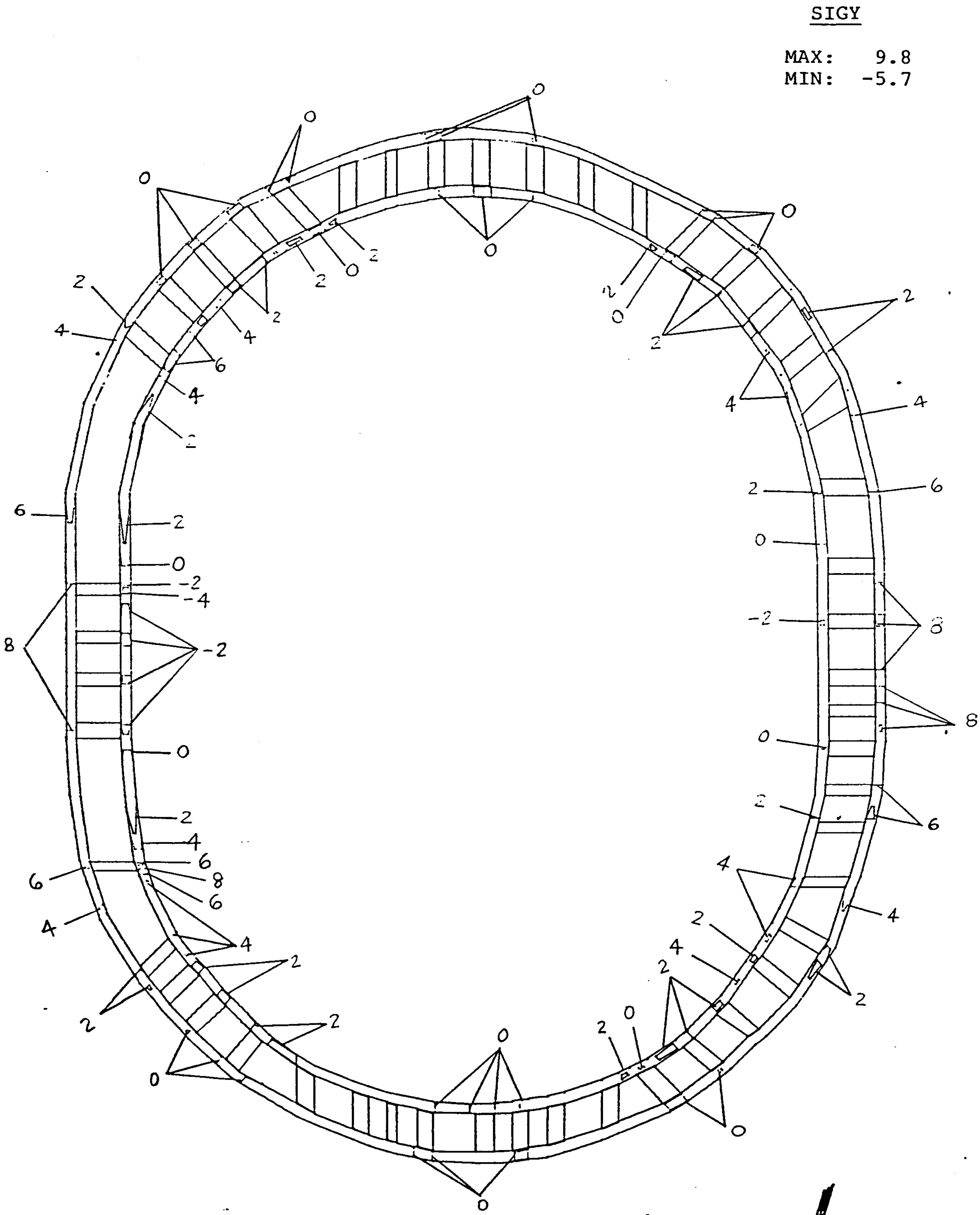

Note: Stresses are in ksi

MSC

0/90 P55/MG HOUSING WITH PRESSURE LOADS ONLY

TAUXY

MAX: 3.6
MIN: -5.4

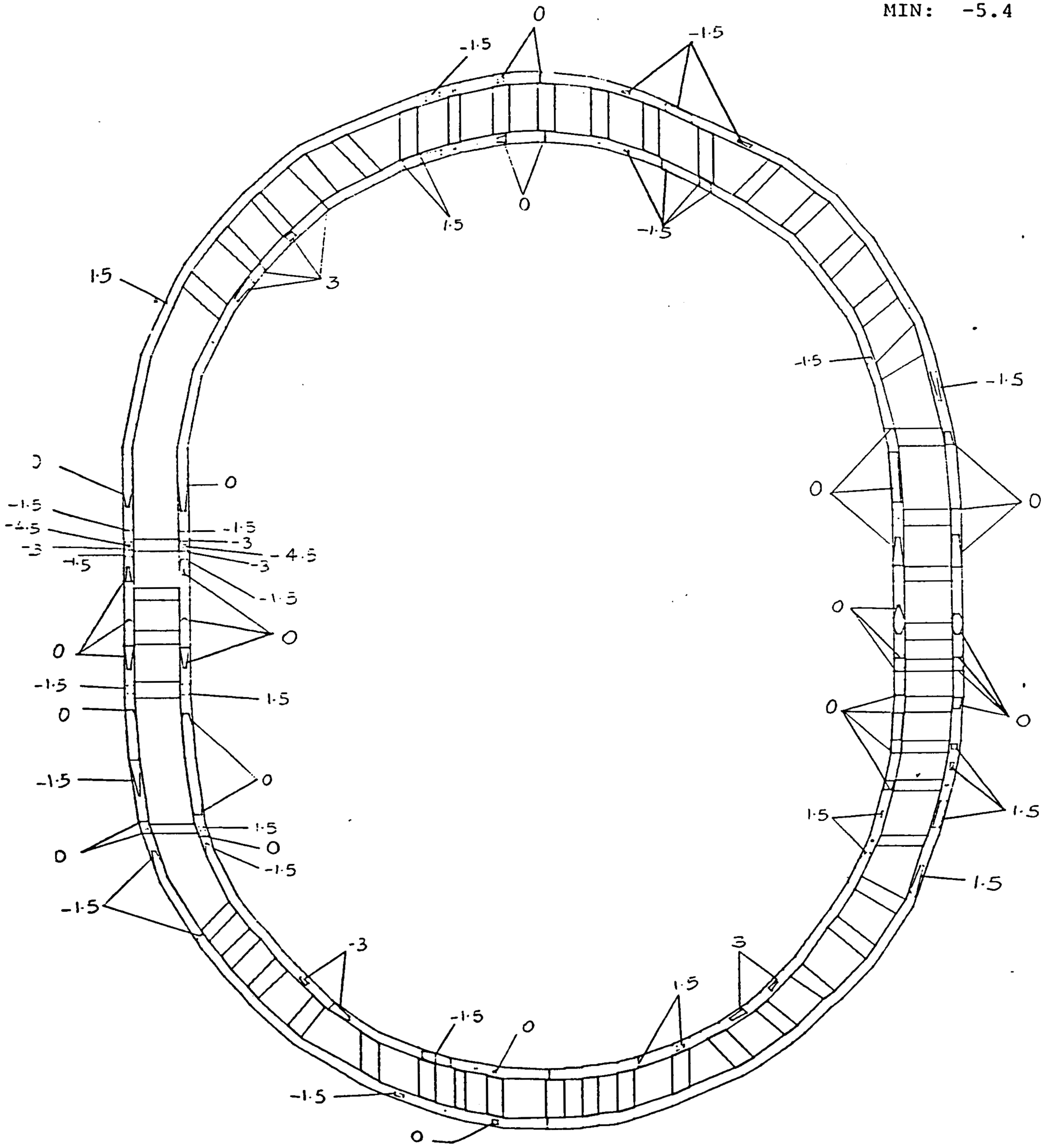

Note: Stresses are in ksi

msc.

THERMAL EXPANSION COEFFICIENTS OF $0^\circ_I/90^\circ_J$ P55/MG (V_F=0.4) COMPOSITES

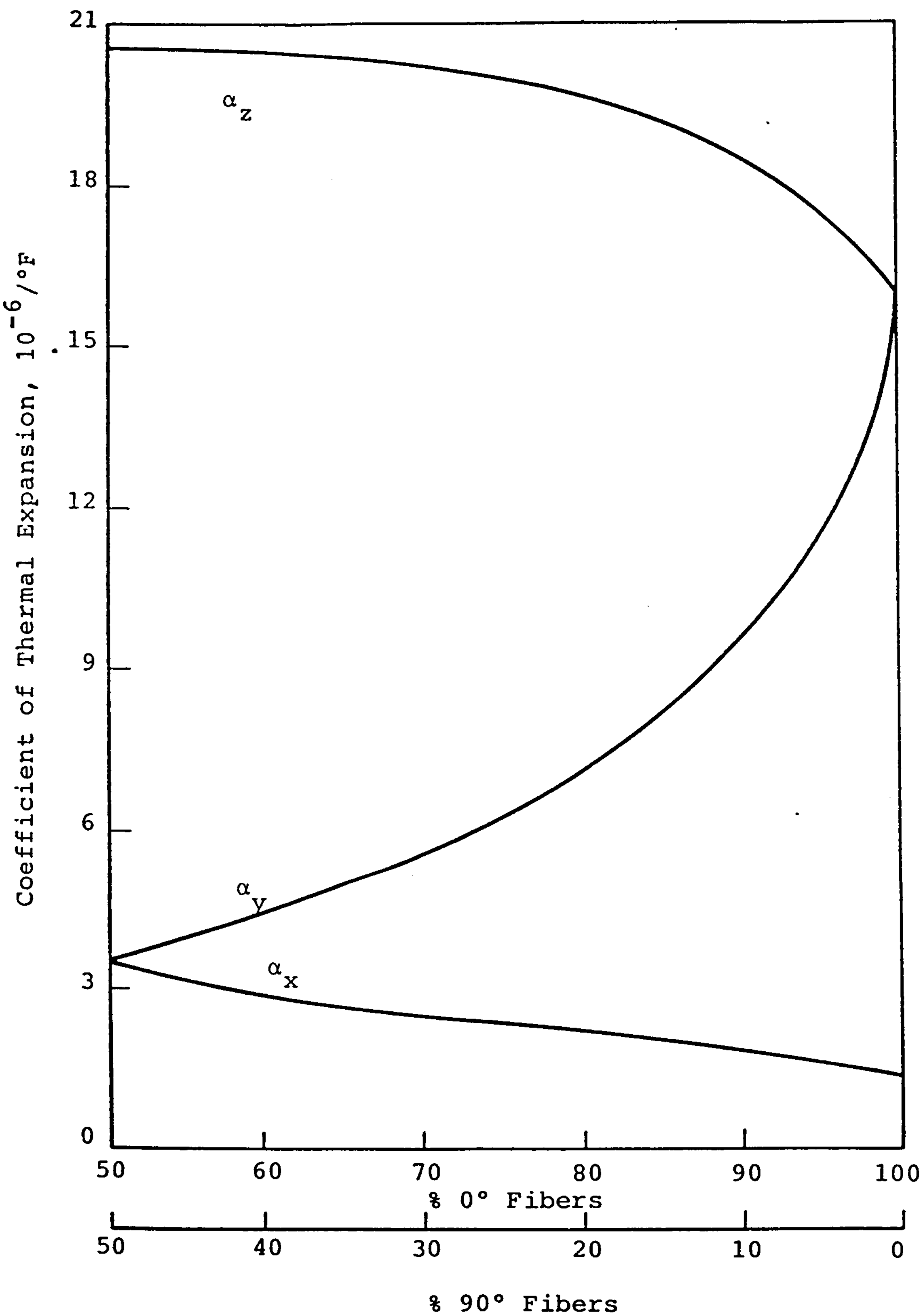

THERMAL EXPANSION COEFFICIENTS OF $0^\circ_I/90^\circ_J$ P55/MG (V_F=0.4) COMPOSITES

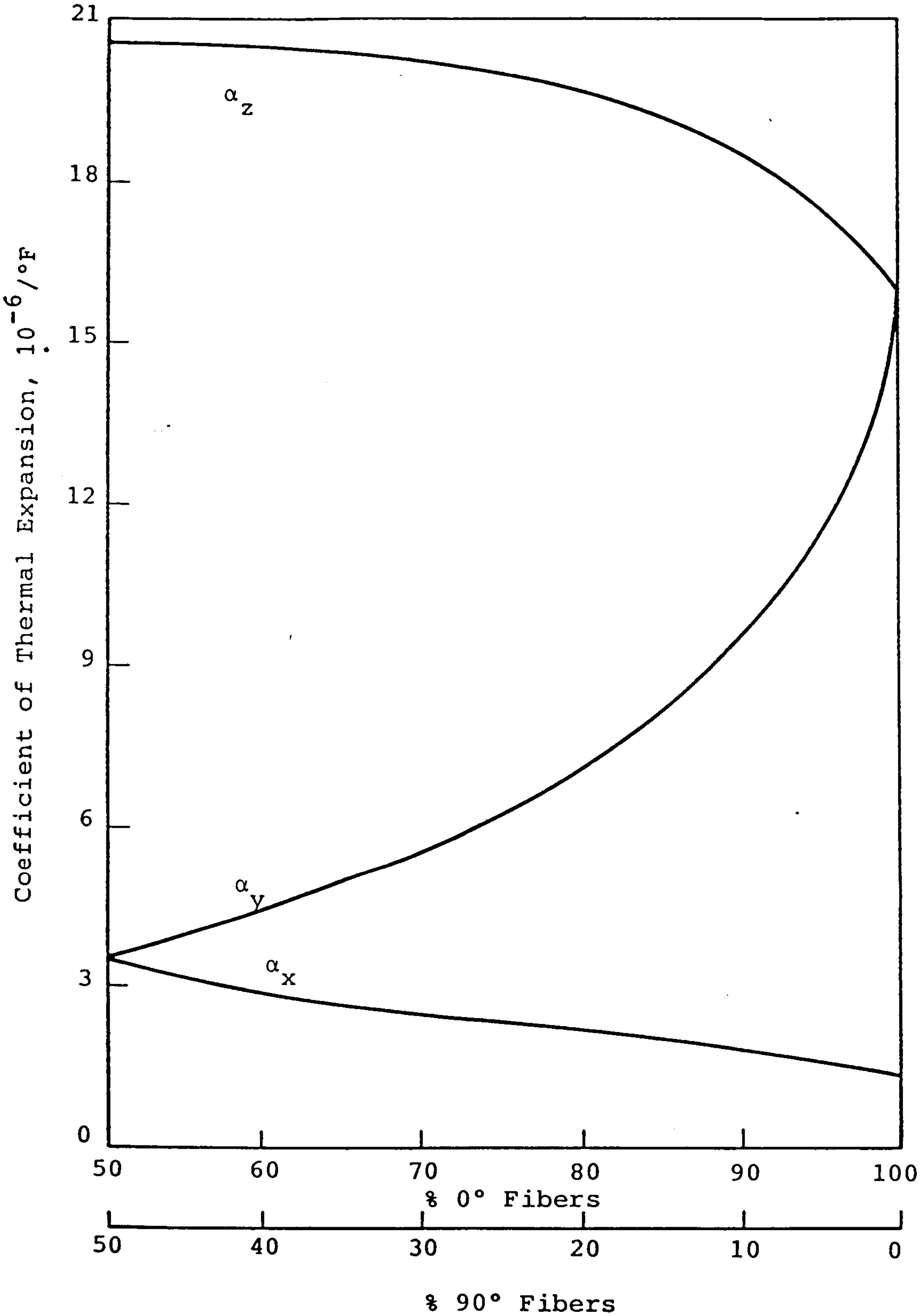

THERMAL CONDUCTIVITIES OF 0° P55/AZ91C COMPOSITES

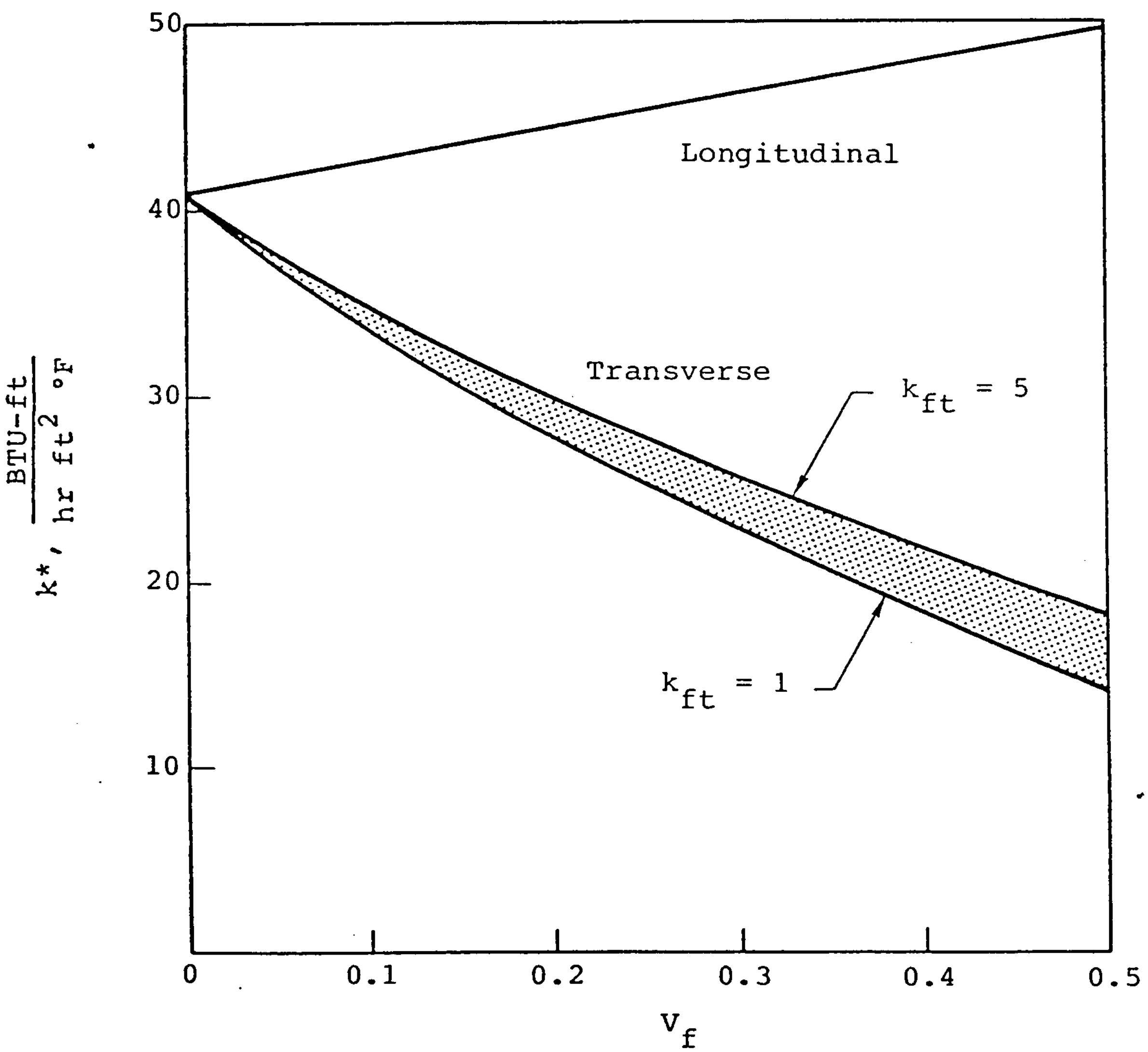

VARIATION OF THERMAL CONDUCTIVITIES OF VARIOUS

P55/MG LAMINATES WITH VOLUME FRACTIONS

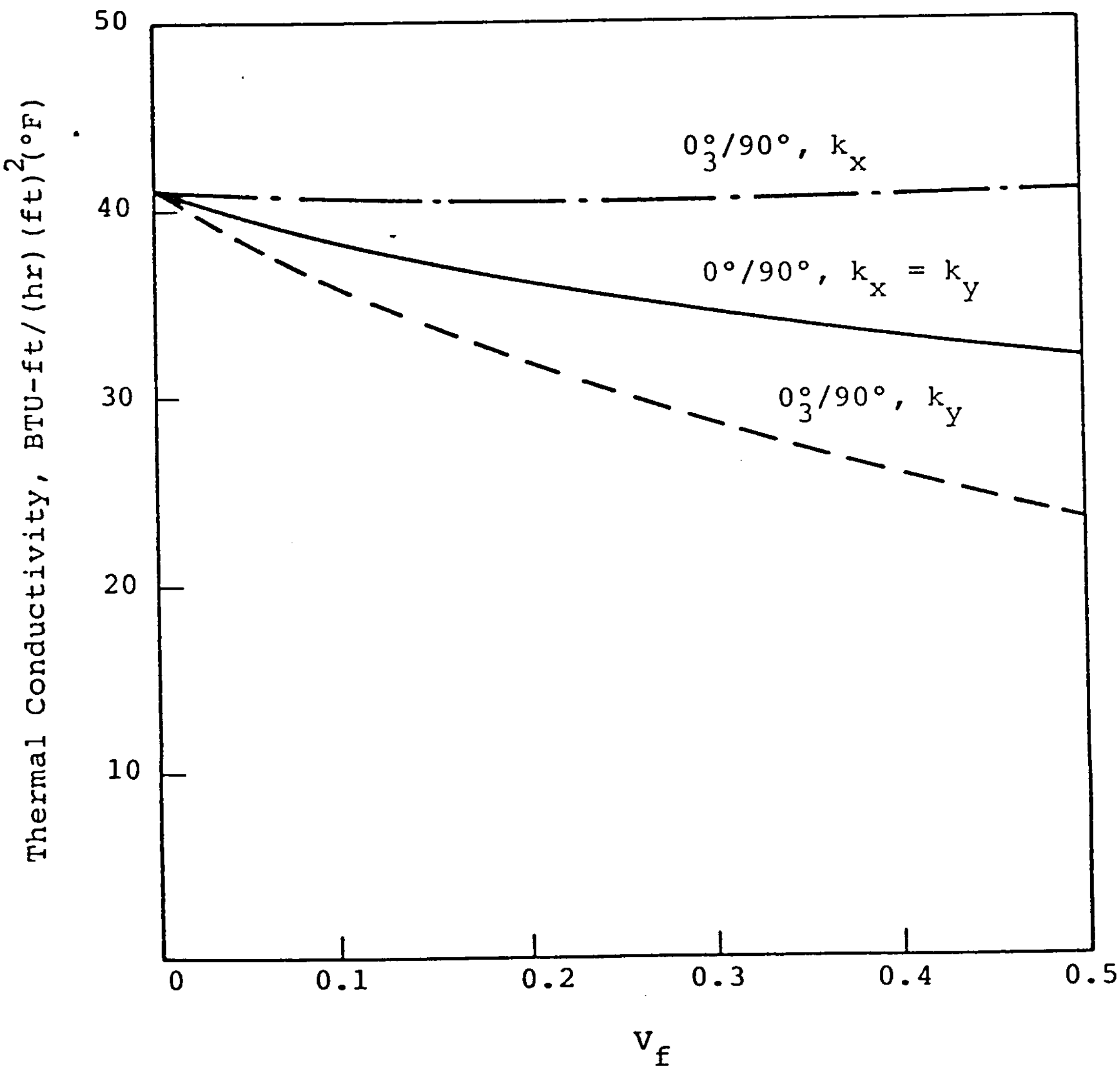

THERMAL CONDUCTIVITIES OF VARIOUS P55/AZ91C (V_F=0.4) COMPOSITES

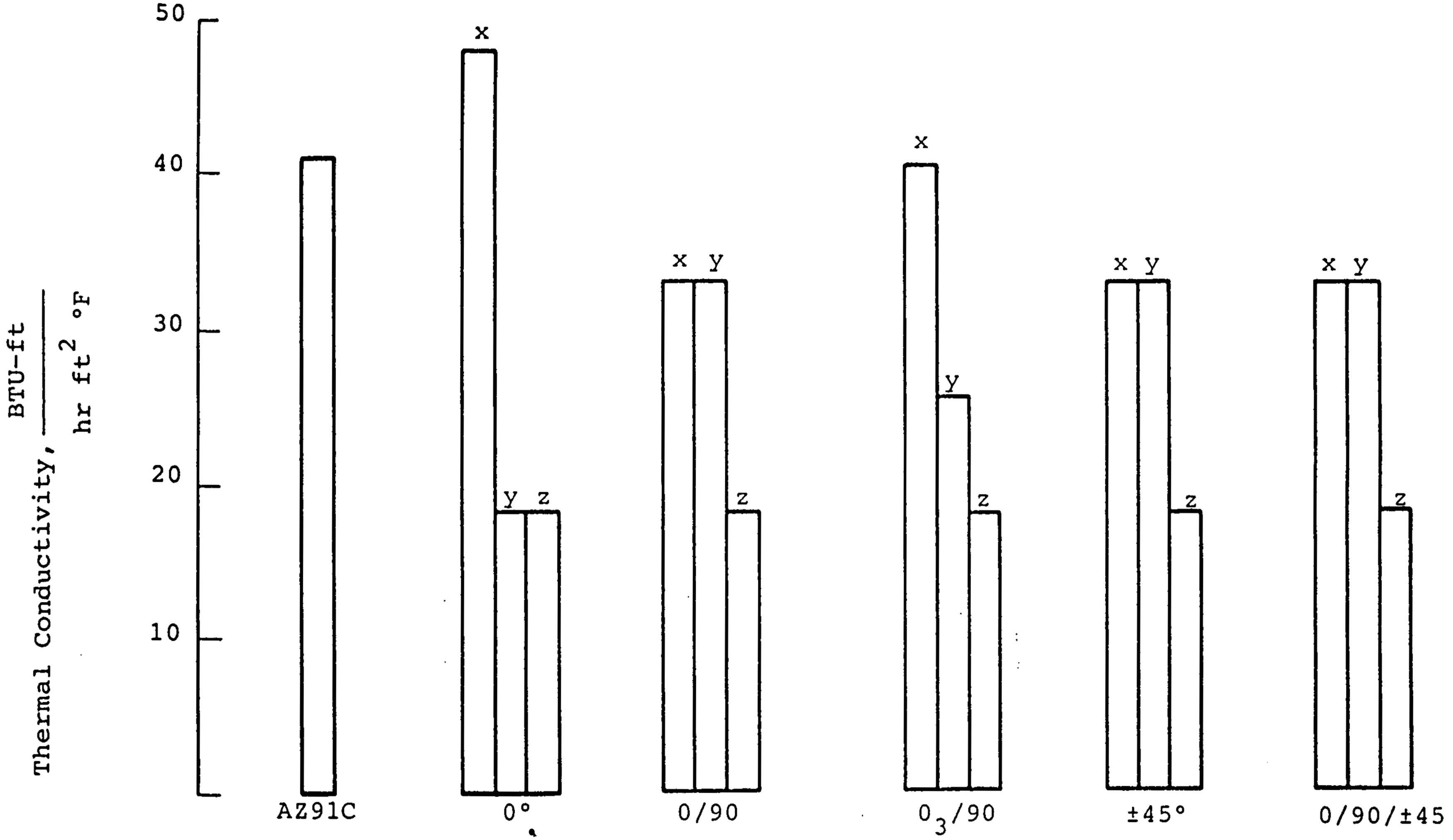

THERMAL CONDUCTIVITY CALCULATIONS

- P55 FIBER
  - AXIAL THERMAL CONDUCTIVITY = 58 BTU/(HR. FT. °F)
  - TRANSVERSE THERMAL CONDUCTIVITY VERY LOW
    - PRECISE VALUE NOT KNOWN, BUT IS NOT VERY SIGNIFICANT AS WILL BE SHOWN

- AZ91C MATRIX THERMAL CONDUCTIVITY = 41 BTU/(HR. FT. °F)

- P55/AZ91C UNIDIRECTIONAL COMPOSITE THERMAL CONDUCTIVITIES
  - $K_L = K_{FA} V_F + K_M V_M$
  - $K_T = K_M \dfrac{K_M V_M + K_{FT}(1+V_F)}{K_M(1+V_F) + K_{FT} V_M}$

COMPARISON OF RT AND ELEVATED TEMPERATURE MODULI

MODULI (MSI)	RT	750°F
0°, E_L^+	21.7	20.3
$0^\circ/90^\circ$, E_L^+	12.8	9.3
$0^\circ_3/90^\circ$, E_Y^+	5.6	4.5
$\pm45^\circ$, E_X^+	4.2	2.4
$+45^\circ_3/-45^\circ$, E_X^+	4.6	1.7

COMPARISON OF RT AND ELEVATED TEMPERATURE STRENGTHS

STRENGTH (KSI)	RT	750°F
$0°$, σ_L^{TU}	68.3	69.4
$0°$, σ_L^{CU}	69.7	53.8 @ 575°F
$0°/90°$, σ_X^{TU}	34.9	40.7
$0°/90°$, σ_X^{CU}	43.1	14.6
$0°_3/90°$, σ_X^{CU}	47.3	30.9
$0°_3/90°$, σ_Y^{TU}	15.0	18.2
$0°_3/90°$, σ_Y^{CU}	33.4	19.0
$\pm 45°$, σ^{TU}	11.4	2.6
$\pm 45°$, σ_X^{CU}	16.7	6.0
$+45°_3/-45°$, σ_X^{TU}	9.2	2.4
$+45°_3/-45°$, σ_X^{CU}	15.4	6.8

COMPARISON OF RT AND ELEVATED TEMPERATURE THERMAL EXPANSION COEFFICIENTS

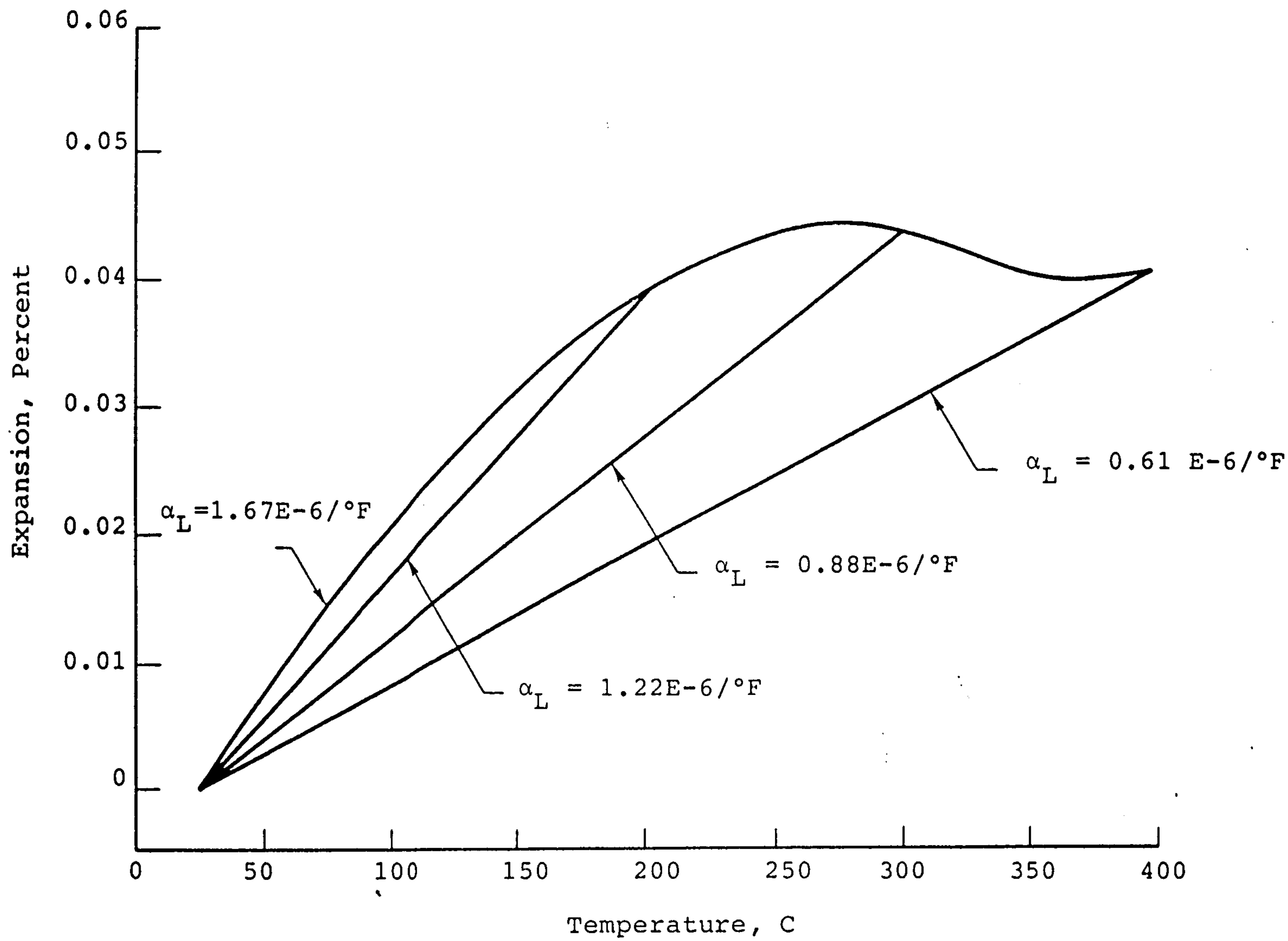

CONCLUSIONS FROM ELEVATED TEMPERATURE TEST RESULTS

- MATRIX DOMINATED PROPERTIES AND STRENGTHS EXPERIENCE LARGE REDUCTIONS COMPARED TO RT VALUES

- FIBER DOMINATED PROPERTIES AND STRENGTHS NOT SIGNIFICANTLY AFFECTED
  - P55 FIBER PROPERTIES DO NOT CHANGE IN THE RANGE 70°F - 750°F

- RESULTS CAN BE EXPLAINED BY CONSIDERING AZ91C-T6 PROPERTIES VERSUS TEMPERATURE

TEMPERATURE, °F	E_M, % RT VALUE	σ_M^{TU}, % RT VALUE
300	85	78
400	70	66
600	46	--

THERMAL ANALYSES

- ONE-DIMENSIONAL HEAT TRANSFER MODEL TO ESTIMATE HOUSING WALL TEMPERATURE
- FUEL SIDE HEAT TRANSFER COEFFICIENT AVAILABLE AS A FUNCTION OF CRANK ANGLE
- COOLANT SIDE HEAT TRANSFER COEFFICIENT ESTIMATED FROM SIZE OF COOLANT PASSAGE, FLOW RATE AND EMPIRICAL HEAT TRANSFER EQUATION:
  - $ST\ PR^{2/3} = 0.023\ RE^{-0.2}$
- EFFECTIVE HEAT TRANSFER COEFFICIENT THROUGH THE WALL OBTAINED FROM (T/K) OF THE WALL MATERIAL
- PARAMETERS USED ON BASELINE A-356 HOUSING TO CHECK VALIDITY OF RESULTS AND THEN USED FOR THE P55/MG CONSTRUCTIONS

VARIATION OF FUEL-SIDE HEAT TRANSFER COEFFICIENT WITH CRANK ANGLE

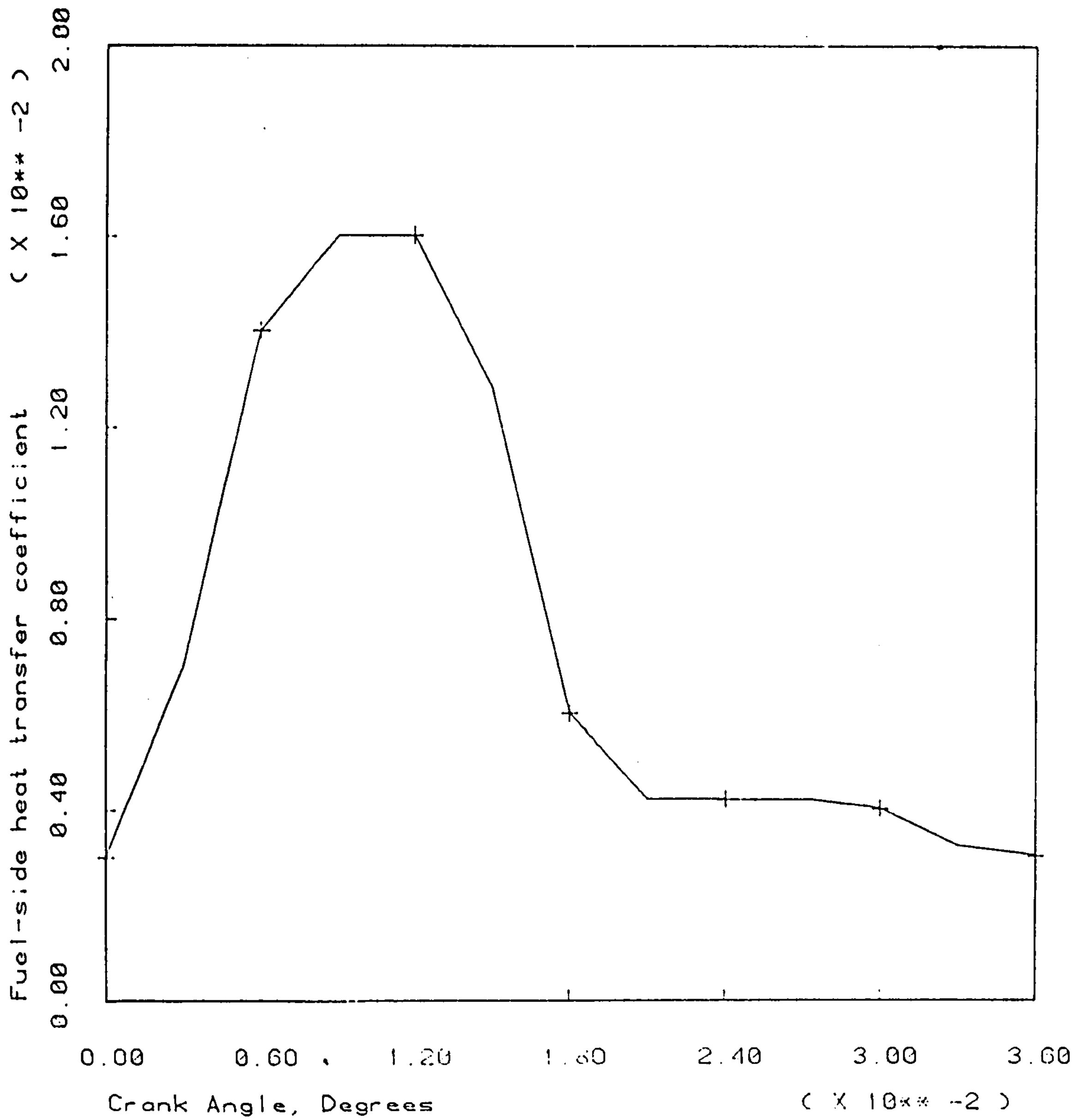

Reference: Atesman, K. M.,
"Heat Transfer in Rotary
Combustion Engines,"
J. Heat Transfer, May, 1975

VARIATION OF ROTOR HOUSING WALL TEMPERATURES WITH CRANK ANGLE

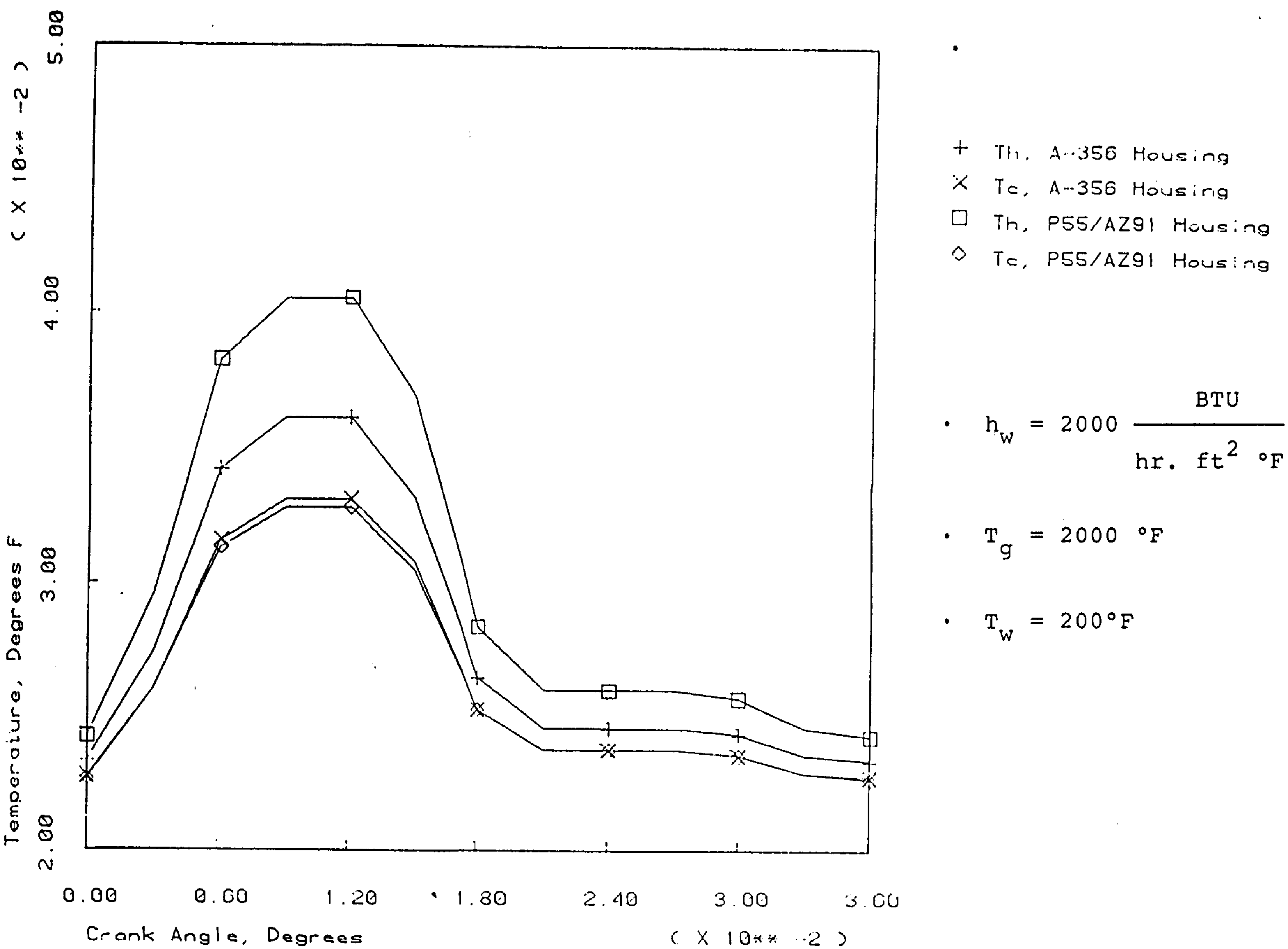

- $h_w = 2000 \dfrac{\text{BTU}}{\text{hr. ft}^2\ °\text{F}}$
- $T_g = 2000$ °F
- $T_w = 200$°F

VARIATION OF ROTOR HOUSING WALL TEMPERATURES WITH CRANK ANGLE

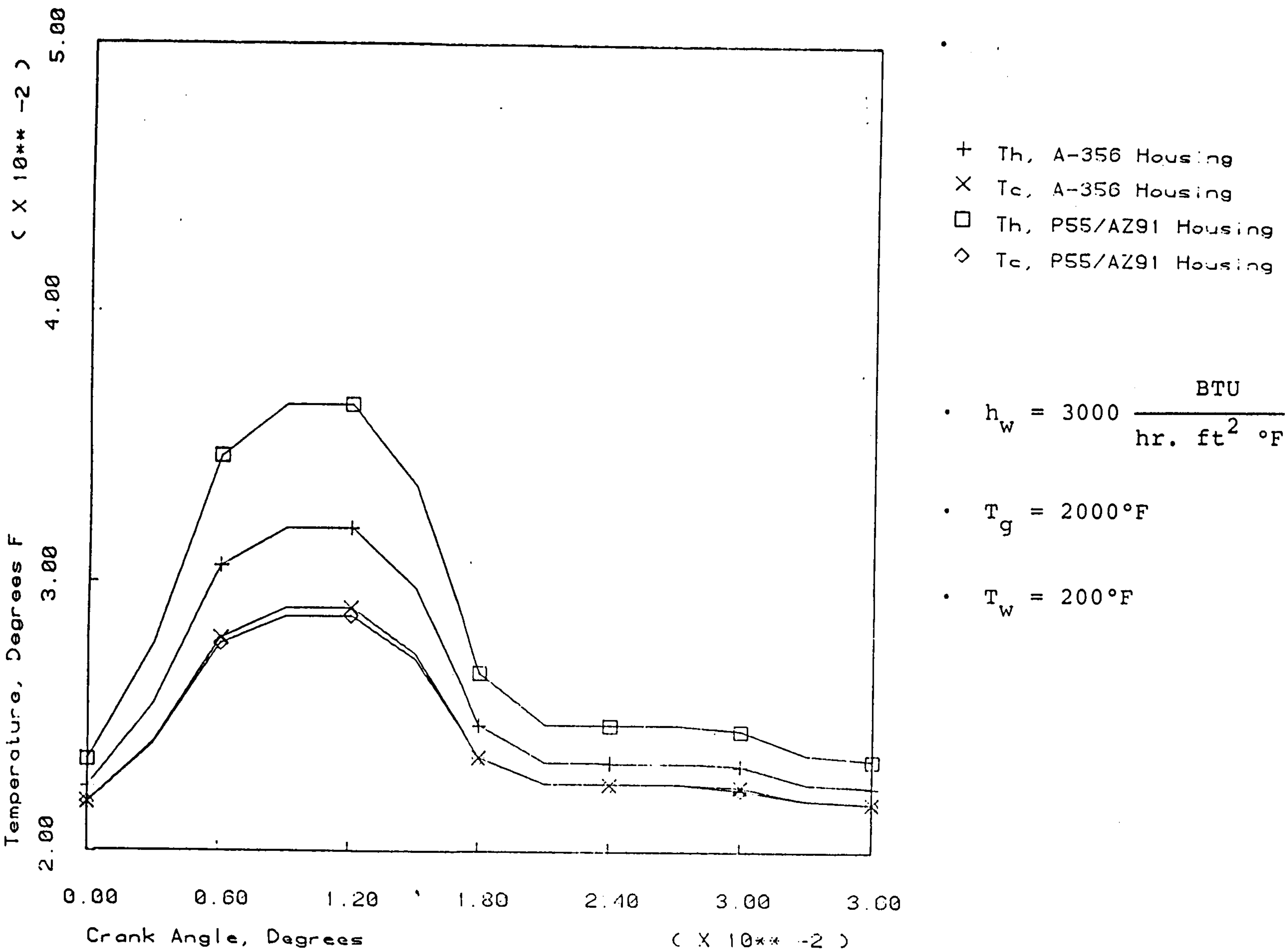

- $h_w = 3000 \dfrac{BTU}{hr.\ ft^2\ °F}$
- $T_g = 2000°F$
- $T_w = 200°F$

ROTOR HOUSING STRESS ANALYSES

- TWO-DIMENSIONAL (PLANE STRAIN) FINITE ELEMENT ANALYSES
- THREE MATERIAL CHOICES
  - A-356 AS THE BASELINE MATERIAL
  - $0^\circ/90^\circ$ P55/MG ($V_F = 0.40$), SAME WALL THICKNESS
  - $0^\circ/\pm45^\circ/90^\circ$ P55/MG ($V_F = 0.40$), SAME WALL THICKNESS
- TWO LOADING CONDITIONS
  - AN INTERNAL PRESSURE OF 200 PSI AT A REFERENCE TEMPERATURE OF 200°F
  - A COMBINED LOAD OF APPLIED TEMPERATURES AND INTERNAL PRESSURE OF 200 PSI
    - TEMPERATURE DISTRIBUTION DETERMINED FROM THERMAL ANALYSIS
    - $T_{REF} = 70^\circ$F

ALLOWABLE STRENGTHS USED FOR STRESS ANALYSES

MATERIAL	TEMP., °F	TENSION, KSI	COMPRESSION, KSI	SHEAR, KSI
A-356	70	33.0	33.0	25.0
	200-300	30.0	30.0	22.5
0°/90° P55/MG	70	34.9	43.1	7.0
	200	36.0	37.6	6.1
	400	37.7	29.1	4.6
0°/±45°/90° P55/MG	70	23.1	29.9	19.5
	200	22.8	26.2	18.5
	400	22.1	20.4	17.0

ALUMINUM HOUSING UNDER PRESSURE LOAD ONLY

SIGX

MAX: 10.3
MIN: 9.4

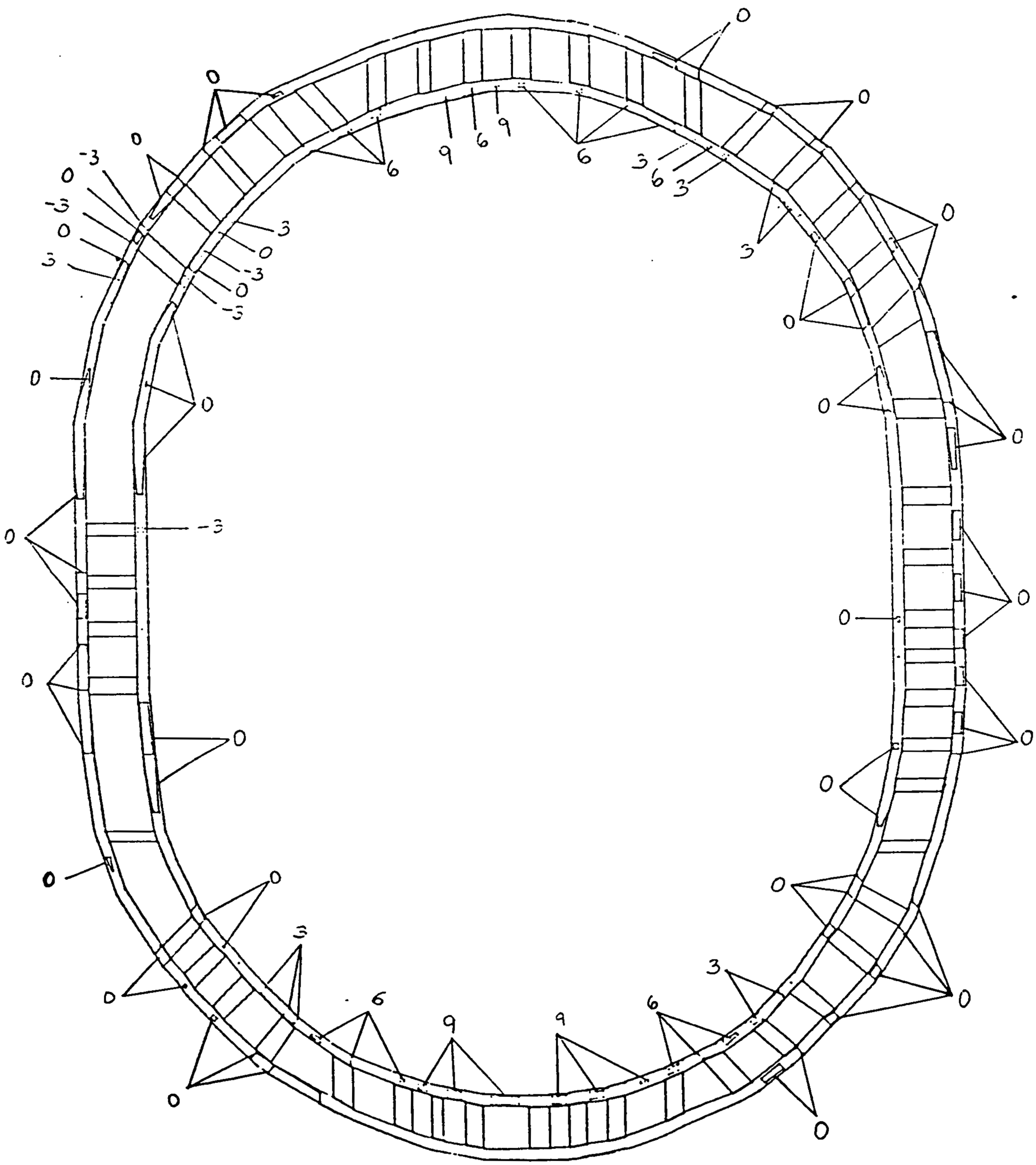

Note: Stresses are in ksi

ALUMINUM HOUSING UNDER PRESSURE LOADS ONLY

SIGY

MAX: 12.0
MIN: -9.2

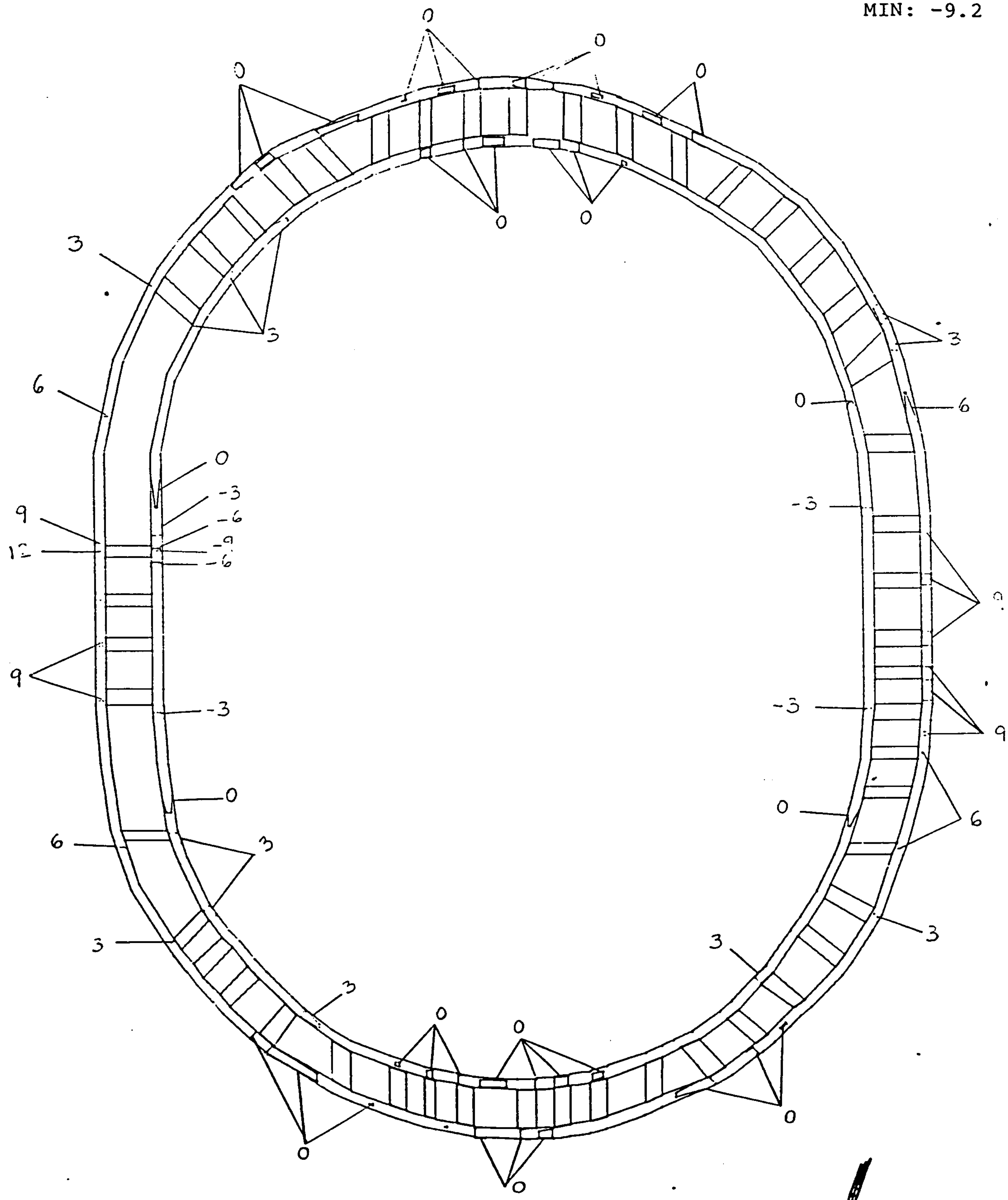

Note: Stresses are in ksi

ALUMINUM HOUSING UNDER PRESSURE LOADS ONLY

TAUXY

MAX: 4.9
MIN:-8.7

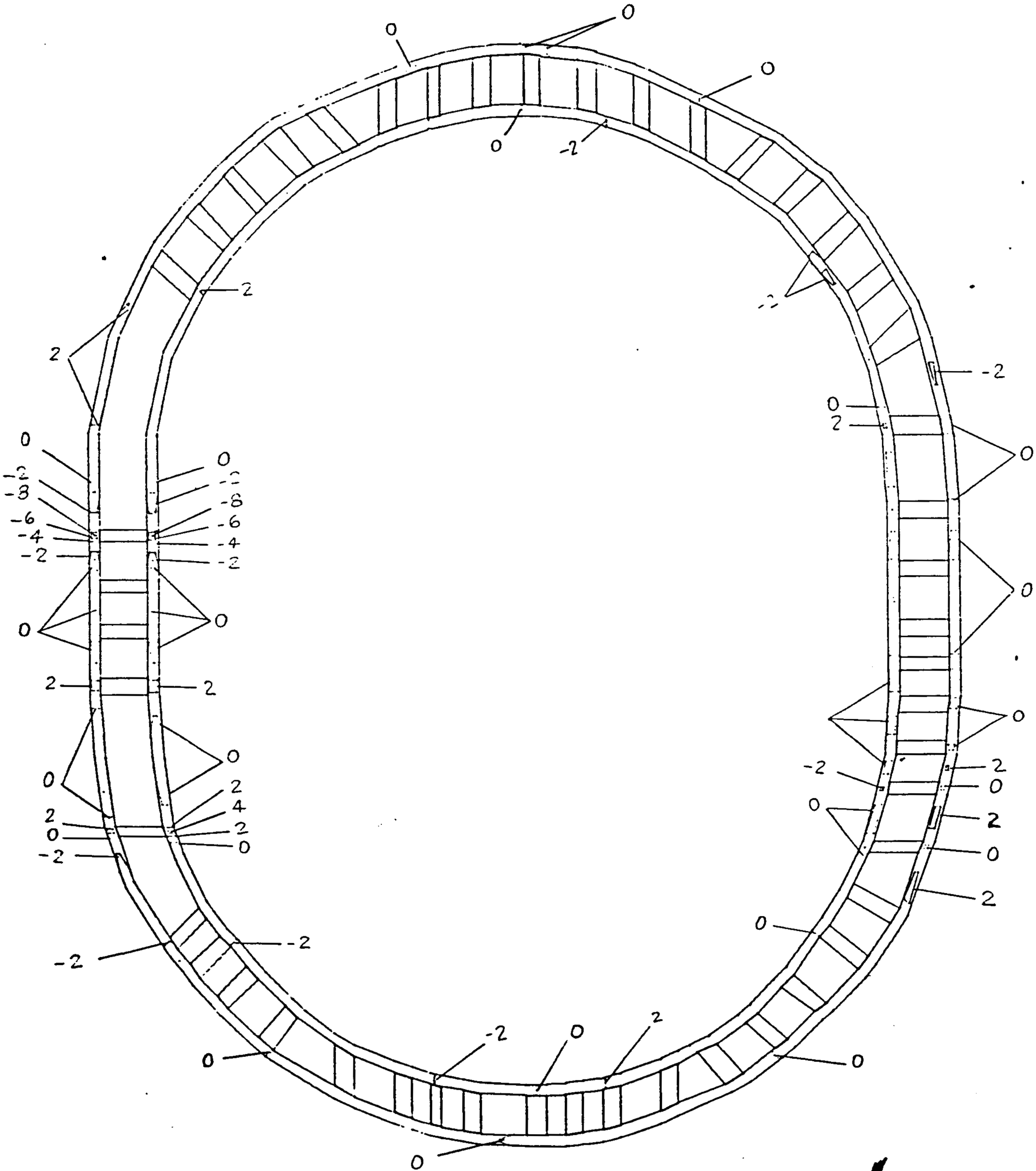

Note: Stresses are in ksi

ALUMINUM HOUSING UNDER TEMPERATURE AND PRESSURE LOADS

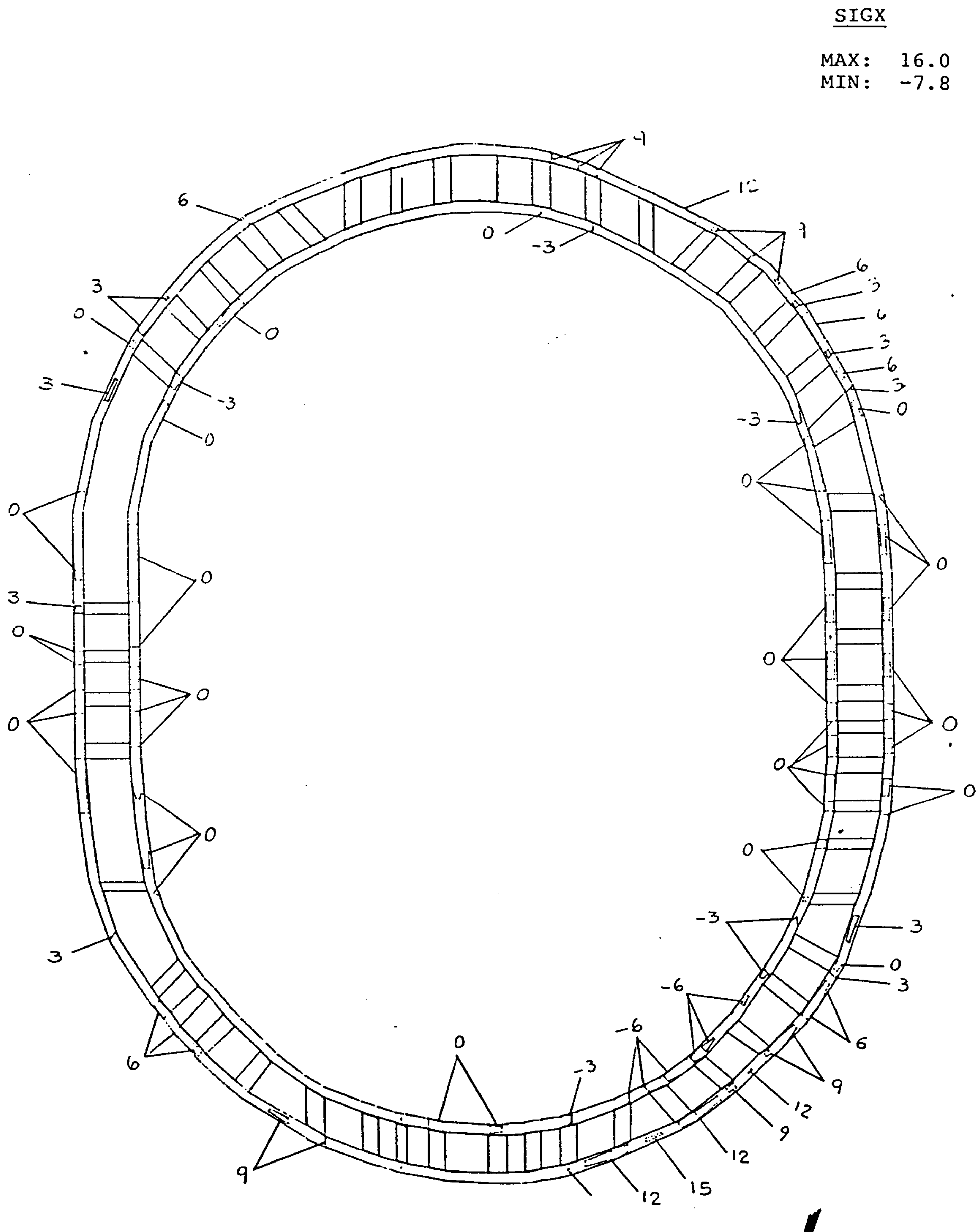

Note: Stresses are in ksi

0/90 P55/MG HOUSING UNDER TEMPERATURE AND PRESSURE LOADS

SIGX

MAX: 5.8
MIN: -7.3

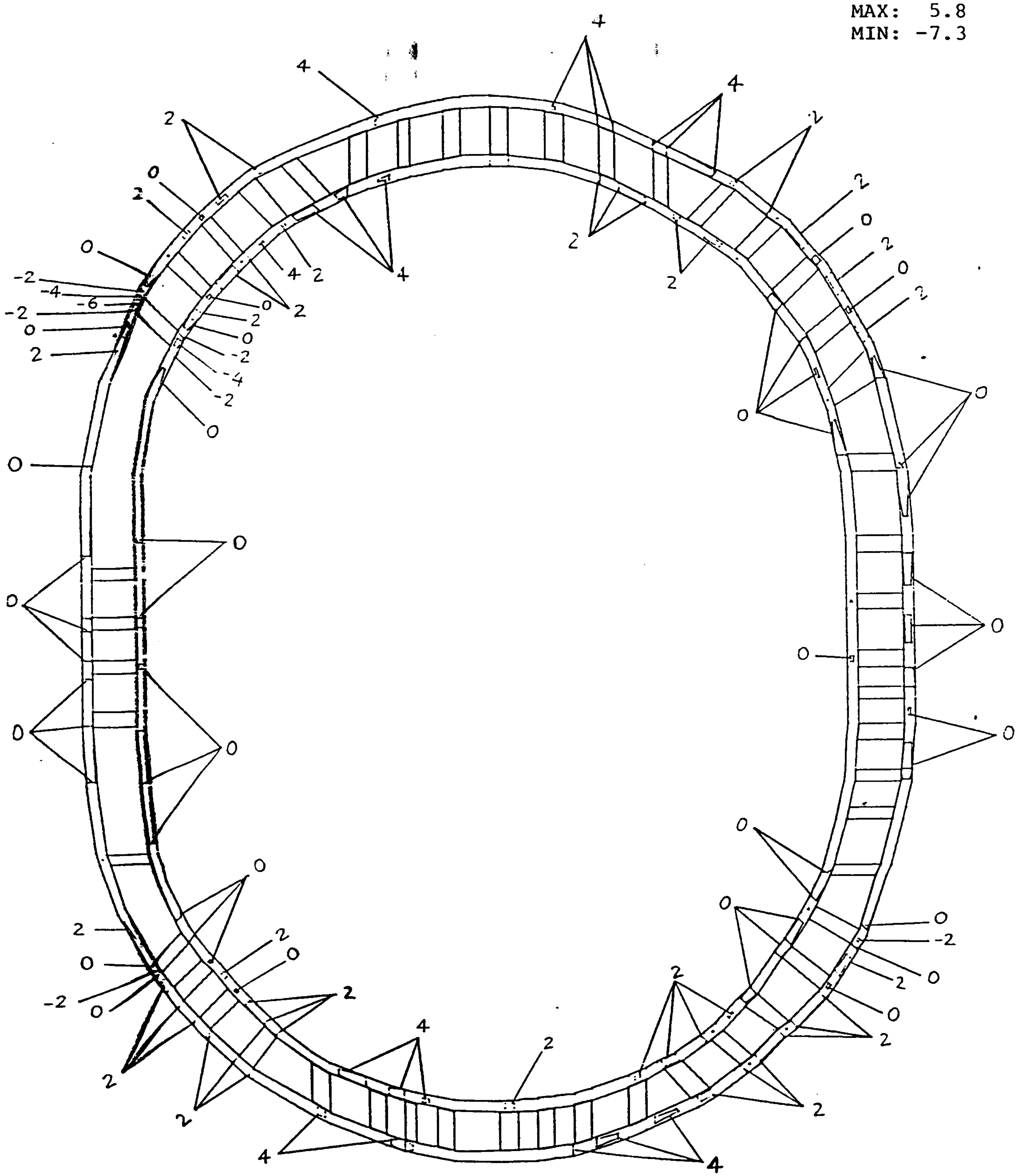

Note: Stresses are in ksi

0/90 P55/MG HOUSING UNDER TEMPERATURE AND PRESSURE LOADS

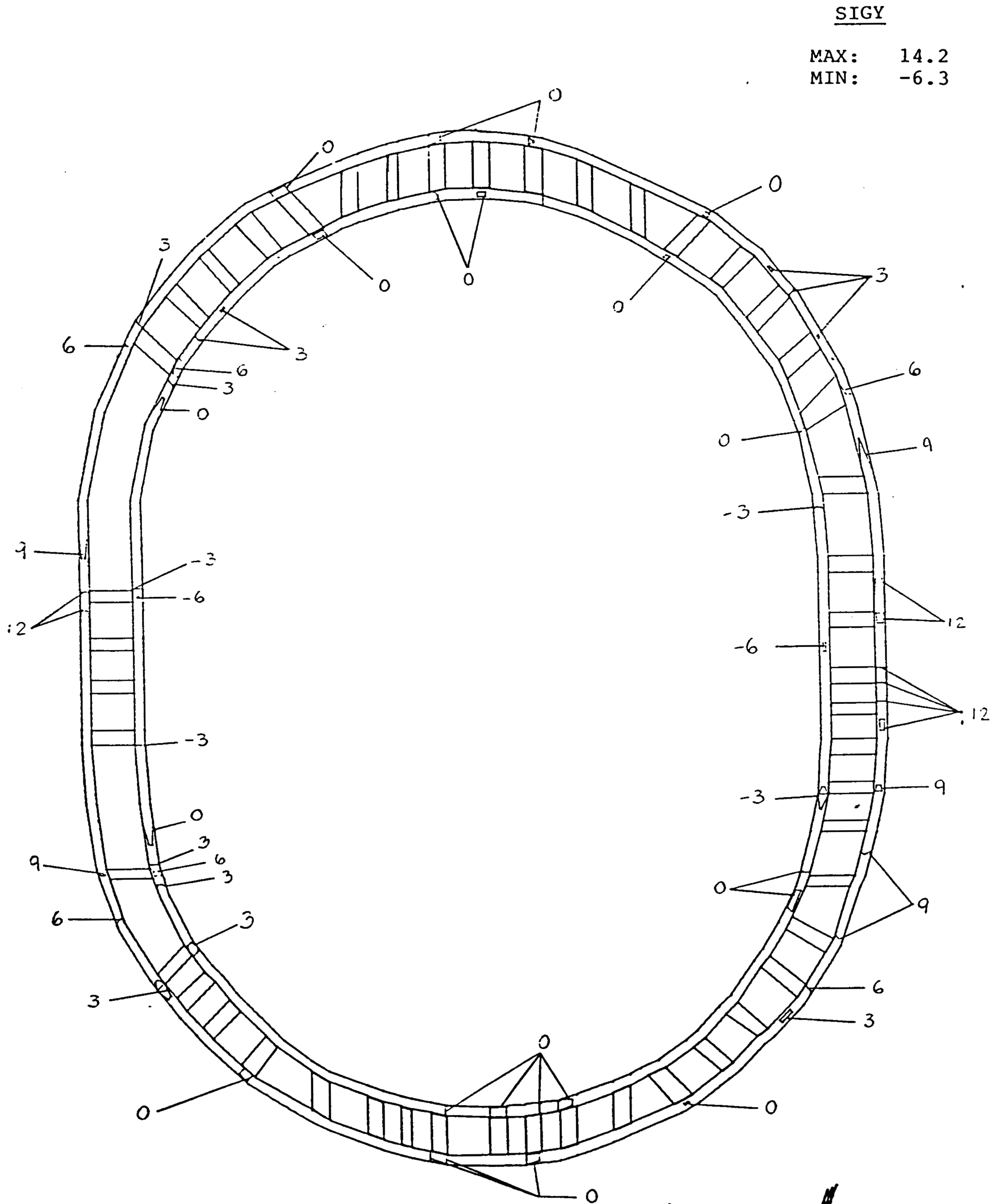

Note: Stresses are in ksi

0/90 P55/MG HOUSING UNDER TEMPERATURE AND PRESSURE LOADS

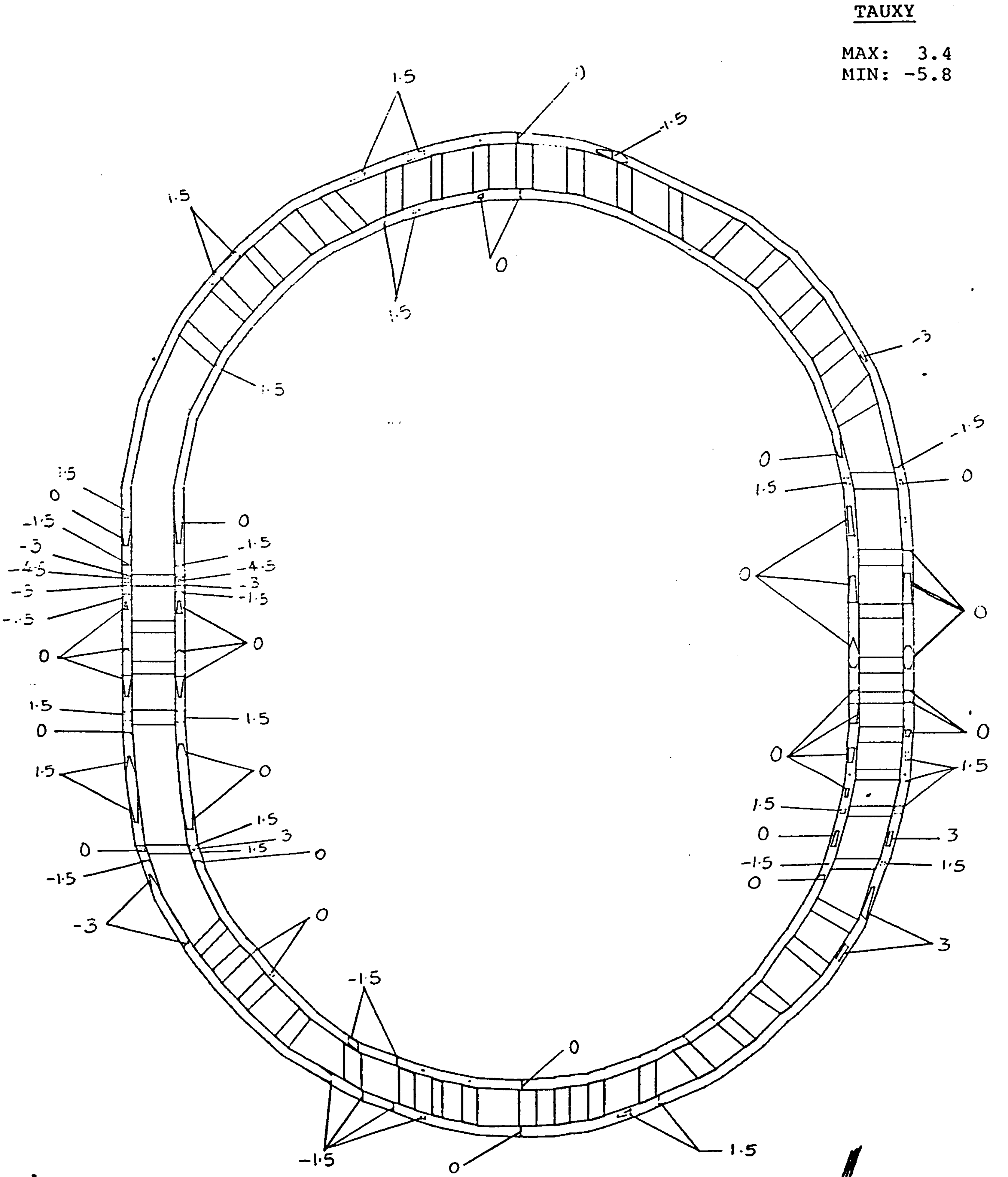

Note: Stresses are in ksi

0/±45/90 P55/MG HOUSING WITH PRESSURE LOADS ONLY

SIGX

MAX: 6.4
MIN: -9.0

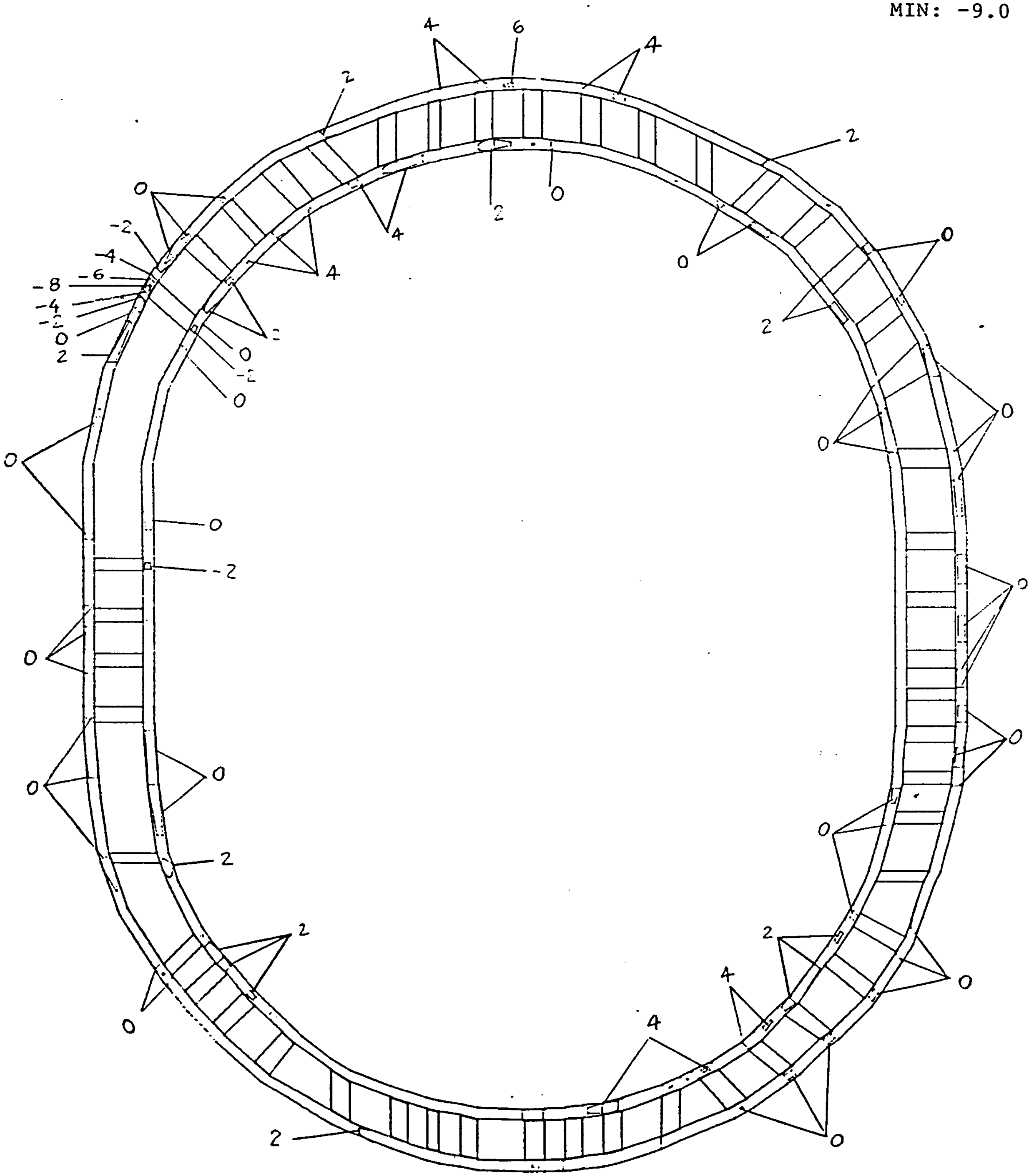

Note: Stresses are in ksi

msc.

0/±45/90 P55/MG HOUSING WITH PRESSURE LOADS ONLY

SIGY

MAX: 9.3
MIN: -6.2

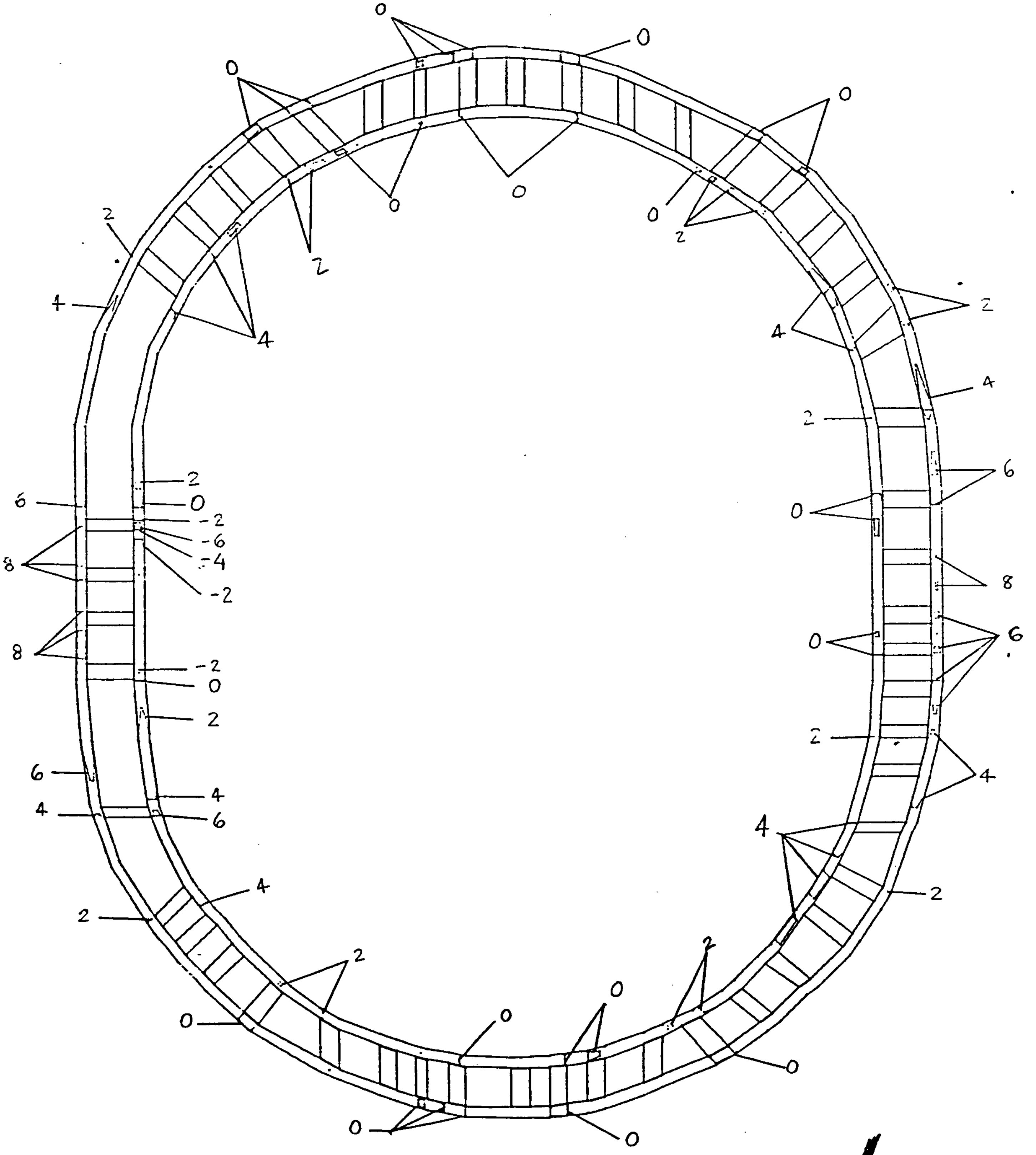

Note: Stresses are in ksi

0/±45/90 P55/MG HOUSING WITH PRESSURE LOADS ONLY

TAUXY

MAX: 4.0
MIN: -7.7

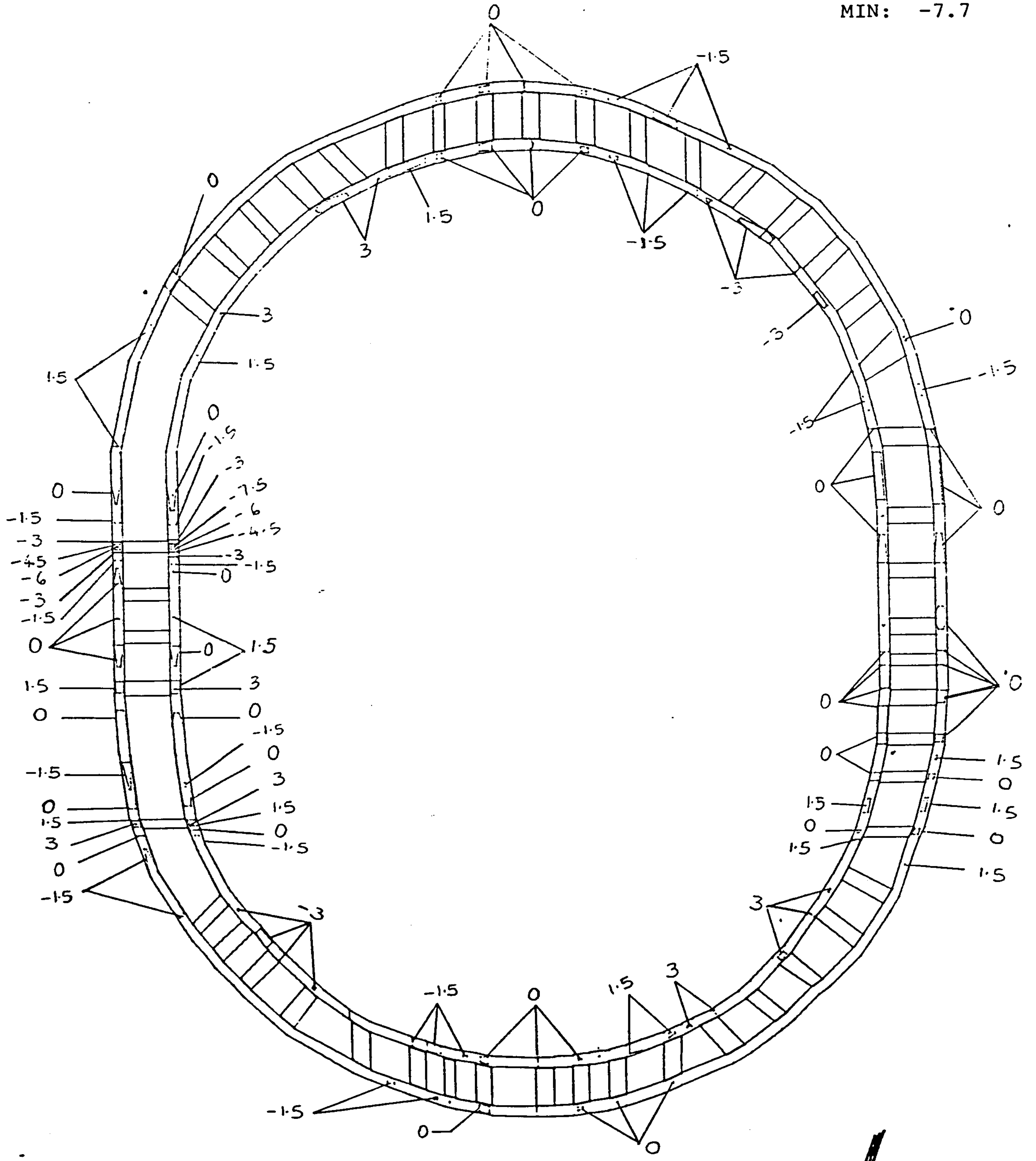

Note: Stresses are in ksi

0/±45/90 P55/MG HOUSING UNDER TEMPERATURE AND PRESSURE LOADS

SIGX

MAX: 6.5
MIN: -7.0

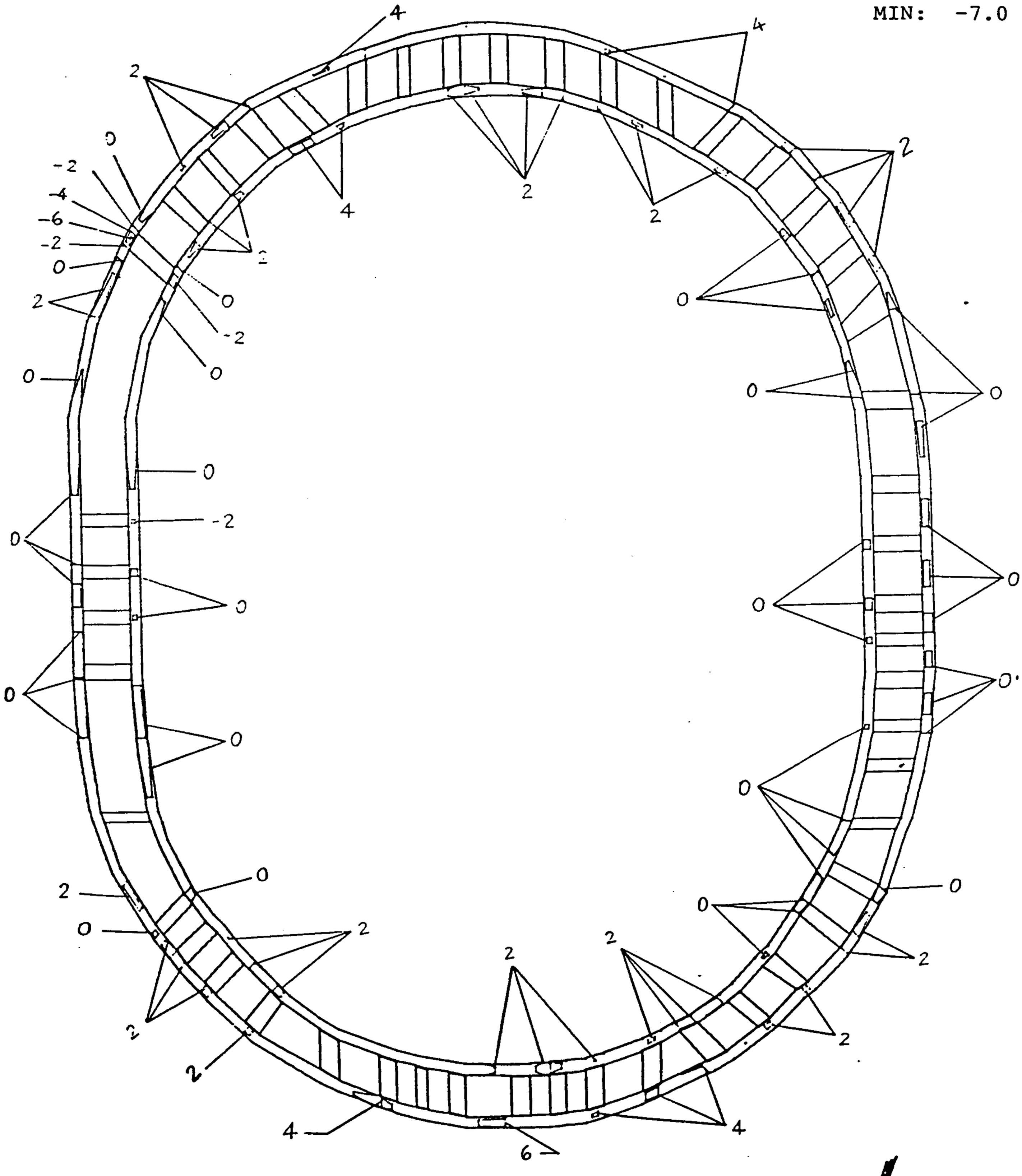

Note; Stresses are in ksi

0/±45/90 P55/MG HOUSING UNDER TEMPERATURE AND PRESSURE LOADS

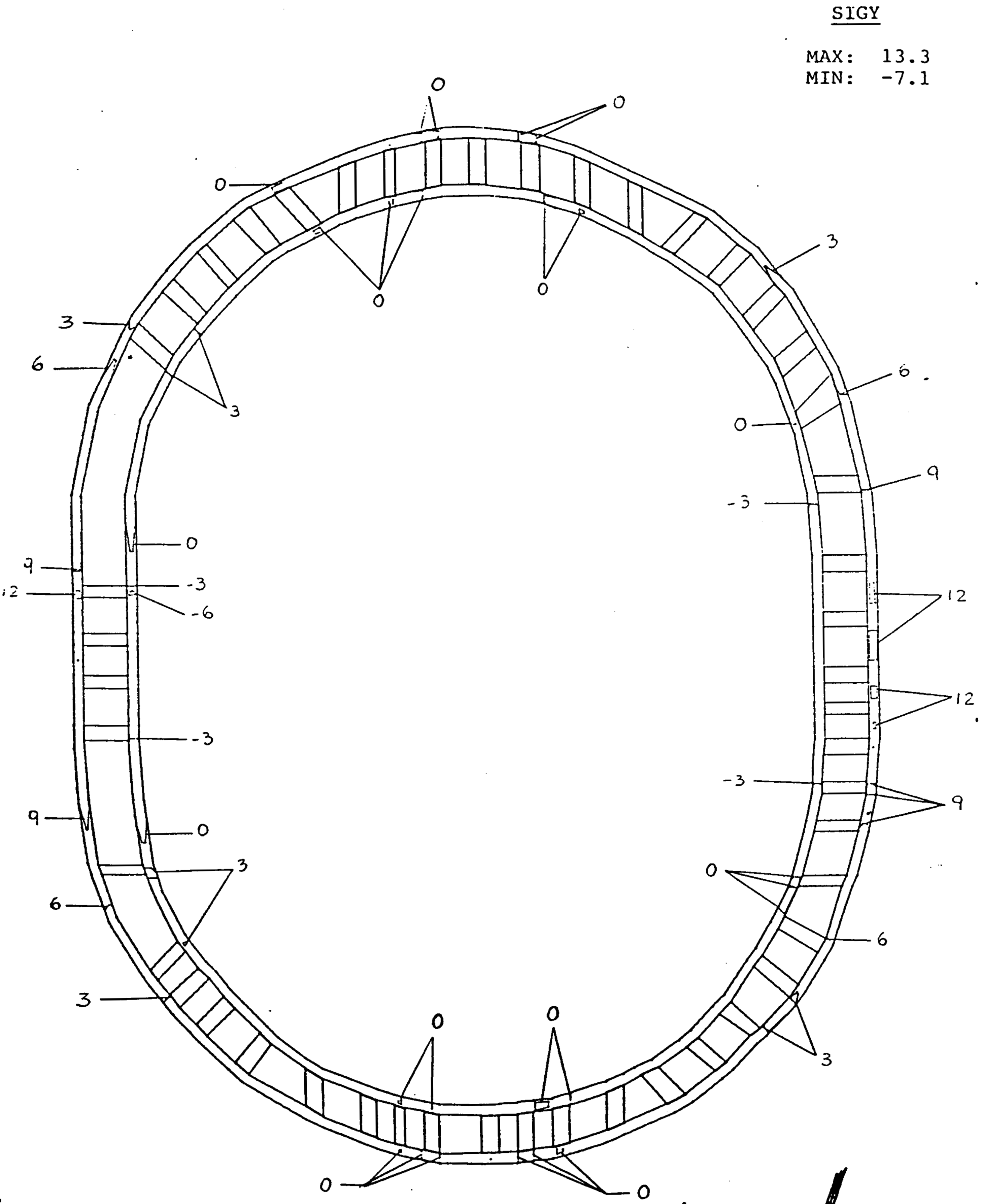

Note: Stresses are in ksi

0/±45/90 P55/MG HOUSING UNDER TEMPERATURE AND PRESSURE LOADS

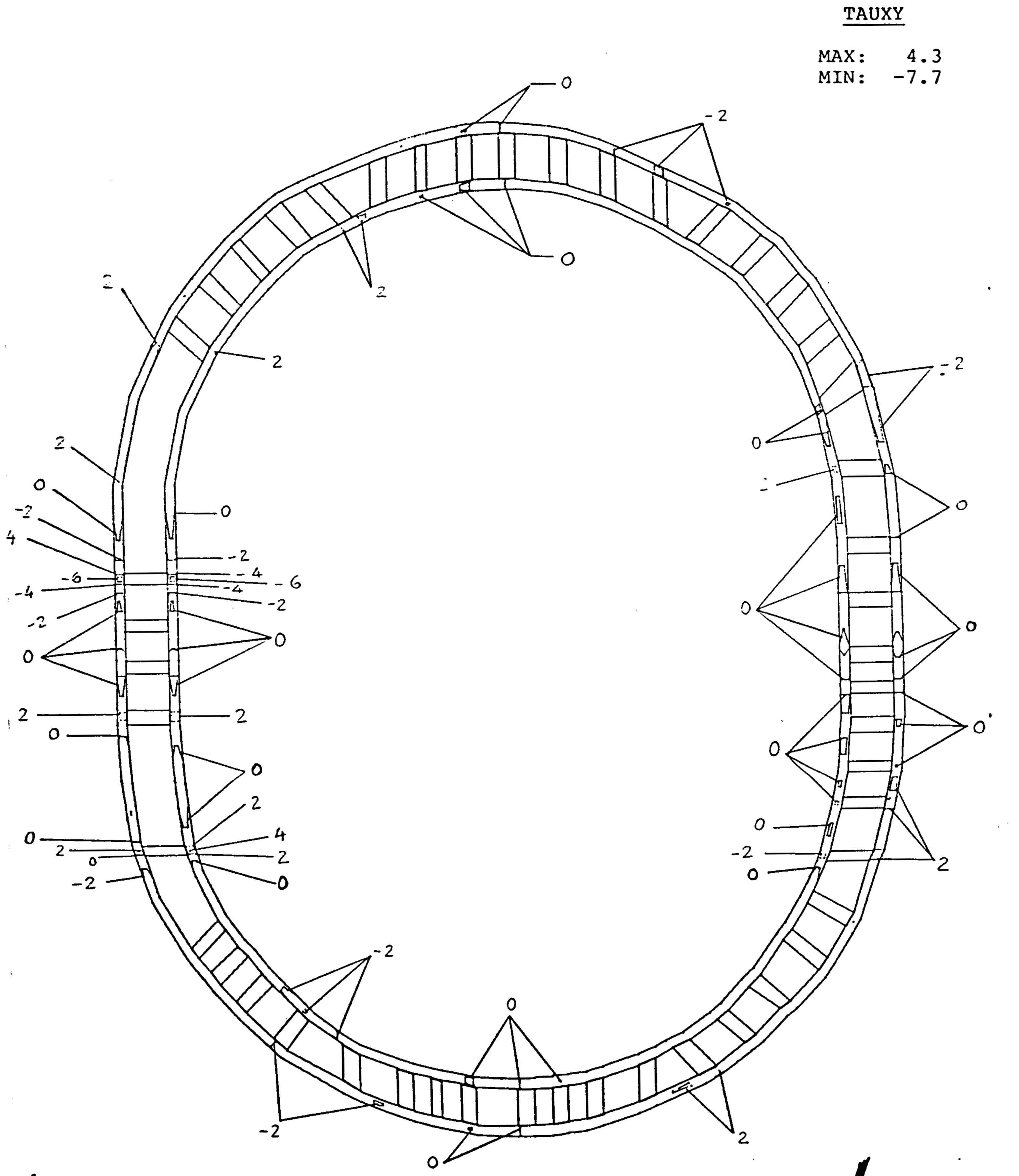

Note: Stresses are in ksi

SUMMARY OF RESULTS OF STRESS ANALYSES

MATERIAL	STRESS	MINIMUM FACTORS OF SAFETY PRESSURE ONLY	PRESSURE + TEMP.
A-356	SIGX	2.91	1.88
	SIGY	2.50	1.01
	TAUXY	2.59	2.01
0°/90° P55/MG	SIGX	4.04	3.99
	SIGY	3.67	2.65
	TAUXY	1.13	0.79
0°/±45°/90° P55/MG	SIGX	2.91	2.43
	SIGY	2.45	1.66
	TAUXY	2.40	2.21

Materials Sciences Corporation

CONCLUSIONS FROM NUMERICAL ANALYSES

- ALUMINUM HOUSING STRESSES DUE TO THERMAL LOADS ARE VERY HIGH DUE TO ALUMINUM'S HIGH CTE
  - AS A RESULT, BASELINE HOUSING EXPERIENCES CRITICALLY HIGH SIGY STRESSES NEAR CRANK ANGLE OF 90°
- LOW IN-PLANE CTE'S FOR P55/MG COMPOSITES RESULT IN LOWER STRESSES EVEN THOUGH TEMPERATURES ARE HIGHER
- LOW SHEAR STRENGTHS OF 0/90 P55/MG ARE A PROBLEM
  - ANALYSIS PREDICTS SHEAR FAILURE FOR COMBINED LOADS
- 0/±45/90 P55/MG HAS A BETTER BALANCE OF PROPERTIES AND IS MUCH BETTER SUITED FOR THESE DESIGN LOADS
- 0/±45/90 P55/MG IS A VIABLE CONFIGURATION IF SOME OF THE INHERENT COMPLEXITIES OF P55/MG METAL MATRIX COMPOSITES CAN BE DEALT WITH

RELATED PROBLEMS ASSOCIATED WITH THE USE OF GR/MG COMPOSITES

- MATRIX YIELDS DUE TO THERMAL CYCLING BETWEEN RT AND OPERATING TEMPERATURE (~400°F)
  - PLASTIC STRAINS ACCUMULATE
  - DIMENSIONAL TOLERANCES MAY BE AFFECTED IF COMPOSITE IS USED IN AS-FABRICATED CONDITION
  - APPROPRIATE PROCESSING WILL REDUCE OR MAY EVEN ELIMINATE MATRIX YIELDING

- MATRIX CREEP EFFECTS
  - CREEP EFFECTS ARE MUCH MORE SIGNIFICANT IN MAGNESIUM AS COMPARED TO ALUMINUM
  - LOWER THERMAL CONDUCTIVITIES OF P55/MG AS COMPARED TO ALUMINUM WILL RESULT IN HIGHER HOUSING TEMPERATURES
  - PROBLEM MAY BE ADDRESSED IN VARIOUS WAYS
    - USE OF HIGHER K FIBERS
    - USE OF BETTER CREEP RESISTANT MG ALLOYS
    - ALTERING COOLING SYSTEM OR USING COATINGS TO KEEP WALL TEMPERATURES WITHIN "SAFE" LIMITS

EFFECTS OF POST-PROCESSING

- INCREMENTAL LAMINATE STRESS ANALYSIS MODEL USING TEMPERATURE DEPENDENT PROPERTIES
- RESIDUAL MATRIX TENSILE STRESS IN THE FIBER DIRECTION OF 3 KSI ASSUMED
- DUE TO MISMATCH OF CTE BETWEEN FIBER AND MATRIX, AS COMPOSITE IS HEATED FROM RT, FIBER IS IN TENSION AND MATRIX IN COMPRESSION
- AS COMPOSITE IS COOLED, MATRIX UNLOADS ELASTICALLY AND HYSTERESIS EFFECTS OCCUR RESULTING IN A RESIDUAL COMPOSITE STRAIN WHEN COMPOSITE IS COOLED DOWN TO RT

CONSTITUENT PROPERTIES USED TO MODEL THERMAL CYCLING

- P55 FIBER PROPERTIES ASSUMED TEMPERATURE INDEPENDENT
  - VALID FOR THE TEMPERATURE RANGE CONSIDERED

- TEMPERATURE DEPENDENT AZ91C PROPERTIES

TEMP., °F	E, MSI	σ_Y T-6	σ_Y F
70	6.50	22.0	14.0
300	5.46	16.5	10.5
400	4.62	14.5	9.3

THERMAL CYCLING OF P55/MG COMPOSITES - F CONDITION

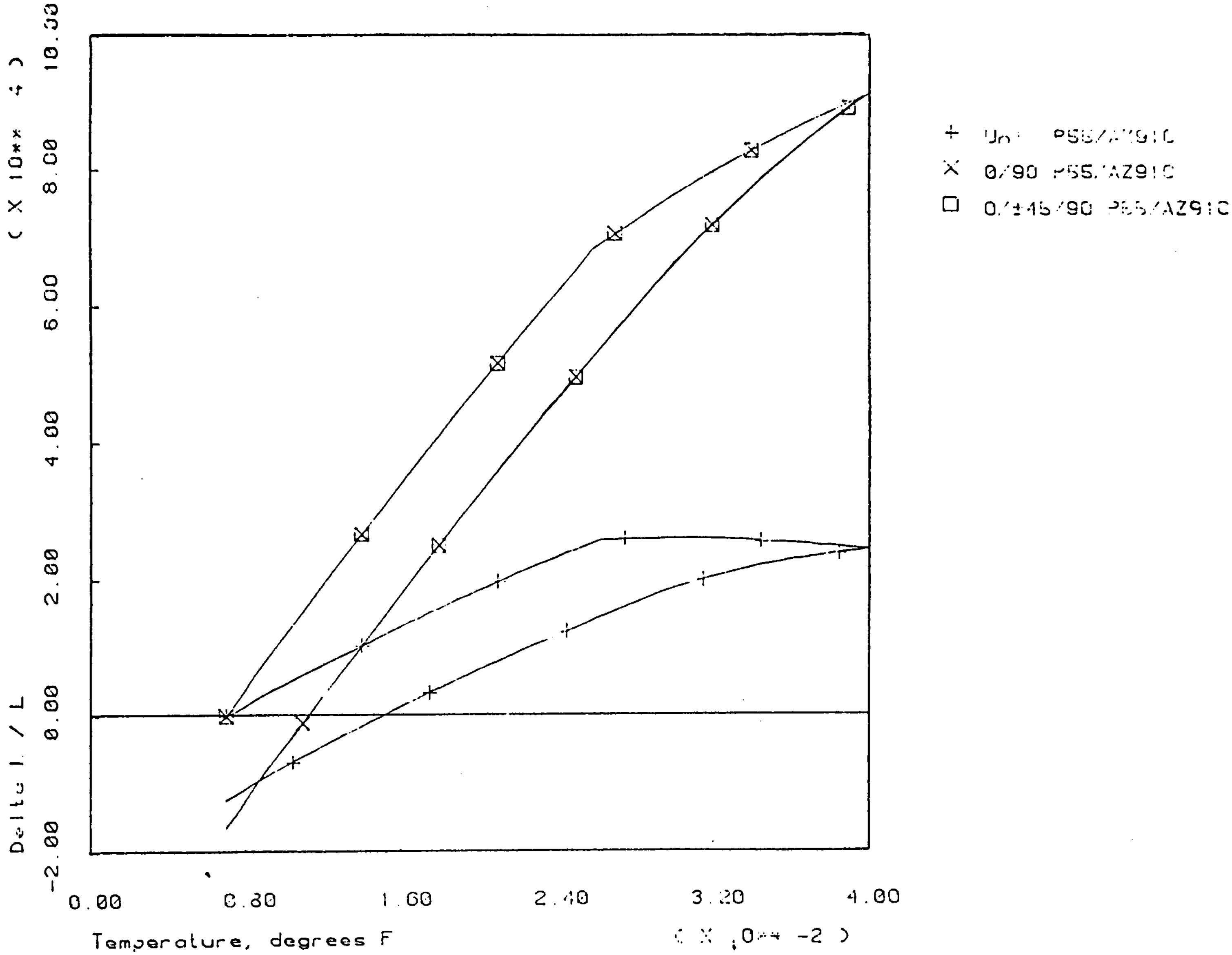

ORIGINAL PAGE IS
OF POOR QUALITY

THERMAL CYCLING OF P55/MG COMPOSITES - T-6 CONDITION

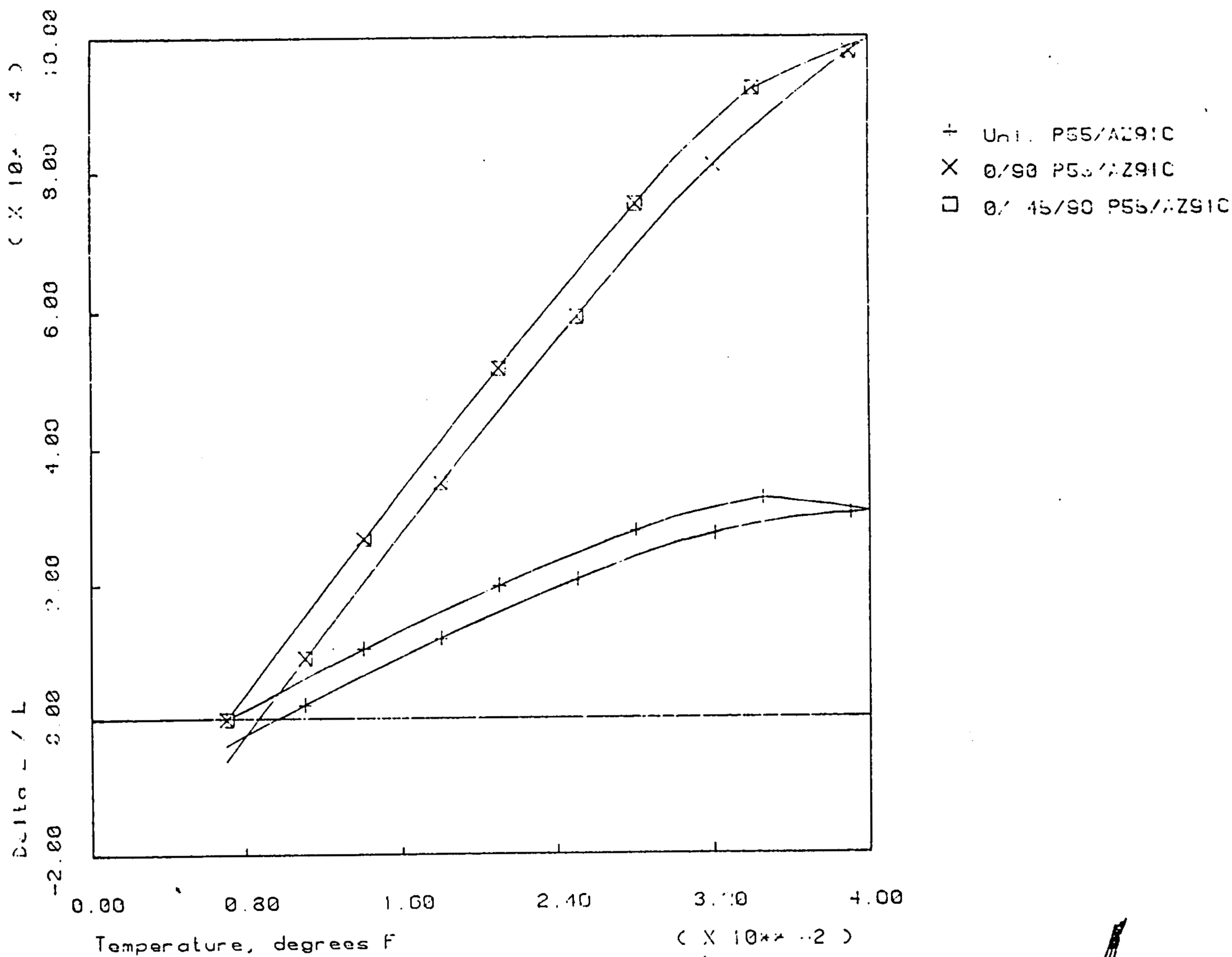

ORIGINAL PAGE IS OF POOR QUALITY

CONCLUDING REMARKS

- FOR THE METHOD OF FABRICATION USED, ANY $0^\circ_I/90^\circ_J$ CONSTRUCTION WILL EXPERIENCE PROBLEMS DUE TO LOW SHEAR STRENGTHS, ESPECIALLY AT ELEVATED TEMPERATURES
- $0/\pm45/90$ CONSTRUCTION IS BETTER SUITED FOR THIS APPLICATION
  - SLIGHTLY LOWER TENSILE AND COMPRESSIVE MODULI AND STRENGTHS BUT IMPROVED SHEAR STRENGTHS, BOTH AT RT AND HIGH TEMPERATURES
  - THERMAL EXPANSION BEHAVIOR AND THERMAL CONDUCTIVITY VALUES ARE NOT AFFECTED
  - SPECIFIC AMOUNTS OF $\pm45^\circ$ LAYERS DIFFICULT TO SPECIFY BECAUSE GOOD DEFINITION OF PRESSURES AND TEMPERATURE DISTRIBUTIONS ARE NOT AVAILABLE AND BECAUSE TESTS ON $0^\circ_I/\pm45^\circ_J/90^\circ_K$ WERE NOT DONE
- POST PROCESSING TO RELIEVE MATRIX RESIDUAL STRESSES AND TO INCREASE MATRIX YIELD STRENGTHS IS RECOMMENDED
  - PLASTICITY EFFECTS ARISING DUE TO CYCLING BETWEEN RT AND OPERATING TEMPERATURES CAN THUS BE REDUCED OR EVEN ELIMINATED

CONCLUDING REMARKS (CONT'D)

- RECOMMEND KEEPING P55/MG WALL TEMPERATURES UNDER 350°F TO REDUCE MATRIX CREEP. COULD CONSIDER:
  - USE OF FIBERS HAVING HIGHER AXIAL THERMAL CONDUCTIVITY
  - USE OF BETTER CREEP RESISTANT MATRIX
  - SLIGHT REDUCTIONS IN WALL THICKNESSES
- ANALYSES ARE PRELIMINARY BECAUSE THEY WERE BASED ON VARIOUS ESTIMATED PARAMETERS
  - NEED BETTER DEFINITION OF HOUSING TEMPERATURE DISTRIBUTIONS
  - NEED ADEQUATE DEFINITION OF INTERNAL PRESSURE LOADS
  - NEED TEST DATA ON $0_I/\pm45_J/90_K$ COMPOSITES FOR INTERMEDIATE TEMPERATURES BOTH ON T-6 AND AS-FABRICATED CONDITIONS
- REFINED FINITE ELEMENT ANALYSES (3-D) ARE RECOMMENDED ONCE MORE SUBSTANTIVE DATA ARE AVAILABLE